Investigation of a Biofilm Reactor Model with Suspended Biomass

Masic, Alma

2013

Investigation of a biofilm reactor model with suspended biomass

Alma Mašić

Lund University

Faculty of Engineering
Centre for Mathematical Sciences
Mathematics

Mathematics
Centre for Mathematical Sciences
Lund University
Box 118
SE-221 00 Lund
Sweden

http://www.maths.lth.se/

Doctoral Theses in Mathematical Sciences 2013:1
ISSN 1404-0034

ISBN 978-91-7473-465-2
LUTFMA-1047-2013

Printed in Sweden by MediaTryck, Lund 2013

Abstract

Biofilms are compact, sessile microbial communities that attach to surfaces in aqueous environments. In wastewater treatment, they are especially important for removal of phosphorus and nitrogen, which, if released into a receiving water body, can cause severe eutrophication. Mathematical models of biofilms in wastewater are used to understand the underlying processes and to describe and analyze biofilm development. Although biofilm reactors always contain an amount of suspended biomass, this biomass is mostly neglected in mathematical models of biofilm reactors. This thesis is based on four papers which investigate the role of suspended biomass in biofilm reactors. A one-dimensional mathematical model of biofilm and suspended biomass in a continuous stirred tank reactor is presented and analyzed in the first paper. The underlying model is a hybrid model of chemostat-like mass balances for the substrate and biomass in the reactor, coupled with a free boundary value problem for the substrate in the biofilm. In a single species single substrate setting, stability conditions for washout and persistence are given. It is found that biofilm and suspended biomass are either both present in the reactor or completely washed out. Numerical simulations show that biofilm dominates over suspended biomass in the longterm reactor performance, but that suspended biomass is relatively more efficient at substrate removal. The model is extended to a microbially and algebraically more complex multi-species multi-substrate model in the third paper, describing two-step nitrification in a Moving Bed Biofilm Reactor (MBBR). Nitrogen enters the reactor in the form of ammonium and leaves as nitrate after an intermediate conversion to nitrite. Numerical simulations show that suspended biomass does not contribute significantly to the overall reactor performance, but is substantial in the intermediate processes. In the second paper, the biofilm model is numerically validated against microelectrode measurements of oxygen gradients across the biofilm depth of a nitrifying biofilm attached to a suspended carrier harvested from an MBBR. Finally, a single species single substrate case with a limited amount of substrate and treatment time is considered as a two-objective optimization problem. With the bulk flow velocity as the control, different classes of admissible functions are investigated. It is found that, given the uncertainties in the initial data, none of the other functions perform better than the constant flow rate, i.e. the uncontrolled reactor.

Populärvetenskaplig sammanfattning

Hantering av avlopp och avfall är en del av alla människors vardag. Vår hälsa och miljö påverkas av metoderna vi tillämpar för att ta hand om rester från hushåll och industrier. Genom teknikens utveckling används idag bakterier i vattenreningsverk där avloppsvatten renas från alla skadliga föremål och föreningar. Med hjälp av matematiska uttryck och analyser, i samspel med biologiska, fysikaliska och kemiska experiment, kan dessa reningsprocesser undersökas och förhoppningsvis förbättras. I den här avhandlingen vänds strålkastarljuset mot så kallade biofilmer, som är betydande för borttagning av kväve och fosfor ur avloppsvatten.

Bakterier som hopar sig på en blöt yta bildar ofta biofilmer med helt andra egenskaper än de fria bakterierna. Biofilmer skyddar bakterierna från exempelvis antibiotika, men de bromsar samtidigt tillflödet av näringsämnen. Ett typexempel på biofilmer är vanligt plack som bildas på tänderna. Om placken inte tas bort kan den bilda tandsten och orsaka karies. Trots att biofilmer ofta kopplas samman med sjukdomar och förfall finns det flera användningsområden där de kan göra nytta.

I avloppsvattenrening har man länge använt bakterier i form av aktivt slam, där bakterierna växer och förökar sig genom att bryta ner olika näringsämnen som finns i avloppsvattnet. En pågående övergödning av vattendrag på grund av för höga halter av kväve och fosfor i reningsverkens utloppsvatten ökar kraven på förbättrade reningsmetoder. Ett sätt att ytterligare rena avloppsvattnet är att använda biofilmer som ger utrymme för specialiserade bakterier att bryta ner kväve och ta upp fosfor. Kväve kommer in till reningsverket i form av ammonium som finns i urin och lämnar det slutligen som oskadlig kvävgas.

Matematiska modeller i form av differentialekvationer har länge använts för att beskriva och förstå bakteriernas mekanismer och deras roll i reningen av vatten. Modellerna varierar i komplexitet och detaljrikedom beroende på hur många element och processer de beskriver. Många är därför mycket komplicerade och svåra att lösa analytiskt och måste beräknas numeriskt med hjälp av datorer. Enklare modeller, där många mindre viktiga processer försummas, kan däremot ofta studeras med exakt matematik.

Biofilmssystem i vattenreningsverk brukar alltid ha en liten andel bakterier som flyter omkring i vattnet. Dessa bakterier, så kallad suspenderad biomassa, kommer antingen in till reaktorn med det orenade vattnet eller lossnar från biofilmen. Den suspenderade biomassan måste tas bort från det renade vattnet innan det kan fortsätta vidare i reningsverket och ut till ett vattendrag. Trots detta försummas den fria biomassan oftast i traditionella biofilmsmodeller.

I den här avhandlingen undersöks effekterna av suspenderad biomassa i matematiska biofilmsmodeller av avloppsvattenrening. En relativt enkel endimensionell modell med en bakteriesort och ett näringsämne presenteras och analyseras både analytiskt och numeriskt. Det visar sig att suspenderad biomassa och biofilm måste samexistera. I ett längre tidsperspektiv kommer biofilmen att dominera den suspenderade biomassan. Suspenderad biomassa är dock relativt sett bättre på att bryta ner näringsämnet än biofilm men effekten är oftast obetydlig eftersom dess andel i allmänhet är ganska liten.

En mer varierande bild ges av en nitrifikationsmodell där två olika bakteriesorter och tre näringsämnen samt syre finns i reaktorn. Lämpliga parametrar framtogs i en första studie där simulerade syrekoncentrationer jämfördes med uppmätta tvärs igenom biofilmen. Ytterligare numeriska simuleringar visar att reaktorns totala prestanda inte påverkas nämnvärt av suspenderad biomassa i och med att biofilmen står för störst andel nedbrytning. Däremot spelar den suspenderade biomassan en tydlig roll i processens mellansteg och mellanprodukter. Slutsatsen är att suspenderad biomassa inte behöver inkluderas i biofilmsmodeller om reaktorns prestationsförmåga står i fokus.

I en efterföljande studie undersöks vad som händer i en situation där tillgången till näringsämnet samt behandlingstiden är begränsade. Frågan ställs om en sådan reaktor kan förbättras genom styrning av flödet mellan förvaringsreaktorn och behandlingsreaktorn. Ett optimerat styrningsproblem formuleras och löses för olika typer av flödesreglering. Den bästa kandidaten, en så kallad off-on-funktion där flödet är avstängt till en början medan bakterierna etablerar sig, är inte avsevärt bättre än ett vanligt konstant flöde. Slutsatsen blir att ett styrt flöde inte har några nämnvärda fördelar gentemot en konstant flödeshastighet.

Preface

This thesis considers the problem of mathematical modeling of biofilm reactors which include suspended biomass. Such a model is formulated and analyzed both mathematically and numerically in the first paper. The next paper investigates a nitrifying biofilm in a Moving Bed Biofilm Reactor through microelectrode measurements and numerical simulations. In the third paper the main model from the first paper is used and extended by introduction of microbial and physical complexity from the nitrification model of the second paper. The extended model is analyzed by means of extensive numerical simulations. In the last paper an optimization problem is presented and studied. The aim of the problem is to find a flow regime between a storage reactor and a treatment reactor that will increase the substrate removal efficiency and decrease process duration.

The work of this thesis has been funded by the Knowledge Foundation, Malmö University and Lund University.

The thesis consists of the following four papers:

I **A. Mašić** and H.J. Eberl, (2012), "Persistence in a single species CSTR model with suspended flocs and wall attached biofilms", *Bulletin of Mathematical Biology*, **74**(4):1001-1026.

II **A. Mašić**, J. Bengtsson and M. Christensson, (2010), "Measuring and modeling the oxygen profile in a nitrifying Moving Bed Biofilm Reactor", *Mathematical Biosciences*, **227**(1):1-11.

III **A. Mašić** and H.J. Eberl, (Aug 2012), "A modeling and simulation study of the role of suspended microbial populations in nitrification in a biofilm reactor", submitted to *Bulletin of Mathematical Biology*.

IV **A. Mašić** and H.J. Eberl, (Feb 2013), "On optimization of substrate removal in a bioreactor with wall attached and suspended bacteria", submitted to *Mathematical Biosciences and Engineering*.

Acknowledgments

I have had the privilege to meet and interact with various people during my years as a PhD student, many of whom have contributed to make this journey worthwhile. First, I would like to thank my supervisors Per Ståhle and Johan Helsing for all their help and advice. Their constructive comments during the examination of this thesis have considerably improved its quality. I would also like to acknowledge the help from my previous supervisors Anders Heyden and Niels Christian Overgaard.

I will forever be most indebted to Hermann Eberl of University of Guelph, Canada. He has been my main collaborator, providing genuine support and guidance along the way. His enthusiasm for and knowledge of mathematics have been contained in countless e-mails and long discussions, which have been crucial for my work. I would particularly like to emphasize the amount of work he has invested in the finalization of this thesis, with an unfailing attention to detail. Collaboration with such a generous and inspiring person continues to be effortless and I hope we will have plenty of opportunities to work together again. I would also like to thank him for inviting me to visit Guelph and devoting his time to our discussions during my research stays. My visits were greatly eased by the assistance and kindness of Mallory Frederick Jutzi, Hedia Fgaier, Ranga Sudarsan, Vardayani Ratti, Blessing Uzor, Fazal Abbas and Sandy Smith, who all welcomed me as one of their own.

My interdisciplinary work would have been a mystery were it not for the considerable help and support I have received from Magnus Christensson, Jessica Bengtsson, Maria Johansson, Eva Tykesson and Jenny Kruuse at AnoxKaldnes in Lund. They have patiently taught me so much about biofilms and wastewater treatment, always providing explanations for a curious mathematician. I would also like to express my gratitude to their colleagues who have shown a friendly work environment and invited me to eat many "fredagsbulle" over the years.

I am sincerely thankful for the generosity and understanding shown by Kalle Åström at the Centre for Mathematical Sciences. Andrey Ghulchak contributed with ideas and helpful conversations, which I truly appreciate. Furthermore, I want to thank Mikael Abrahamsson at the mathematical library, who has eagerly helped me find many important, but obscure books and papers. I have had several interesting discussions with Robert Almstrand, Malte Hermansson and Fred Sörensson of Gothenburg University and would

like to thank them for all their competent and insightful comments.

I was fortunate to be able to share my experience with fellow graduate students Mattias Hansson and Ketut Fundana. They have selflessly provided support and encouragement, especially during the rough patches of this project. The help of Sami Brandt, who started out as a post-doc and became a friend of ours, is highly appreciated. I will miss all our joint activities, many of which have turned into anecdotes. Good future to all of us!

Christina Bjerkén and Ulf Hejman of Malmö University showed enthusiasm and competence during our short collaboration, which I am very grateful for. It has also been a pleasure to spend time with the graduate students involved in the research program Biofilms – Research Center for Biointerfaces at Malmö University.

Without my family and friends, who have provided endless support and appreciation, I would not have been where I am today. I will always cherish the love and kindness they have shown me.

Stort tack till mina kära vänner Arsine Bellarian, Džana Džemidžić, Karin Fremling och Aida Hadžialić som alltid har trott på mig. Den här avhandlingen hade inte blivit så bra utan det villkorslösa stöd ni har givit mig. Även Šeherzada Čatak och Berina Ibrović har hjälpt mig och stöttat mig. Jag är lyckligt lottad som har sådana underbara vänner.

Ich bedanke mich auch herzlich bei Maren Kus, für ihre Freundschaft, Unterstützung, Aufmerksamkeit und Gastfreundschaft.

Mojim dragim roditeljima Fatimi i Ramizu, najveće hvala na podršci i povjerenju koje su mi pokazali. Vaša beskonačna ljubav, pomoć i bodrenje su mi olakšali i omogućili put kroz moje dugogodišnje školovanje. Pružili ste mi veliki oslonac u životu i uvijek ste se trudili da osigurate bolju budućnost za mene i za Adnana. Zbog toga ću vam vječno biti zahvalna i ponosna na sve što sam postigla. Moj lijepi i voljeni brat Adnan mi je također uvijek pružao podršku i pomoć, na čemu sada iskreno zahvaljujem (yoshi hugs!). Nana Ružica i deda Ismet su s ponosom i ljubavlju pratili moje uspjehe, ohrabrivali me i podupirali. Deda bi sada sigurno bio presretan da je dočekao objavljivanje mog rada. Hvala vam oboma na potpori. Također zahvaljujem mojoj dragoj tetki Melihi, tetku Samiru i rodicama Nejli, Sabini i Emini, koji su bili uz mene, pružali mi pomoć i povjerenje. Hvala i ostaloj rodbini u Bosni i Hercegovini i širom svijeta.

Posebno hvala mojim prijateljima na velikodušnoj podršci: Ajana Sadiković, Ajdin Sadiković, Irma Hodžić i Zlatan Balta, Lamija i Edin Karabegović, Mehmed Jakić, Mirza Jelačić, Senad Zjajo.

Podršku mi je također pružila i porodica Čolo. Konačno hvala mom dragom Atifu, koji je bio uz mene u dobru i u zlu, uvijek sa velikim razumijevanjem i dubokom ljubavlju. Tvoja podrška, pamet, nježnost i briga su mi mnogo značile. Ti si jedna poduzetna i maštovita duša, koja me inspiriše i motiviše. Hoćemo li sada na more?

Contents

Abstract iii

Populärvetenskaplig sammanfattning v

Preface vii

Acknowledgments ix

1 Introduction 1
- 1.1 Background . . . 1
- 1.2 Overview of the thesis . . . 2

2 Biofilms in wastewater treatment 7
- 2.1 Biofilms . . . 7
  - 2.1.1 Heterogeneity: spatial structure, diffusion gradients and microbial populations . . . 9
  - 2.1.2 Harmful and beneficial biofilms . . . 14
  - 2.1.3 Attachment and detachment . . . 15
- 2.2 Wastewater treatment . . . 17
  - 2.2.1 Moving Bed Biofilm Reactor . . . 19
  - 2.2.2 Nitrification . . . 20

3 Biofilm modeling 23
- 3.1 Mathematical models in biology . . . 23
  - 3.1.1 Chemostat . . . 24
  - 3.1.2 Conservation of mass, diffusion and transport . . . 27
- 3.2 Biofilm models . . . 29
  - 3.2.1 Overview . . . 29
  - 3.2.2 The one-dimensional Wanner-Gujer model . . . 30
  - 3.2.3 Biofilm models in wastewater applications . . . 32

3.2.4 Advantages and disadvantages of simple models 36

4 Conclusions and outlook **43**

Bibliography **47**

Paper I **59**

Paper II **90**

Chapter 1

Introduction

1.1 Background

Biofilms are ubiquitous microbial aggregates that coat surfaces in an aqueous environment. As aggregates they exhibit different features than free floating cells, for example an increased antibiotic resistance and the experience of concentration gradients from the bulk liquid toward the inner parts of the biofilm. The best and most studied example of beneficial biofilms is their use in wastewater treatment. Bacteria have been used in biological treatment even before biofilms were considered, for example in trickling filters, where wastewater was trickled over a bed of rocks on which bacteria had accumulated. The bacteria typically consume substrates from the wastewater and produce compounds that are safe for release into the environment. Here, the term substrate is used in a biochemical sense, denoting a substance that provides energy for the metabolism of the bacteria. Biofilms are used in wastewater treatment to allow for slow growing bacteria to grow and remain in the reactor while treating the wastewater. Removal of nitrogen and phosphorus has increased in significance due to possible eutrophication in water bodies that receive wastewater discharges when high levels of these chemical compounds are released. Nitrogen is, therefore, removed in an aerobic process called nitrification in which ammonium is converted first to nitrite and then to nitrate by two different bacterial species.

Mathematical models of wastewater treatment processes and biofilms in particular have been used to understand the underlying mechanisms and structures of these complex processes. The more we learn about biofilms from laboratory studies the more components we can incorporate into our models. On the other hand, the results from a mathematical study (either analytical or numerical) may confirm hypotheses or ask new questions which close the loop in a symbiotic relationship between experimentalists and mathematicians. There now exist all kinds of different models ranging from simple one-dimensional to complicated three-dimensional descriptions of biofilm wastewater pro-

cesses. Simpler models allow for more analysis, but may often lack in proper description of biofilm structure or heterogeneity. Complicated models involve many components and produce a detailed multi-dimensional description and can often only be solved numerically using large computation power.

Biofilm systems always have a certain amount of suspended biomass present in the reactor, even if it is much less than the biomass found in an activated sludge reactor. The suspended biomass, a result of detachment from the biofilm and possibly addition of biomass through the influent, can (re-)attach to the biofilm. However, traditional biofilm models have typically neglected the existence and effects of suspended biomass in the reactor, even when the detachment process is included. While this can be a reasonable assumption for certain lab-scale reactors in which suspended biomass is almost immediately washed out, it may be important for biofilm reactors where the suspended biomass is retained long enough for (re-)attachment to occur, which influences biofilm growth.

The main objective of this thesis is to investigate the role of suspended biomass in biofilm reactor models. Suspended biomass and biofilms interact through attachment and detachment of bacterial cells. In this thesis, the following questions, among others, are asked: How much does suspended biomass contribute to the reactor performance? Which mode of growth will dominate, sessile or suspended? Is it possible for the two biomass forms to out-compete each other? When is it necessary to include suspended biomass in biofilm models?

The investigation is based on a dynamic one-dimensional mathematical model of biofilm and suspended biomass in a continuous stirred tank reactor, which is presented in this thesis. The model is mathematically and numerically analyzed. Furthermore, the single species single substrate model is extended through incorporation of microbial complexity in order to represent a nitrifying moving bed biofilm reactor in a wastewater setting. The nitrification model is assessed through comparison with microelectrode measurements of oxygen concentration gradients. Finally, optimization of a bioreactor by control of the flow rate is investigated.

1.2 Overview of the thesis

Due to the interdisciplinarity of the thesis, the biological background is given in Chapter 2 and the mathematical framework in Chapter 3. Both chapters are mainly intended as an overview of the research field and to provide the necessary context for the problems addressed in the papers. Conclusions and future work are presented in Chapter 4. The scientific contributions of this thesis are contained in the four papers that follow in the last part of the thesis. They are also summarized here below with specified author contributions.

PAPER I — Persistence in a single species CSTR model with suspended flocs and wall attached biofilms

Alma Mašić and Hermann Eberl

In this paper we investigate the role of suspended biomass in a biofilm reactor. We formulate and study a one-dimensional mathematical model of suspended and wall-attached microbial populations and resource dynamics in a continuous stirred tank reactor (CSTR). The starting model is a free boundary value problem for a parabolic partial differential equation which we formally can rewrite as a model of ordinary differential equations (ODE) and then study with elementary ODE techniques. For a single species single substrate setting our analysis shows that the stability of the washout equilibrium depends on the dilution rate and on the growth and decay rates of the suspended flocs and the biofilm. We compare our results with the algebraically and physically less complex Freter model (a model of a chemostat with wall-attachment) and find that the Freter results largely carry over. If the trivial equilibrium is unstable the system will attain a non-trivial equilibrium at which biomass is present in the reactor in both modes of growth. Numerical simulations show that biofilms will dominate as mode of growth in a majority of the studied cases. The longterm behavior of the system depends on operating conditions of the reactor. Furthermore, it is observed that suspended biomass is relatively more efficient at substrate removal than biofilms are.

Author contribution: AM and HE constructed the model, developed the theory and analyzed the results. AM implemented the model and outlined and performed the numerical experiments. Manuscript was written and reviewed by AM and HE.

PAPER II — Measuring and modeling the oxygen profile in a nitrifying Moving Bed Biofilm Reactor

Alma Mašić, Jessica Bengtsson and Magnus Christensson

In this paper we validate the nitrification model against experimental data and identify realistic parameters for the model. We demonstrate an experimental microelectrode setup, used to measure oxygen gradients in a nitrifying biofilm on a suspended carrier from a Moving Bed Biofilm Reactor (MBBR) at different flow velocities. We incorporate the CSTR equation into a mathematical biofilm model of Wanner-Gujer type and simulate the oxygen gradients numerically with model parameters from several sources. The underlying biofilm model is a combined hybrid-parabolic free boundary value problem for which validation of parameters suggested in the literature and identification of parameters that are unique to this setup are performed. Our results show a dependence of biofilm and mass transfer boundary layer thickness on the bulk flow rate, implying that a decrease of the boundary layer would enhance the utilization of oxygen. Moreover, we establish a relationship between the erosion parameter and the bulk flow rate.

Author contribution: JB designed and performed the microelectrode measurements, AM constructed the model and developed and performed the numerical simulations. AM and JB analyzed and interpreted the results and wrote and reviewed the manuscript with contributions from MC.

PAPER III — A modeling and simulation study of the role of suspended microbial populations in nitrification in a biofilm reactor

Alma Mašić and Hermann Eberl

The presence and effects of suspended biomass in biofilm reactors are usually neglected in traditional biofilm models. We therefore investigate the importance of suspended biomass in a nitrifying biofilm reactor. In this paper we introduce the microbial complexity from Paper II into the model presented in Paper I, i.e. we study a one-dimensional mathematical model of a nitrifying MBBR with biofilms and suspended biomass. The resulting model is an ODE system that is coupled to a hyperbolic free boundary value problem by a semi-linear system of second order two-point boundary value problems. The complexity of the model prevents extensive analysis thereof but allows for numerical simulations. Our results show that the incorporation of suspended biomass may be neglected if the objective of the study is the overall reactor performance. However, inclusion of suspended biomass would be significant if detailed descriptions of the intermediate steps and products of the nitrification process are required.

Author contribution: AM constructed the model and analyzed the results with advice from HE. AM implemented the model and outlined and performed the numerical experiments. Manuscript was written and reviewed by AM and HE.

PAPER IV — On optimization of substrate removal in a bioreactor with wall attached and suspended bacteria

Alma Mašić and Hermann Eberl

In Papers I and III we assumed an infinite supply of substrate and studied longterm effects with regard to suspended biomass in a biofilm reactor. In this paper we pose an optimization problem for the one-dimensional single species single substrate model presented in Paper I with the aim to increase substrate removal efficiency and decrease process duration. We assume that a storage tank with a limited amount of substrate is connected to the biological treatment reactor through a controllable flow. The resulting optimal control problem is singular and leads to chattering control, which is not feasible from a practical perspective. Our results show that the optimization problem is rather insensitive to changes in the flow rate that deviate from the constant flow rate. We compute numerical solutions for specific off-on flow rate functions and find that they marginally improve the

reactor performance. Since they depend on initial data which cannot be controlled, we propose that a search for a different control than the constant flow rate is not necessary.

Author contribution: AM and HE constructed the model, developed the theory and analyzed the results. AM implemented the model and outlined and performed the numerical experiments. Manuscript was written and reviewed by AM and HE.

Chapter 2

Biofilms in wastewater treatment

2.1 Biofilms

Bacteria are prokaryotic microorganisms that are found in abundance almost everywhere on Earth. Many of them play a crucial role in nutrient cycles and human health, while others are detrimental to the environment and our well-being. With increased knowledge about the ubiquity and diversity of biofilms, improved investigative methods and interdisciplinary approaches, the biofilm research field has grown significantly since the beginning of the 1980s. Biofilms are most easily defined as layered aggregates of microbial populations attached to each other or to solid surfaces in aqueous environments or submerged in a liquid [16, 18]. They are typically embedded in a gel-like matrix (EPS, extracellular polymeric substances) produced by the bacteria themselves, comprised of polysaccharides, proteins, extracellular DNA etc. [33]. Together they form a very complex and differentiated community with a behavior unlike that of planktonic bacteria [119]. Although this description may appear very broad, it captures something that is common to all biofilms. Apart from that, what identifies biofilms is their wide diversity and adaptation to many different situations. For example, biofilms occur naturally in human bodies (e.g. as dental plaque), in household plumbing, on ship hulls, in hot springs, on frozen glaciers along with other locations [17]. Biofilms are in some way more different than they are similar.

A typical biofilm development has three stages: (i) attachment, (ii) growth, (iii) detachment, see Figure 2.1. In the initial attachment phase, bacteria adhere to coated solid surfaces, among which we find both organic and inorganic materials [9, 106]. The wet surfaces are coated with a thin film consisting of nutrients, proteins and other molecules, to which microbial cells adsorb. They initiate production of EPS, which entraps nutrients, microbial products and other organic and inorganic matter. This leads to an irreversible mode of attachment and a commencing aggregation.

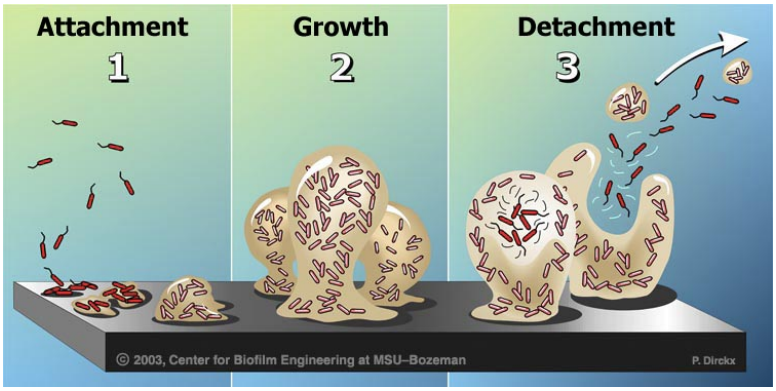

Figure 2.1: The three stages of biofilm development. Image used with permission, courtesy of Peg Dirckx, Montana State University.

During the second stage of biofilm growth and maturation, the bacteria within the biofilm experience an environment much different from that of planktonic bacteria. The EPS matrix surrounds and protects the biofilm bacteria, provides nutrients and "neighbors" who can communicate through cell-to-cell signaling (quorum sensing) [81]. The biofilm attains a complex three-dimensional dynamic structure. It is throughout this stage that biofilms develop their heterogeneous traits, such as structural diversity and distribution of populations.

The final stage of the biofilm development contains detachment of cells into the surrounding medium. Detachment processes can roughly be divided into an active and a passive form [50]. The latter involves external forces such as shear stresses, predation by higher organisms etc. which cause a loss of biomass. Cells can leave the biofilm structure individually or in larger clumps. Active detachment is initiated by the bacteria internally, leading to a dispersal of cells. Detached cells are able to attach and form new colonies downstream of the biofilm that they originated from.

What distinguishes biofilms from free floating bacteria are mainly three features, namely: the gel-like EPS-matrix that encapsulates the microorganisms within a biofilm and provides a specific environment, the exposure to concentration gradients of dissolved components across a biofilm instead of bulk liquid concentrations, and the very difficult eradication of biofilms that exhibit a strong resistance to antibiotics and drugs [20]. Thus, biofilms are able to survive in many different environments where free floating bacteria would be eliminated, wherefore bacteria preferentially reside in biofilms.

The following sections will only cover those elements of biofilm literature that provide a context and are relevant to this dissertation, rather than presenting an extensive literature overview.

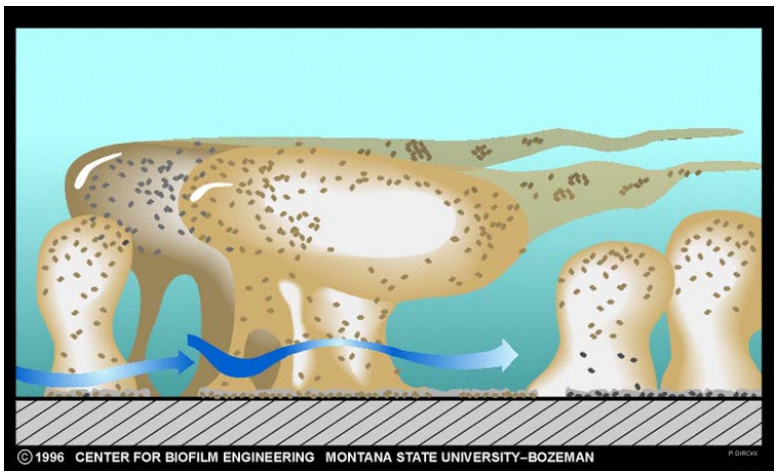

Figure 2.2: Typical biofilm mushroom-like structure with liquid channels. Image used with permission, courtesy of Peg Dirckx, Montana State University.

2.1.1 Heterogeneity: spatial structure, diffusion gradients and microbial populations

A mature biofilm is very responsive to its surroundings and is able to adapt to external changes. As a result, biofilms express various features in chemical, biological and physiological composition as well as structural arrangement [105], which have been observable through advances in microbiological and in particular microscopic tools. The confocal laser scanning microscope (CLSM) has notably enabled studies and visualizations of living, functional and hydrated biofilms more or less in their natural form.

Spatial structure

In the initial phases of biofilm formation the bacteria constitute a thin and patchy layer, which does not yet provide all the benefits of a joint sessile mode of growth, like protection of washout. The length scale of a bacterium is in the range of micrometers, wherefore the early biofilm is only a couple of micrometers thick. However, as the biofilm matures, it reaches thicknesses in the range of millimeters and on some occasions even centimeters. To the naked eye a biofilm is often perceived as a slime layer. Bacteria within a biofilm are encapsulated by the EPS matrix which is interspersed with water channels that provide transport of nutrients and other molecules throughout the complex structure [23].

The three-dimensional structure of a biofilm generally depends on the environment in which the biofilm is situated [121]. Substrate concentration and availability (or dosage intervals in laboratory experiments) along with hydrodynamic conditions are among the

factors that affect biofilm formation and development. A typical image of a biofilm is the so called mushroom structure, where liquid channels penetrate the bottom of the porous mushroom shaped biomass [110], see Figure 2.2. In Figure 2.3 a variety of different biofilm structures is shown, ranging from thin and dense to thick and porous biofilms which are attached to plastic surfaces in a wastewater treatment environment. The color of the biofilm varies depending on the type of bacteria, on chemical reactions that take place in the biofilm and on the properties of the surrounding liquid.

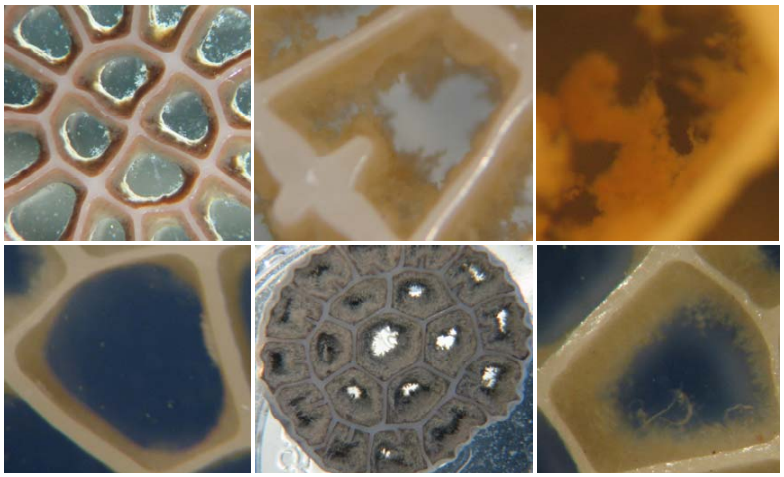

Figure 2.3: Photographs of various biofilms attached to white plastic surfaces in wastewater treatment. The plastic walls are approximately 0.1 to 0.15mm thick and 0.2 to 0.5mm long. Images used with permission, courtesy of AnoxKaldnes, Sweden.

Diffusion gradients

In diffusion, particles move from areas with high concentration to areas with low concentration down the concentration gradient without fluid motion. This process requires no input of energy from the particles and is, therefore, often called a passive process which is much slower than advection (transport of solutes within a fluid by its bulk flow). A porous biofilm with water channels as depicted in Figure 2.2 allows advection even within the aggregate. On the other hand, in a cell cluster where bacteria are densely packed advection cannot take place due to physical obstacles, wherefore substrates must be transported into and through the aggregate by diffusion. As a consequence, diffusion limitation arises in biofilm systems as the diffusion distance increases substantially across a complex biofilm structure [104].

The application of microsensor measurements in biofilm research has enabled visualization and direct observation of the distribution of a substrate in a living biofilm [18].

In combination with CLSM images, the heterogeneous structure of a biofilm has been revealed. The earliest and most studied microsensor used in biofilms was a sensor that measures the oxygen concentration inside biofilms. Therefore, mostly aerobic and relatively thin biofilms could initially be analyzed. However, by now there exists a variety of reliable microsensors measuring chemical composition across biofilms, e.g. pH, ammonium, carbon dioxide [22].

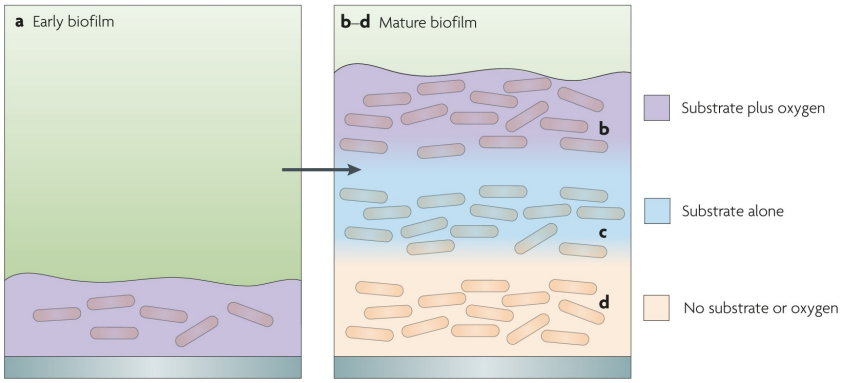

Figure 2.4: Heterogeneity in a single species biofilm, where oxygen and substrate are present in a thin biofilm at an early stage (**a**), but sequentially depleted within a mature biofilm (**b-d**). Image used with permission from [105], courtesy of Nature Publishing Group.

A layering in biofilms has been shown through measurements of oxygen and substrate concentrations [105], see Figure 2.4. The layering was a result of limited availability of substrates and oxygen due to diffusion and reaction. In a young and thin biofilm, the oxygen and the substrate reach the bottom of the biofilm through diffusion from the biofilm-bulk interface. As the biofilm grows thicker the oxygen only penetrates a certain distance from the surface (Figure 2.4b) before it is depleted by the bacteria. Oxygen limitation in Figure 2.4c occurs due to diffusion and uptake in layer b, assuming that the substrate is not the limiting factor. The intermediate layer becomes anaerobic with substrate availability but a lack of oxygen, i.e. a different environment than in the upper layer. The substrate- and oxygen-free bottom layer is created when the substrate is depleted in the intermediate layer.

In a multi-layered biofilm there are several chemical components possible for measurement. In Figure 2.5 three typical concentration gradients across a biofilm are shown [105]. Substrates are available in the bulk liquid and diffuse into the biofilm from the surface. The substrate concentration decreases from right to left in Figure 2.5a due to the consumption of substrate in the biofilm. Although generally most attention is given to diffusion of matter entering the biofilm, diffusion occurs in all directions down the gra-

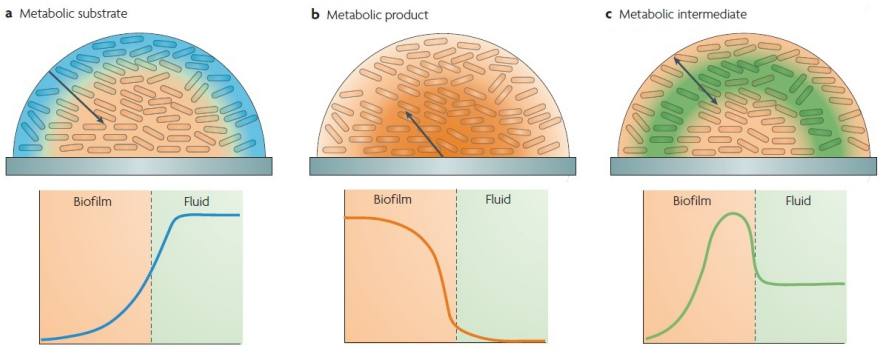

Figure 2.5: Three typical concentration gradients that arise in biofilms due to reaction-diffusion interactions for a substrate (blue; **a**), a product (orange; **b**) and an intermediate compound (green; **c**). Image used with permission from [105], courtesy of the Nature Publishing Group.

dients. For a product generated by the bacteria the concentration gradient is the opposite of that of a substrate (see Figure 2.5b), with molecules diffusing out of the biofilm into the bulk liquid. The concentration of an intermediate compound usually peaks in the middle layer of the biofilm and the compound diffuses from that layer both deeper into the biofilm as well as out into the bulk liquid.

The liquid flow velocity parallel to the surface is close to zero directly at the biofilm/liquid interface, even when the overall liquid flow is larger. A boundary layer, i.e. a thin liquid layer with negligible flow, forms between the biofilm surface and the surrounding liquid. In the boundary layer, molecules are transported only by diffusion [26]. The thickness of the boundary layer depends on the biofilm surface and on the flow regime, often in terms of laminar or turbulent flow. It has been shown through oxygen microelectrode measurements on a biofilm in a flow chamber that a higher flow rate as well as a rough biofilm surface make the boundary layer thinner [125]. This effect on the boundary layer thickness can be significant for biofilm activity, in particular for aerobic biofilms that require high concentrations of oxygen.

Oxygen concentration was measured inside a biofilm attached to a suspended carrier from a Moving Bed Biofilm Reactor (MBBR) process with the use of microelectrodes in Paper II (see also Section 2.2.1). The oxygen concentration gradients displayed a steady decrease from their bulk concentration to depletion deeper in the biofilm, leading to oxygen limitation. A correlation was shown between the boundary layer thickness and the flow velocity.

Populations

Early studies of bacterial populations were based on isolation and cultivation of single species bacteria on nutrient-rich media. However, many bacterial cells harvested from natural biofilms could not be cultured and, therefore, not studied. The turning point to resolve this issue arrived with the employment of molecular tools, most notably in situ hybridization with rRNA probes [2]. Further combinations of fluorescence in situ hybridization (FISH) with CLSM allowed identification and three-dimensional visualization and localization of microbial populations within biofilms.

Organisms, and thereby bacteria, are usually divided into groups based on the manner they obtain energy, their ability to fix carbon and the type of molecule they use as an electron donor [38, Ch.1]. Organic molecules (e.g. sugars and fats) serve as electron donors for organotrophs and inorganic molecules (e.g. iron, ammonia, hydrogen sulfide) for lithotrophs. In addition, autotrophs utilize carbon dioxide as a carbon source while heterotrophs are unable to fix carbon dioxide and require organic compounds as their carbon source.

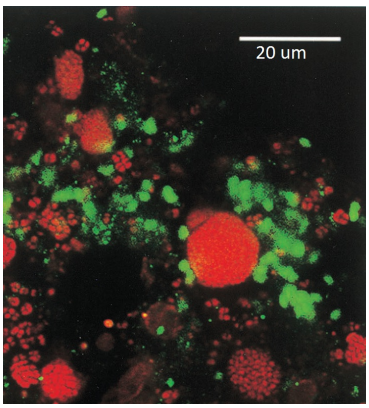

Figure 2.6: CLSM image of a FISH-stained biofilm with nitrite oxidizing bacteria (green) surrounding the clusters of ammonia oxidizing bacteria (red). Image used with permission from [77], courtesy of ASM Journals.

Environmental micro-niches created by diffusion-reaction interactions allow diverse bacterial species to cohabit the same biofilm, whereby a multi-species biofilm is formed. Bacterial cells easily adapt to the local surroundings and respond to the concentration gradients, which often results in a stratification where different species occupy specific layers in the biofilm [71]. The cooperation and competition between species in a biofilm can often be exemplified through situations where the waste of one species is a substrate for the other. A typical illustration of these dynamics are the aerobic nitrifying biofilms in a process known as nitrification [101]. Close interactions between the ammonia oxidizing

bacteria (AOB) and the nitrite oxidizing bacteria (NOB) arise as a result of the dependence of NOB on AOB for substrate supply, i.e. AOB convert ammonia to nitrite which is further converted to nitrate by the NOB. These interactions often lead to small clusters of nitrite oxidizing bacteria being close to or surrounding large clusters of ammonia oxidizing bacteria, interspersed throughout the biofilm [77, 100], instead of exhibiting a distinct stratification, see Figure 2.6.

2.1.2 Harmful and beneficial biofilms

Bacterial biofilms can play both beneficial and detrimental roles in their environment depending on whether their formation is controlled or unintentional [11]. A strong motivation for research into biofilms has been their persistence and resistance to antimicrobial agents which cause severe medical effects and pose problems in the public health [40]. However, recent advances in biofilm research [96] are opening doors toward utilizing bacterial biofilms commercially in the industrial production of chemicals.

Harmful biofilms

Over the years, clinical and public health microbiologists have studied numerous infectious diseases from a biofilm perspective. Medical device-associated infections were first observed in the early 1980s through detection of bacteria deposited on the surface of indwelling devices and were the first clinical infections where a correlation to biofilms was identified [26, 40]. Microorganisms contaminate medical devices and form single or multi-species biofilms, which subsequently cause severe infections in the human host. Due to inherent biofilm resistance to antimicrobial agents these infections are very difficult to cure [19]. Among the many examples of devices, which in association with biofilms are known to cause infections [19], urinary catheters, sutures, contact lenses, central venous catheters and mechanical heart valves can be mentioned.

Microorganisms may also form biofilms on damaged human tissue and cause chronic infections. A common ailment is dental plaque, a biofilm found on tooth surfaces. Dental plaque is formed regularly in healthy persons, but may alter its microflora to contain more cariogenic strains, which can rapidly metabolize dietary sugars to acid, decreasing the local pH [64]. If left untreated, the biofilms can cause infection, tooth demineralization and tooth loss. The advantage of the easy biofilm accessibility is the possibility to mechanically remove biofilms through toothbrushing.

The unwanted deposition and growth of biofilms does not only cause problems in relation to human health, it is also a common disturbance in water and industrial systems where it is referred to as biofouling [32]. The phenomenon is characterized by the development of a biofilm which interferes with the proper operation of a water pipe or reactor. Bacteria are always present in the liquid phase of water systems and may utilize nutrients available in the water for biomass production, why it is difficult to prevent biofilm formation. A typical example of surfaces that are predisposed to biofouling are

ship hulls. Colonized surfaces can significantly reduce the speed of ships, thereby increasing fuel costs. Furthermore, microbially influenced corrosion (MIC), a broad term for mechanisms by which biofilms affect corrosion of metals, is a serious problem with widespread effects throughout our society. So far only a few mechanisms have been fully described and quantified, among which the corrosion by sulfate-reducing bacteria is the most known example [58].

Beneficial biofilms

The most successful example of the benefit of biofilms is their ability to remove unwanted compounds from wastewater in order to safely release the treated water back into the environment. Bacteria have long been used in the biological treatment of wastewater in removal of organic matter, phosphorous and nitrogen [72]. The biological treatment incorporates various biofilm-forming bacteria that feed on nutrients present in the water. They produce compounds that are either further degraded by other bacteria or in a secondary treatment, or that can safely be released into a receiving water body. Some compounds, like phosphorous, are only taken up by the bacteria without conversion and moved from the water phase to the biomass.

In the field of bioremediation, a process in which microorganisms are employed instead of physicochemical methods to remove pollutants, the usefulness of biofilms is well established. One of the advantages of biological decontamination is the rare production of toxic intermediates [82], which otherwise tend to persist in the environment, enter the food web and act as mutagenic or carcinogenic agents on mammals. Recent developments of biofilms in wastewater bioreactors involve bioremediation of heavy metals like zinc, copper and nickel.

2.1.3 Attachment and detachment

The life cycle of a biofilm starts with the arrival of bacteria and ends with their departure, i.e. the processes attachment and detachment as depicted in Figure 2.1. Particular attention has been given to biofilm attachment from a human health perspective where biofilm formation is undesired [25]. On the other hand, detachment is considered to be an important factor in the field of wastewater treatment where stable biofilms serve a purpose [60]. In terms of nomenclature, both attachment and detachment are very broad terms, encompassing several processes.

Attachment

Several factors are assumed to be involved in the initial attachment of bacterial cells to a surface. Among those are mass transport, conditioning of the surface, hydrophobicity, surface charge and roughness [79]. Organic and inorganic molecules, along with the bacteria, are transported to the surface and accumulate at the solid-liquid interface,

constituting what is commonly known as a conditioning film [57]. The film contains a higher concentration of nutrients compared to the bulk liquid, with physiochemical properties that differ from the original unaltered surface [99].

Essentially, bacterial adhesion can be divided into two steps: reversible and irreversible attachment [79]. The former incorporates the transport of bacteria close enough to the surface to allow initial interaction between cells and (conditioned) surfaces. In this step bacterial cells are able to leave the biofilm and can be easily removed by rinsing, etc. The second step of adhesion involves production of EPS that binds firmly to the surface, entering an irreversible mode of attachment [27]. In this stage, bacteria cannot be removed without physical or chemical intervention, e.g. scrubbing or chemical cleaners.

Bacterial cells may also attach to the surface of a developed biofilm, a process which, however, is poorly understood. Knowledge about the mechanisms of biofilm formation plays a significant role in research about detrimental biofilms, as discussed in Section 2.1.2. Attachment is also crucial in wastewater treatment applications where suspended biomass and biofilms are present in the same reactor and an exchange of biomass is observed, see Section 3.2.3.

Detachment

The final stage of the biofilm development involves active and passive loss of cells to the bulk liquid, either individually or in clusters. Detachment is a complex phenomenon, representing several different mechanisms and factors that cause biomass loss, see Figure 2.7. Overall, it is a process of great importance that regulates biomass accumulation, production of suspended solids and biological survival strategies [37].

Generally, detachment is divided into five categories of processes [50, 69]: (i) abrasion, (ii) grazing, (iii) erosion, (iv) sloughing and (v) dispersion. Grazing and abrasion are passive processes, erosion and sloughing can be both active and passive, whereas dispersion is always an active removal of cells, which involves mechanisms that are initiated by the bacteria themselves. The processes are not exclusive, i.e. several modes of detachment can occur within the same biofilm.

Abrasion and erosion are the release of cells or small portions of the biofilm, but differ in mechanism [21]. Abrasion is caused by collision with submerged particles in the bulk liquid [36]. On the other hand, erosion is caused by fluid shear in a flowing system with biomass loss occurring when shear forces exceed the cohesiveness of the biofilm [109].

In grazing, higher order organisms cause removal of biomass through predation on bacteria in the biofilm. This process is poorly understood, but is believed to be an important factor controlling biofilm dynamics [46, 80].

Sloughing involves detachment of large intact portions of the biofilm in discrete events, at times removing entire segments of biofilm from the substratum. Studies have shown that local hydrodynamic conditions in relation to biofilm structure trigger biofilm detachment, where an increase in flow velocity causes an increased amount of detachment from the biofilm that is affected by the shear forces [63, 112]. The local angle at which

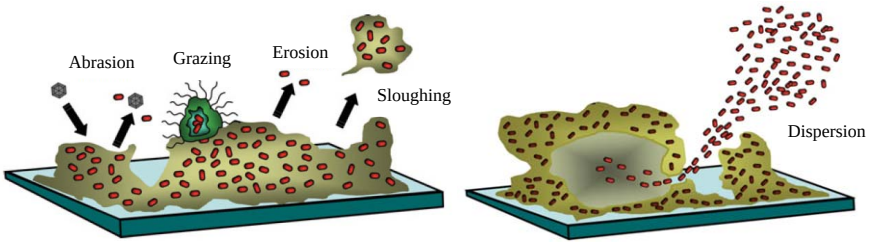

Figure 2.7: Five modes of detachment in biofilms: abrasion, removal of biomass caused by collision with particles; grazing, loss of biomass due to predation by higher order organisms; erosion, continuous removal of cells due to fluid shear; sloughing, dislodging of large biofilm portions; dispersal, active distribution of planktonic cells from a void within the biofilm. Image used with permission from [21], courtesy of Springer.

the shear stress acts on the biofilm determines the mode of detachment as either erosion or sloughing [73].

Dispersion is the release of unattached cells from a void within the biofilm, requiring active participation of bacteria. Contrary to erosion and sloughing, dispersion does not depend on fluid shear and can occur in the absence of flow [21]. It has been postulated that dispersion is an escape mechanism for biofilm bacteria due to poor conditions in their surroundings [98]. Furthermore, dispersion allows transport of bacteria to new colonization sites, a phenomenon referred to as seeding [50].

Comprehension of the mechanisms of biofilm detachment is crucial in several applications. In wastewater treatment, erosion and sloughing due to fluid shear forces impact the formation and the performance of a biofilm [60]. On the other hand, knowledge about biofilm detachment might lead to the development of clinical tools and methods to regulate biofilm formation or to promote its detachment [21].

Detachment is a significant factor in mathematical modeling of biofilms in wastewater. There are a number of different detachment models derived either from empirical or theoretical considerations. In Papers I-IV a detachment term is used that represents the sum of all detachment-like processes. The effect of the interaction between attachment and detachment rates on the overall outcome was investigated in Paper III.

2.2 Wastewater treatment

Wastewater management has developed over the years from collection and discharging without treatment to collection and treatment before disposal and possible reuse. Serious health concerns instigated better designs and planning of wastewater management. Industrial wastewaters differ depending on the type of industry and may contain complex

or toxic substances, while municipal wastewater mostly consists of organic matter and nutrients in either solid or soluble form. This thesis will exclusively address municipal wastewater treatment.

The objectives of (municipal) wastewater treatment are to remove contaminants and, thereby, to produce a safe effluent which can be discharged into receiving water bodies without harming the environment. Generally, wastewater treatment is performed in three major steps: primary, secondary and tertiary treatment [91]. Primary treatment typically consists of screening and settling where large particles and objects are removed and heavy and light solids are separated from the fluid. It is followed by a secondary treatment in which a biological process takes place where microorganisms remove suspended and dissolved organic matter, as mentioned in Section 2.1.2. The increased knowledge of the effects of chemicals and toxic compounds has resulted in the need for a tertiary treatment, which can be for example chemical or biological. Typically it involves disinfection, odor control and removal of the nutrients nitrogen and phosphorous.

Microorganisms are used in the second step to remove organic matter from the fluid most often in a process commonly known as activated sludge. The process requires an aerated reactor, a settling tank, sludge recirculation and removal of excess sludge [111]. The biomass is kept in suspension in an aerated reactor where the biochemical reactions take place. It is followed by a settling tank, in which the biomass sinks to the bottom, separating it from the clarified effluent. The settled biomass is mainly recirculated to the aerated reactor, to preserve a high concentration of biomass, which otherwise would be discharged. The remaining part, excess sludge, is removed and further treated in the sludge treatment stage.

Due to eutrophication, i.e. the over-enrichment of receiving water sources with mineral nutrients [15], the tertiary treatment stage involves removal of nutrients. Increased amounts of phosphorus (P) and nitrogen (N) in a lake or sea enhance the proliferation of algae and bacteria. This in turn leads to oxygen-free bottom waters due to high respiration by the biomass, thereby causing loss of fish and other aquatic animals naturally occurring in the water. Although eutrophication is a natural process, the superfluous addition of nutrients aggravates the development, wherefore discharge of P and N has been increasingly regulated in wastewater treatment. Removal of P and N is added as a tertiary treatment stage, with the latter discussed in more detail in Section 2.2.2.

Bacteria in the form of activated sludge or biofilms are not only used in secondary treatment, but are also present in tertiary treatment. They can be used for removal of both phosphorus and nitrogen. Biofilm processes and the reactor setups differ from those of activated sludge. Instead of being suspended in the liquid, biofilm biomass is attached to a surface that is submerged in the liquid. Therefore, there is no need for settling and sludge recirculation. Biofilms provide means for slow growing bacteria to grow and remain in a reactor. Many different biofilm reactors are available in contemporary wastewater engineering, from fixed bed reactors such as the trickling filter, submerged fixed-film reactors such as the rotating biological contactor to fluidized bed reactors such as the

upflow sludge blanket [66]. Section 2.2.1 will cover the Moving Bed Biofilm Reactor, in which biofilms are attached to suspended media that move freely in the liquid.

2.2.1 Moving Bed Biofilm Reactor

The moving bed biofilm reactor (MBBR) process was developed in Norway in the late 1980s to overcome the problems of existing biofilm systems used in wastewater treatment, while implementing the best features of the activated sludge process [74]. It has since become a common process used in treatment plants worldwide, either as an added treatment unit in an existing plant or as an integral part of the plant.

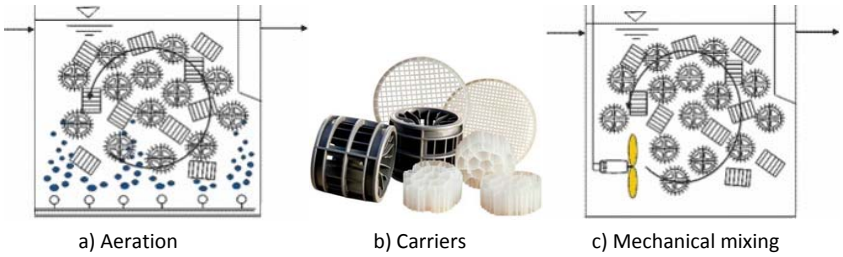

Figure 2.8: a) Aerobic tank with suspended carriers and aeration from the bottom. b) Different kinds of carriers. c) Anoxic tank with suspended carriers and mechanical mixing. Images used with permission, courtesy of AnoxKaldnes, Sweden.

In an MBBR the biomass is attached to carriers (Figure 2.8b) that are suspended in the water. The carriers are mixed in the liquid either through rising coarse air bubbles due to aeration (Figure 2.8a) or through mechanical mixing in oxygen-free processes (Figure 2.8c), and kept from leaving the reactor by a sieve. The carriers are designed with the biofilm area as the key parameter. A reactor can be filled with varying amounts of carriers, although the standard filling fraction is 40 to 65%. Here, the filling fraction is the volume of carrier elements relative to the water volume of the reactor in which they are suspended.

The MBBR process requires no sludge recirculation nor a large sedimentation tank, which gives it a great advantage over the activated sludge process [95]. Furthermore, it is easily managed and can often be set up using existing tanks, thereby being cost effective. The process is compact due to high concentration of biomass which can be differentiated with respect to bacterial species. However, the MBBR has increased operational costs due to larger power requirements for aeration/mixing, in particular to maintain activity during low loading phases, and a higher initial cost of carrier acquisition. Moreover, the effluent from an MBBR must be treated in order to remove the sloughed off biofilm from the treated water. This can be achieved through a variety of biomass separation methods such as sedimentation, flotation or filtration after the MBBR [75, 76]. The MBBR effluent contains several types of particulates, among which the sloughed off biomass and

the influent particulate matter are the most significant [47]. Compared with a standard activated sludge reactor there is approximately ten times less suspended biomass to be separated in the MBBR effluent, but still enough to require treatment. Hence, there is always a certain amount of suspended biomass present even in pure MBBR systems. The MBBR process is used in the mathematical models throughout this thesis, with particular focus on the interaction between attached and suspended biomass in Papers I, III and IV.

2.2.2 Nitrification

The agricultural development during recent years, with emphasis on fertilization of cropland, has increased the need for nutrient removal. High nitrogen loads promote eutrophication, which is harmful for the environment. Nitrogen is, therefore, removed from wastewater through sequential processes called nitrification and denitrification, which convert ammonium-nitrogen from the wastewater to nitrogen gas and in lesser amounts nitrous oxide, safe for release into the atmosphere. An additional nitrogen pathway exists through the process anammox (anaerobic ammonium oxidation), which, however, will not be discussed in this thesis.

Nitrification is a process in which ammonium (NH_4^+) is sequentially oxidized to nitrate (NO_3^-) with the intermediate component nitrite (NO_2^-) [59]. The chemical reactions are expressed as:

$$(i): \quad NH_4^+ + 1.5O_2 \rightarrow NO_2^- + 2H^+ + H_2O \tag{2.1}$$

$$(ii): \quad NO_2^- + 0.5O_2 \rightarrow NO_3^- \tag{2.2}$$

where the first reaction *(i)* is performed by ammonium oxidizing bacteria (AOB) and the second reaction *(ii)* by nitrite oxidizing bacteria (NOB), i.e.

$$NH_4^+ \xrightarrow{\text{AOB}} NO_2^- \xrightarrow{\text{NOB}} NO_3^-. \tag{2.3}$$

These bacteria use nitrogen as an electron donor, oxygen as an electron acceptor and fix carbon from carbon dioxide, wherefore they are classified as chemolithoautotrophs, see Section 2.1.1. Nitrification is an aerobic process, i.e. requires oxygen for the reactions to take place, why maintaining a high concentration of dissolved oxygen is a crucial task. If no other inhibitions are present, the first reaction *(i)* is the rate-limiting step of the overall conversion from ammonium to nitrate [122].

The two most common bacterial genera of AOB are the *Nitrosomonas* and *Nitrosospira* [55]. For NOB, the two most common genera are the *Nitrobacter* and *Nitrospira* [12]. AOB and NOB co-habit the same space within a biofilm and benefit from the physical proximity during the nitrification process [83], previously discussed in relation to Figure 2.6. NOB consume the product that is the outcome of the first reaction performed by AOB, thereby relieving the latter from toxic waste. Optimal temperatures for growth of

pure cultures were shown to be 35°C and 38°C for AOB and NOB, respectively [39]. The specific growth rates for AOB are higher than for NOB at temperatures above 15°C, while the opposite occurs at lower temperatures [42]. The MBBR processes used in Papers II and III are assumed to operate at a temperature of 10°C, to represent nitrification in a colder climate. The chosen temperature is far from the optimal temperature range, bringing about slower growth rates for both species and an advantage for NOB over AOB, resulting in different interactions than would have occurred at room temperatures. In comparison with heterotrophic bacteria that consume organic matter, the growth rates for AOB and NOB are much slower. The nitrifiers, therefore, benefit from the protected surfaces on the carriers in an MBBR, which allows them to form a stable biomass without being exposed to the risk of washout. Heterotrophic biomass, on the other hand, works very well in an activated sludge process.

Several factors that influence nitrification kinetics, i.e. the rates of chemical processes, have been identified. With regard to bacteria the kinetics refer to growth of nitrifying bacteria and the reaction rates in nitrification. It has been empirically determined that microbial growth in general follows so called Monod kinetics [65]. The Monod equation states that microbial growth is limited by the nutrient concentration

$$\mu(S) = \mu^{\max} \frac{S}{K_S + S} \tag{2.4}$$

where μ [time^{-1}] is the specific growth rate of the bacteria, $\mu^{\max}$ [time^{-1}] the maximum specific growth rate, S [mass·length^{-3}] the concentration of the limiting substrate and K_S [mass·length^{-3}] the half-saturation coefficient, i.e. the substrate concentration when $\mu = 0.5\mu^{\max}$. K_S and $\mu^{\max}$ are empirical constants that differ between species and depend on environmental factors. In nitrification, disregarding oxygen, growth of AOB is limited by the ammonium concentration while NOB is limited by the nitrite concentration. The Monod equation displays a steep growth curve for lower substrate concentrations, which levels off with an increasing substrate and asymptotically approaches its maximum rate, see Figure 2.9.

The kinetics and, thereby, the overall nitrification rate, is affected by several factors [59]. High concentrations of free ammonia or nitrous acid inhibit AOB and NOB, respectively. Furthermore, both species are inhibited by the presence of heavy metals like copper and nickel and other toxic compounds. The slow growth and the limited number of nitrifying bacteria renders them especially susceptible to such compounds; no other bacteria can take over the role of nitrification. Temperature has a significant effect on microbial activity, reaching a maximum at the optimal temperature. Nitrifying bacteria are able to survive at extreme temperatures ranging from 5 to 50°C [39]. Several phenomena are involved in the overall effects of temperature on the nitrification rate, for example the diffusion mass transport and half-saturation coefficient [126]. These dependencies should be taken into account in mathematical modeling, to ensure the utilization of appropriate parameters.

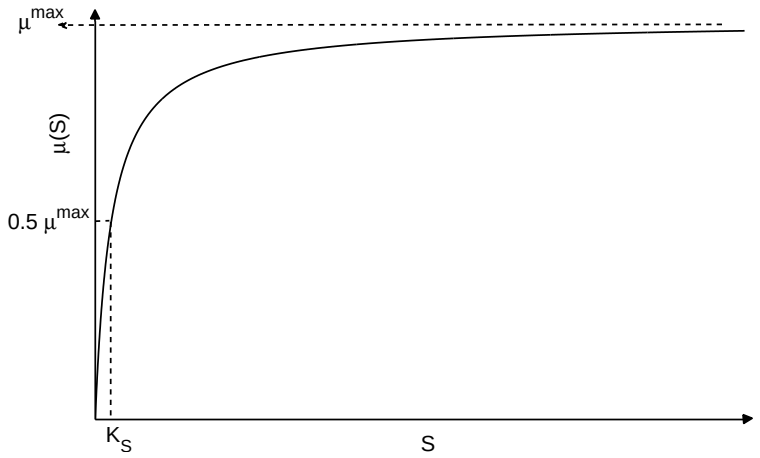

Figure 2.9: The Monod equation for microbial growth rate $\mu(S)$ on substrate S at a maximum specific growth rate μ^{max} and a half-saturation coefficient K_S.

Apart from substrate availability, it is also crucial that a high level of dissolved oxygen (DO) is present in a nitrification reactor. The nitrifiers are obligate aerobes and require the presence of oxygen for growth. Low DO will limit the nitrification rate, particularly in biofilm applications where diffusion of oxygen into the biofilm will pose a second obstacle for oxygen availability. In general, it is believed that a DO level below 2 mg/l is limiting for nitrifying bacteria in biofilms [13]. Due to diffusion and reaction oxygen may become limiting in the depths of a biofilm even though the bulk concentration has a sufficient level of DO. The affinity for oxygen differs between AOB and NOB, where the latter generally requires a higher DO concentration for microbial growth [83]. In wastewater treatment biofilm reactors there is a possibility for organic matter to enter the nitrification reactor. If organic matter is present it will serve as a substrate for heterotrophic bacteria which will compete for oxygen and space with nitrifying bacteria [13]. A heterotrophic layer may form on top of the nitrifiers in the biofilm and limit the oxygen penetration. As long as the nitrifiers are reached by a high enough oxygen concentration they will establish themselves and remain in the depths of the biofilm [35]. In these cases, the heterotrophic layer is often beneficial to the nitrifiers because it protects them from detachment.

Chapter 3

Biofilm modeling

3.1 Mathematical models in biology

Fibonacci (1175-1250) is often named as a pioneer in mathematical biology due to his number series that aimed to represent the reproduction of rabbits [54]. The series, in which the next number is the sum of its two predecessors, has later also been found in other parts of nature, for example in the growth of certain shells and most notably in the distribution of seeds in a sunflower. Over the centuries people have shown interest in understanding and deciphering our surroundings. The field of biology encompasses all living organisms, ranging from studies of among others plants and animals, cells and molecules to evolution, populations and genetics. The resulting catalog of mathematical models in biology therefore displays a similar range from small scale to large scale, simple to complex, linear to nonlinear etc. Examples of biological phenomena described by mathematical models include the predator-prey model of Lotka and Volterra, infectious disease models, tumor cell growth models and fishery management models [70]. A common misconception about mathematical models is that they are supposed to explain and depict a phenomenon in detail, reproducing the real life behavior to its fullest. This is, however, not the case. Mathematical models are a helpful tool that through simplification of the observed phenomenon can bring the theoretical or experimental work forward. It has been claimed that, more often than not, the mathematical model will predict biologically infeasible results [29, Ch.3]. But the subsequent investigation of the causes thereof may shed light onto the phenomenon itself as well as pose questions which will point the researchers in a new direction. The most fundamental processes in biofilms are microbial growth and mass transfer. In the next two sections the mathematical framework for these two concepts will be briefly reviewed, which will be needed later on.

3.1.1 Chemostat

In many subfields of biology it is common to study the population growth of organisms. In microbiology it is usually done through an experiment where microorganisms are suspended in a nutrient-rich liquid in which they proliferate [29]. Their growth is typically observed through an increase in volume and density. Depending on the circumstances during the experiment most microorganisms show a growth that can be characterized as logistic or exponential. A more realistic type of bacterial growth is the saturated nutrient consumption rate, where the growth rates are nutrient-dependent. Monod kinetics (previously discussed in Sec. 2.2.2), described by the equation $\mu(S) = \mu^{\max}\frac{S}{K_S+S}$ in (2.4), shows a growth rate that is proportional to the substrate concentration if nutrient availability is limited and levels off to a constant value if nutrients are available in abundance, see Figure 2.9.

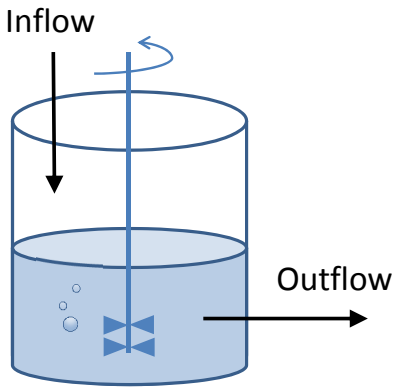

Figure 3.1: The chemostat with stirring and continuous inflow and outflow.

A bioreactor with stirring and continuous inflow and outflow is called a chemostat [102]. The chemostat provides a dynamic system for population studies and is extensively used in laboratory experiments. Nutrient is continuously supplied through the inflow and continuously removed through the outflow, while the liquid volume in the reactor is kept constant, see Figure 3.1. Various microorganisms, with concentrations $x_i(t)$ [mass·length^{-3}] for the $i = 1, \ldots, n$ species, are suspended in the reactor. Let Q [length^3·time^{-1}] denote the flow rate, V [length^3] the reactor volume and S^0 [mass·length^{-3}] the concentration of the input nutrient. It is assumed that all components that are necessary for bacterial growth are in excess except one limiting nutrient, denoted by $S(t)$. The flow rate Q and the input concentration S^0 are kept constant along with all other parameters that affect microbial growth. The rates of change for the bacteria

and the nutrient can be summarized as *growth-washout* and *inflow-washout-consumption*, respectively. It is often convenient to discuss the chemostat in terms of the dilution rate D [time^{-1}], which is obtained through $D = Q/V$ and has the same unit as the growth rate $\mu(S)$.

The competition between n competitors for one growth-limiting substrate can be expressed with the nondimensional system

$$\begin{aligned} \dot{S} &= 1 - S - \sum_{i=1}^{n} x_i \mu_i(S) \\ \dot{x}_i &= x_i(\mu_i(S) - 1), \quad i = 1, \ldots, n \end{aligned} \tag{3.1}$$

with $S(0) \geq 0$ and $x_i(0) > 0$, where $0 \leq S, x_i \leq 1$. The system has been nondimensionalized, why the concentrations S and x_i are now measured in units of S^0 and time in units of D^{-1}. It is assumed that nutrient uptake by the bacteria equals immediate bacterial growth. The general monotone response functions $\mu_i(S)$ ("the growth functions") are positive with $\mu_i(0) = 0$, increasing and continuously differentiable. Monod kinetics are most often used as growth functions in a chemostat.

Let b_i be the *break-even concentration* defined as the unique solution to $\mu_i(S) = 1$. If the solution does not exist, let $b_i = +\infty$. The biological interpretation of b_i is the nutrient concentration for which a microbial growth rate is obtained that is equal to the dilution rate. The equations for x_i in (3.1) are numbered such that $0 < b_1 < b_2 \leq \ldots \leq \infty$. Microbial species 1 requires a smaller nutrient concentration than species 2 and thus has an advantage in the competition. With the nondimensionalization the microbial concentrations are expressed in their nutrient equivalent, i.e. how much nutrient was used to achieve that particular concentration. Define Σ as

$$\Sigma = S + \sum_{j=1}^{n} x_j - 1. \tag{3.2}$$

It follows that

$$\lim_{t\to\infty} \Sigma(t) = 0 \Longleftrightarrow \lim_{t\to\infty} \left(S(t) + \sum_{j=1}^{n} x_j(t) \right) = 1. \tag{3.3}$$

The system (3.1) can now be rewritten in the variables $\Sigma, x_1, \ldots, x_n$ as

$$\begin{aligned} \dot{\Sigma} &= -\Sigma \\ \dot{x}_i &= x_i \left(\mu_i \left(1 + \Sigma - \sum_{j=1}^{n} x_j \right) - 1 \right), \quad i = 1, \ldots, n \end{aligned} \tag{3.4}$$

Solutions of (3.1) and (3.4) exist and are non-negative and bounded. Using (3.3) and considering the system (3.4) restricted to the invariant hyperplane $\Sigma = 0$, the system can be simplified to

$$\dot{x}_i = x_i \left(\mu_i \left(1 - \sum_{j=1}^{n} x_j \right) - 1 \right), \quad i = 1, \ldots, n \tag{3.5}$$

on the positively invariant domain $\Omega = \left\{ x \in \mathbb{R}^n_+ : \sum_{j=1}^n x_j \leq 1 \right\}$ with $x_i(0) > 0$.

All microbial competitors with a break-even concentration that is equal to or exceeds the nutrient concentration in the reactor, i.e. $b_i \geq 1$, are deemed inadequate as they will eventually be eliminated from the reactor. Thus, only adequate competitors with $0 < b_i < 1$ are considered. Let x_1 be an adequate competitor and let

$$E_1 = (1 - b_1, 0, 0, \ldots, 0) \tag{3.6}$$

be the equilibrium point for $(x_1, \ldots, x_n)$ in (3.5) at which only species x_1 survives. Consideration of equilibrium points for other adequate species for some $j \geq 2$ is not necessary for the statement of the main result about competitive exclusion.

Theorem 3.1.1. *Let $x(t)$ be a solution to (3.5) in Ω for which $x_1(0) > 0$. Then*

$$\lim_{t \to \infty} x(t) = E_1. \tag{3.7}$$

The theorem states that the microbial species with the smallest break-even concentration will outcompete all other species in a chemostat and remain alone in the reactor. Lyapunov functions and the LaSalle corollary of Lyapunov stability theory are used to prove the theorem. By defining the sets $\Delta_A = \left\{ x \in \Omega : \sum_j x_j = 1 - b_1 \right\}$, $\Delta_B = \left\{ x \in \Omega : \sum_j x_j < 1 - b_1 \right\}$ and $\Delta_C = \left\{ x \in \Omega : \sum_j x_j > 1 - b_1 \right\}$, it is shown that a solution that starts in Δ_C either moves to Δ_B or remains in Δ_C and converges to E_1. Solutions in Δ_B remain in the set and converge to E_1.

Theorem 3.1.1 presents a mathematical result which has subsequently been confirmed with biological experiments. In a proper chemostat setting with several species competing for one nutrient, the microbial species with the smallest break-even concentration will eliminate all other species from the reactor. The result is used by microbiologists to design chemostat experiments. The chemostat is often used for bacterial enrichment and harvesting [29, Ch.4]. Further applications include steady state analysis of different organisms and interactions and competition between populations. However, the result rests on the assumption that the growth of each competitor is described by a monotone function and that there is no interaction between the competitors. The principle of com-

petitive exclusion does not hold if one species has a (non-competitive) growth advantage over the other [31], if there is a direct exchange of biomass between the species, or if one of the species is protected from washout. The latter two aspects need to be considered in biofilm reactors with suspended growth, which requires an extension of the above theory.

3.1.2 Conservation of mass, diffusion and transport

The principle of mass conservation states that all mass/matter/energy in an isolated system is conserved. The mass conservation equation can be derived by use of the divergence theorem [24, Ch.2].

Let $V \in \mathbb{R}^d$, $d = 1, 2, 3$, denote the fixed control volume containing a substance with concentration $C(t,x)$ and let ∂V denote the closed surface boundary of V. The mass $M(t)$ of the substance contained in V is the volume integral

$$M(t) = \iiint_V C(t,x)\, dV \tag{3.8}$$

where dV is the differential element of the volume V. Conservation of mass implies that

$$\text{rate of change of } M \text{ in } V = \underbrace{\text{production in } V}_{\text{source}} - \underbrace{\text{outflux through } \partial V}_{\text{sink}} \tag{3.9}$$

which is mathematically expressed as

$$\frac{dM}{dt} = \iiint_V R\, dV - \oiint_{\partial V} J \cdot n\, dS \tag{3.10}$$

where R is the local production rate and where the second term on the right hand side is a surface integral of the total flux J of the substance in the direction of the outward normal n through the differential surface elements dS on ∂V. Applying the divergence theorem the surface integral can be converted into a volume integral

$$\oiint_{\partial V} J \cdot n\, dS = \iiint_V \operatorname{div} J\, dV. \tag{3.11}$$

Substituting (3.11) into (3.10) and using (3.8) leads to

$$\frac{d}{dt} \iiint_V C(t,x)\, dV = \frac{dM}{dt} = \iiint_V R\, dV - \iiint_V \operatorname{div} J\, dV \tag{3.12}$$

which can be rewritten under one integral as

$$\iiint_V \left(\frac{\partial C}{dt} - R + \operatorname{div} J \right) dV = 0. \tag{3.13}$$

Since the equality in Equation (3.13) has to hold for any arbitrary volume V it follows that

$$\frac{\partial C}{dt} - R + \operatorname{div} J = 0. \tag{3.14}$$

The conservation law is expressed in its integral form in (3.13) and in its differential form in (3.14).

The expression for the flux J can be adapted to the situation at hand. An important transport process for particles is diffusion, in which the random and irregular motion of individuals in a group results in a movement on a macroscopic level [70]. Diffusion transports matter down the concentration slope, i.e. from high to low concentration, also known as Fick's first law. The law states that the flux J is proportional to the gradient of the concentration C

$$J = -D_c \nabla C \tag{3.15}$$

where D_c [length^2·time^{-1}] is the diffusion coefficient that measures the efficiency of particle dispersal and ∇ denotes the gradient. Diffusion is in general a fast process locally, but an extremely slow process on longer distances [29, Ch.9]. The diffusion-reaction equation follows from (3.14) and (3.15):

$$\frac{\partial C}{\partial t} = R - \nabla \cdot (-D_c \nabla C) \tag{3.16}$$

where $\nabla \cdot = \operatorname{div}$, which becomes

$$\frac{\partial C}{\partial t} = R + D_c \nabla^2 C \tag{3.17}$$

if D_c is constant. The equation is a semilinear parabolic partial differential equation and requires appropriate initial and boundary conditions.

Another mode of particle transport, advection (transport of particles in a fluid by the fluid flow), was discussed in Section 2.1.1. Advective flux can be described by uC where u [length·time^{-1}] is the average flow velocity of the liquid. Let the flux J denote both diffusive and advective flux

$$J = -D_c \nabla C + uC \tag{3.18}$$

which, when substituted into (3.14), gives the general transport equation, also known as

the advection-diffusion-reaction equation

$$\frac{\partial C}{\partial t} = R + D_c \nabla^2 C - \nabla(uC). \tag{3.19}$$

The transport equation, or versions thereof, will be discussed in Section 3.2 as a suitable representation of biofilm development.

3.2 Biofilm models

3.2.1 Overview

Before the breakthrough of new tools like the confocal laser scanning microscope and the microelectrode measurements that enabled detailed observation, biofilms were roughly perceived as homogeneous layers of biomass that could grow by consuming a substrate delivered with the bulk liquid. Biofilm models are changing with advances in microbiology and with the increase in possible applications. Even within a given application there is an evolution of the model as we learn more about the biofilm system and its environment on a physical, chemical and biological level [53]. Still, there are several obstacles that need to be tackled, like the influence of macroscale physical factors on biofilm composition and structure. The main difficulty is to incorporate all processes of such a complex system, on a wide variety of time and length scales into an exhaustive and understandable model [113]. For example, despite the increasing knowledge about biofilms there is a lack of understanding of the crucial processes attachment and detachment of biomass, which govern much of the development of a biofilm. The complexity of these processes is rarely visible in the mathematical models where an ad hoc technique has been used in most models to describe detachment by a rate proportional to the square of the biofilm height.

The varying levels of biofilm description are also apparent in mathematical models which contain different levels of complexity. The most significant distinctions are made between one-dimensional (1D) and two- and three-dimensional models (2D/3D), dynamic and steady state models, and single species/substrate and multi-species/-substrate models. An increased modeling and process complexity implies an increased mathematical and numerical complexity which makes the choice of model a trade-off decision. Biofilm models in wastewater engineering were comprehensively compared in [114], where it was found that numerical 1D models describe the wastewater process well and are much easier to work with than 2D/3D models. The multi-dimensional models require numerical treatment and large computing power while the 1D models often allow for mathematical analysis. The focus of this thesis will be on the one-dimensional biofilm model, introduced in detail in the next section.

3.2.2 The one-dimensional Wanner-Gujer model

The seminal paper by Wanner and Gujer in 1986 [116], in which a one-dimensional multi-species continuum biofilm model was presented, was the continuation of several works published on this topic in the early 1980s [51, 92, 93, 115]. While the previous works had often made several simplifying assumptions, neglecting certain processes or describing the biomass or the substrates at a steady state, Wanner and Gujer used as few assumptions as possible and derived a dynamic multi-species biofilm model so general that it could easily be adapted to different situations, serving as an important mathematical tool in biofilm research. The model treats the biomass as a continuum and rests on the assumption that all changes in biomass and dissolved compounds occur in the direction perpendicular to the substratum. Furthermore, by observing mass conservation principles the formulated model describes the dynamics and spatial distribution of microbial species and substrates in the biofilm, predicts the evolution of the thickness of the biofilm and also allows for biomass detachment due to sloughing and shear stress.

Let $f_i(t,z)$ denote the volume fraction of species i, $i = 1,\dots,n_x$, at the time t and the distance z from the substratum, at which $z = 0$, and set up the microbial mass balance as

$$\frac{\partial f_i}{\partial t} = \left(\mu_{o,i} - \frac{\partial u}{\partial z}\right) f_i - u\frac{\partial f_i}{\partial z} = \mu_{o,i} f_i - \frac{\partial}{\partial z}\left(u f_i\right) \tag{3.20}$$

with initial conditions $f_i(0,z)$, where $\mu_{o,i}(t,z)$ is the observed specific growth rate for species i and $u(t,z)$ denotes the velocity at which the microbial mass moves perpendicular to the substratum. The flux $g_i(t,z)$ of microbial species i in the outward direction from the substratum can be expressed as $g_i(t,z) = u(t,z)\rho_i f_i(t,z)$, where ρ_i is the constant biomass density for species i. Using the assumption that the sum of the volume fractions of all species equals 1, i.e. $\sum f_i = 1$, and summing Equation (3.20) over all the n_x species it follows that

$$\frac{\partial u}{\partial z} = \bar{\mu}_o(t,z), \qquad \text{with } \bar{\mu}_o(t,z) = \sum_{i=1}^{n_x} \mu_{o,i}(t,z) f_i(t,z) \tag{3.21}$$

where $\bar{\mu}_o(t,z)$ denotes a mean observed specific growth rate of the biomass. From Equation (3.21) an expression for u can be obtained

$$u(t,z) = \int_0^z \bar{\mu}_o(t,s)\,ds \qquad \text{with } u(t,0) = 0 \tag{3.22}$$

with the velocity being equal for all species. The biofilm thickness $\lambda(t)$ changes at the biofilm-liquid interface at a velocity $u_\lambda(t) = \frac{d\lambda}{dt}$, which with the addition of a biomass

exchange term $\sigma(t)$ between the biofilm and the bulk liquid results in

$$u_\lambda(t) = u(t,\lambda) + \sigma(t) = \int_0^\lambda \bar{\mu}_o(t,s)ds + \sigma(t). \tag{3.23}$$

In a case study in [116] the function $\sigma(t)$ describes shear stress through the expression

$$\sigma(t) = -E\lambda(t)^2, \tag{3.24}$$

where E [length^{-1}·time^{-1}] is a constant. Equations (3.20) and (3.21) yield another form of the mass balance equation

$$\frac{\partial f_i(t,z)}{\partial t} = \big(\mu_{o,i}(t,z) - \bar{\mu}_o(t,z)\big) f_i(t,z) - u(t,z)\frac{\partial f_i(t,z)}{\partial z}, \quad i = 1,\dots,n_x - 1. \tag{3.25}$$

Analogously, the mass balance for the substrates is obtained

$$\frac{\partial S_k(t,z)}{\partial t} = \frac{\partial}{\partial z}\left(D_k \frac{\partial S_k(t,z)}{\partial z}\right) + r_k(t,z) \tag{3.26}$$

with initial conditions $S_k(0,z)$, for the substrate concentration $S_k(t,z)$ of compound k, $k = 1,\dots,n_s$, where D_k is the diffusion coefficient for substrate k and $r_k(t,z)$ the observed reaction rate. Equation (3.26), a diffusion-reaction equation, fits into the framework of Section 3.1.2 along with Equation (3.20), which is an advection-reaction equation. The boundary conditions at the substratum ($z = 0$) are no-flux conditions given by

$$\frac{df_i(t,0)}{dt} = \big(\mu_{o,i}(t,0) - \bar{\mu}_o(t,0)\big) f_i(t,0) \quad \text{and} \quad \frac{\partial S_k(t,0)}{\partial z} = 0 \tag{3.27}$$

and the boundary conditions at the biofilm-liquid interface ($z = \lambda$) are

$$\frac{\partial S_k(t,\lambda)}{\partial z} = \frac{D_{l,k}}{\lambda_l D_k}\big(S_{l,k}(t) - S_k(t,\lambda)\big) \quad \text{or} \quad S_k(t,\lambda) = S_{l,k}(t) \tag{3.28}$$

where the former includes mass transfer limitation and the latter neglects it. The thickness of the mass transfer boundary layer is denoted by λ_l, $D_{l,k}$ is the diffusion coefficient and $S_{l,k}$ is the substrate concentration of substrate k in the bulk liquid. The specific reaction rates r_k and the specific growth rates $\mu_{o,i}$ can be defined in any form, but are defined with Monod expressions in the case studies in the article [116].

The fully dynamic model allows for studies of relatively complex microbial interactions. A standard time scale argument, which recognizes the difference between the very fast diffusion process for the substrates and the relatively slow growth process of biomass, enables a separation of the processes and a pseudo-steady state approach. Thus, it is possible to work with one process at a time while the other process is considered to be at

a pseudo-steady state. This approach reduces the computational effort, but maintains accuracy. Investigation of the biomass volume fractions can reveal a heterogeneous layering within the biofilm with respect to the different species. Wanner and Gujer used a heterotrophic-autotrophic setting in wastewater treatment (where the species both compete for oxygen) and numerical simulations to demonstrate the abilities of their model.

Most applications use biofilm models in the context of numerical simulations. Only a few studies are known where biofilm models have been approached with analytical techniques. Existence and properties of solutions and of the corresponding steady-state solutions of a one-dimensional biofilm model have been addressed in [88, 107]. Further extensions to [107] with focus on persisters and antimicrobial treatment were presented and studied in [14, 108]. In analogy with the study in Paper I, the overall community productivity and system equilibria for a one-dimensional biofilm model was investigated in [52].

3.2.3 Biofilm models in wastewater applications

The state-of-the-art biofilm model in wastewater treatment was introduced in 1996 in [117], which was an extension of the Wanner and Gujer model from [116]. The continuum approach and the one-dimensionality of the previous model were maintained while new processes and more flexibility was added in order to account for new experimental findings. For example, porosity within the biofilm was included, allowing for liquid phase volume fractions between the biofilm's particulate components. Furthermore, the net result of biofilm cell movements within the biofilm was modeled by an effective diffusive flux. The model was developed for a wastewater application in which an aerobic heterotrophic-autotrophic biofilm in a completely mixed bulk liquid consumes organic matter and ammonium. The two species compete for space and oxygen and are governed by the processes growth, inactivation and respiration. Inert matter is formed through inactivation of active biofilm cells, constituting a third biofilm species.

Implementation of the model in AQUASIM [90] created a template for biofilm models in wastewater treatment, allowing for modifications in order to represent the specific systems at hand. It is an accessible and valuable tool for understanding biofilm processes and is, therefore, widely used in many different applications. The one-dimensional model has also been implemented in many other software packages, e.g. BioWin, GPS-X, Simba and STOAT, with a comprehensive overview in [7].

Mass transfer and utilization of substrate in an autotrophic biofilm system [45] as well as growth and decay in an autotrophic-heterotrophic biofilm [44] were investigated experimentally with the aim of verifying and improving the model of [117]. A different context was presented in [94] where the model was used to describe tolerance of biofilms with respect to antibiotics based on the mechanism of slow growth and nutrient limitation. The model was also successfully adapted to the wastewater application of nitrification and denitrification by biofilms growing on sand grains in a sand filter [120]. Others com-

bined removal of nitrate with removal of phosphorus in a biofilm reactor for enhanced biological phosphorus removal and investigated diffusion limitation [30]. A more complex system was presented in [5] where a mixed-culture biofilm containing autotrophic denitrifiers, sulfate reducing bacteria and heterotrophs performs oxidized nitrogen, sulfur and selenium removal.

Despite the wide applicability of different software packages there is a limitation on the dimensionality of the model. One of the main assumptions is that the biofilm is planar and one-dimensional, which does not suffice for describing a proper biofilm structure. To broaden the understanding of the structure-environment-activity relation it is necessary to use multi-dimensional models that describe spatial heterogeneity in multiple directions. Pure continuum models like [1] and [28], often extending the work of Wanner and Gujer, have been introduced along with other approaches like cellular automata [86] and individual based modeling [84]. While multidimensional models offer more complexity and detailed descriptions of the processes, particularly with respect to biofilm structure [87], they also require greater computational effort and a higher level of input and control from the user. Moreover, the use of multi-dimensional models is restricted to very small domains, much smaller than a lab or full scale reactor. The advantages and disadvantages of simple models will be further discussed in Section 3.2.4.

As biofilms in wastewater treatment are mostly used for nitrogen and phosphorus removal, these applications prevail among the biofilm models. Nitrification, i.e. conversion of ammonium to nitrate by autotrophic bacteria, is sometimes combined with organic matter removal (aerobically by heterotrophic bacteria), denitrification [118] (anoxic conversion of nitrate to nitrogen gas by heterotrophic bacteria) or with the anammox process [41] (anoxic conversion of ammonium and nitrite to nitrogen gas by anammox bacteria). Typically, nitrification is modeled either as a one-step or a two-step process. Wanner and Gujer in [116] used the former model in combination with presence of heterotrophic bacteria to account for removal of organic matter, see the stoichiometric matrix in Table 3.1. Substrates are denoted by S_k, volume fractions by f_i, biomass density by ρ_i, half-saturation Monod coefficient by K, endogenous respiration constant by b, inactivation constant by k, maximum specific growth rate by μ^{max} and biomass yield by Y. In their model the ammonium is not converted to anything, it is only consumed and thereby removed. For two-step nitrification, where ammonium is converted to nitrite and further to nitrate, the autotrophic part in Table 3.1 is divided into several processes for the two species AOB and NOB and two more substrates are introduced. An example is given in Table 3.2 from [10]. The included processes are growth, inactivation and aerobic and anoxic endogenous respiration for the biomass compounds AOB (X_{AOB}) and NOB (X_{NOB}) respectively for the involved dissolved compounds oxygen S_{O2}, ammonium S_{NH4}, nitrite S_{NO2} and nitrate S_{NO3}. The anoxic reduction factor for endogenous respiration is denoted by η and the production of inert matter X_I in endogenous respiration by f_{XI}. By extending nitrification into two steps the model complexity is increased and a more realistic description of the process is obtained. However, when nitrification is used as a

submodule in a larger model it may be desirable to maintain the one-step description in order to allow for more modules without complicating the model extensively.

It is already apparent that biofilm models contain many parameters and constants, whose number increases with increasing model complexity. In a relatively simple model described in Table 3.1 there are 16 parameters that need to be determined or chosen from literature. Many parameters are difficult or even impossible to determine through measurements in wastewater treatment plants or in laboratory experiments [68]. Furthermore, numerous parameters are specific to the environment they were measured in and depend strongly on temperature or pH. Usually the van't Hoff-Arrhenius equation is used to estimate temperature effects on biological reaction rates $\mu = \mu_{20}\vartheta^{T-20}$, where a reference rate μ_{20} measured at $T = 20°\text{C}$ and a dimensionless temperature coefficient ϑ are used to calculate the rate at a new temperature T [126].

Activated sludge modeling is more defined with regard to both model and parameter choice [68]. The activated sludge model No. 1 (ASM1, [43]) and its follow-ups ASM2 and ASM3 have become established reference points and serve as templates for new models. It is therefore reasonable that these models are used as submodules in Integrated Fixed-film Activated Sludge (IFAS) models, also known as hybrid models [61]. The combined activated sludge-biofilm technology emerged in the mid-1990s as an upgrade of an existing activated sludge reactor to enhance nitrogen and phosphorus removal [89]. Addition of fixed-film media to an activated sludge reactor circumvents reconstruction and extension of the reactor, which would otherwise have been required to overcome treatment problems of an insufficient reactor. The added media prolong the solids retention time in the reactor by allowing growth of biofilms which remain in the system without a significant load increase to the final clarifier. Moreover, it increases the amount of slow-growing nitrifying bacteria that provide year round nitrification. IFAS combines "the best of two worlds" and maintains both suspended biomass in the form of activated sludge and attached biomass as biofilms. Mathematical modeling of IFAS has followed the growth curve of experimental advances and a significant amount of work has been devoted to the engineers and practitioners [6]. Some models are used to evaluate stability and effectiveness of an IFAS upgrade [62]. The models are often largely complex as there are many processes taking place with numerous compounds involved.

There is a natural exchange of biomass between the biofilm and activated sludge, connecting the two forms of biomass aggregates. Already in [117] it was concluded that the simultaneously occurring processes attachment and detachment are very important in biofilm systems. Although often neglected in biofilm models, these processes are crucial in IFAS models. Due to the complexity of the processes, as discussed in Section 2.1.3, there is a lack of understanding of the interaction between suspended and attached biomass [48]. More research has been done in connection with detachment than attachment as the former has proven to be slightly easier to control and follow. It is also visible in the different mathematical expressions for detachment rates which range from simple first rate equations to involved expressions concerning hydrodynamics [8]. However, most often

Table 3.1: Stoichiometric matrix from [116].

	Biomass compound i			Substrate compound k			
Process j	1 (Het)	2 (Aut)	3 (Inert)	1 (Organics)	2 (Amm)	3 (Oxy)	Process rate P_j
Heterotrophic (H)							
1. Growth	$+1$	–	–	$-\frac{1}{Y_H}$	–	$-\frac{\alpha_H - Y_H}{Y_H}$	$\mu_H^{max}\rho_H f_H \frac{S_3}{K_{3H}+S_3}\frac{S_1}{K_1+S_1}$
2. Endogenous respiration	-1	–	–	–	–	-1	$b_H\rho_H f_H \frac{S_3}{K_{3H}+S_3}$
3. Inactivation	-1	–	$+1$	–	–	–	$k_H\rho_H f_H$
Autotrophic (A)							
4. Growth	–	$+1$	–	–	$-\frac{1}{Y_A}$	$-\frac{\alpha_A - Y_A}{Y_A}$	$\mu_A^{max}\rho_A f_A \frac{S_3}{K_{3A}+S_3}\frac{S_2}{K_2+S_2}$
5. Endogenous respiration	–	-1	–	–	–	-1	$b_A\rho_A f_A \frac{S_3}{K_{3A}+S_3}$
6. Inactivation	–	-1	$+1$	–	–	–	$k_A\rho_A f_A$
Observed growth and conversion rates		$\mu_{o,i} = \sum_j \frac{P_j \nu_{ij}}{f_i \rho_i}$			$r_k = \sum_j P_j \nu_{kj}$		

Table 3.2: Stoichiometric matrix from [10] with two-step nitrification.

	Biomass compound i			Substrate compound k				
Process j	X_{AOB}	X_{NOB}	X_I	S_{O2}	S_{NH4}	S_{NO2}	S_{NO3}	Process rate P_j
Ammonium oxidizing bacteria (AOB)								
1. Growth	$+1$	–	–	$-\frac{3.43-Y_{AOB}}{Y_{AOB}}$	$\frac{-1}{Y_{AOB}}$	$\frac{1}{Y_{AOB}}$	–	$\mu_{AOB}^{max} X_{AOB}\frac{S_{O2}}{K_{O2,A}+S_{O2}}\frac{S_{NH4}}{K_{NH4,A}+S_{NH4}}$
2. Aerobic endogenous respiration	-1	–	f_{XI}	$-(1-f_{XI})$	–	–	–	$b_{AOB} X_{AOB}\frac{S_{O2}}{K_{O2,A}+S_{O2}}$
3. Anoxic endogenous respiration	-1	–	f_{XI}	–	–	–	$-\frac{1-f_{XI}}{2.86}$	$\eta b_{AOB} X_{AOB}\frac{K_{O2,A}}{K_{O2,A}+S_{O2}}$
4. Inactivation	-1	–	$+1$	–	–	–	–	$k_{AOB} X_{AOB}$
Nitrite oxidizing bacteria (NOB)								
5. Growth	–	$+1$	–	$-\frac{1.14-Y_{NOB}}{Y_{NOB}}$	–	$\frac{-1}{Y_{NOB}}$	$\frac{1}{Y_{NOB}}$	$\mu_{NOB}^{max} X_{NOB}\frac{S_{O2}}{K_{O2,N}+S_{O2}}\frac{S_{NO2}}{K_{NO2,N}+S_{NO2}}$
6. Aerobic endogenous respiration	–	-1	f_{XI}	$-(1-f_{XI})$	–	–	–	$b_{NOB} X_{NOB}\frac{S_{O2}}{K_{O2,N}+S_{O2}}$
7. Anoxic endogenous respiration	–	-1	f_{XI}	–	–	–	$-\frac{1-f_{XI}}{2.86}$	$\eta b_{NOB} X_{NOB}\frac{K_{O2,N}}{K_{O2,N}+S_{O2}}$
8. Inactivation	–	-1	$+1$	–	–	–	–	$k_{NOB} X_{NOB}$

out of convenience the simple expression $\sigma = -E\lambda^2$ from Wanner and Gujer [116] is used. Attachment rate r_{at}, when included in models, is typically modeled proportionally to the biomass X, i.e. $r_{at} = k_{at}X$ for some constant k_{at}.

Keeping in mind the complexity of the attachment and detachment processes it is unsurprising that many pure biofilm models oversimplify these processes and generally neglect the influence of any suspended biomass [68]. Even in pure biofilm applications like the MBBR there is a significant accumulation of suspended biomass that requires a secondary clarifier, see Section 2.2.1. Although the amount of biomass is ten times less than in an activated sludge reactor, the biomass may still significantly contribute to reactor performance. These systems differ from the IFAS technologies in which suspended biomass is desired and purposefully cultured. In a biofilm system the suspended biomass emerges mainly through detachment from the biofilm and possibly through particulate influent.

There are few studies of biofilm models in the literature which include the role of suspended biomass. The most established and studied model of the interaction between suspended and attached biomass is the Freter model [3, 4, 34, 49, 103], where suspended and wall-attached bacteria compete for a nutrient. The wall-attached bacteria form a monolayer on the reactor wall, experiencing the same substrate and growth conditions as suspended biomass. A biofilm on the other hand can display significant heterogeneity, in particular with respect to diffusion concentration gradients, see Section 2.1.1, whereby the Freter model presents a too simplistic description of wall-attached bacterial growth. A similar model was introduced in [97] with mass balances for the substrates, suspended biomass and the biofilm including a detachment and attachment rate. However, based on the assumption that a very thin biofilm is formed, the model did not include the effects of diffusion within the biofilm. An extension of the model was presented in [78] where the substrate diffusion mechanism in the biofilm was incorporated. Both models were studied numerically, investigating steady state solutions and reactor performance.

A simple mathematical model is presented and analyzed mathematically and numerically in Paper I. The one-dimensional dynamic model describes the interaction of suspended biomass and biofilm in a continuous-flow biofilm reactor through detachment and attachment. Diffusion concentration gradients are experienced by the biofilm in a direction perpendicular to the substratum. The simplicity of the model allows for mathematical analysis of the trivial equilibrium while numerical simulations demonstrate the contributions of suspended biomass to reactor performance.

3.2.4 Advantages and disadvantages of simple models

The term simple model typically refers to a model that is one-dimensional in space and possibly relying on further assumptions regarding dynamics and substrate fluxes. More assumptions lead to a simpler model because less processes and phenomena need to be considered by the model. Fewer and/or lower-leveled assumptions logically lead to an

Table 3.3: Summary of differing features between analytical (A), pseudo-analytical (PA), 1D numerical (N1) and 2D/3D numerical (N2/N3) models. A minus sign (–) means that the feature cannot be simulated by the model, a plus sign (+) that it can be simulated and a circle (○) that it may be simulated with restrictions. Table reproduced from [114] with permission from IWA Publishing.

Feature	A	PA	N1	N2/N3
Development over time (dynamic)	–	–	+	+
Heterogeneous biofilm structure	–	–	○	+
Multiple substrates	○	○	+	+
Multiple microbial species	○	○	+	+
External mass transfer limitation	○	○	+	+
Hydrodynamics	–	–	–	+

increase in model complexity and capability. The four types of models used in [114] can be used to demonstrate the characteristics of the different models, summarized in Table 3.3. According to the study in [114], the analytical and pseudo-analytical models are able to simulate the least amount of features while the multi-dimensional models can simulate all of them. Some features may be simulated with certain restrictions, for example heterogeneity in biofilm structure can be obtained in the numerical one-dimensional model but only in one dimension. The Wanner-Gujer model from Section 3.2.2 is essentially N1, the one-dimensional numerical model.

Biofilm models emerged as simple one-dimensional descriptions and have evolved into complex multi-dimensional models as our understanding of the underlying biofilm processes has broadened [67]. The increased details of a multi-dimensional model allow us to capture all features of a biofilm system. However, at the same time they require large computing power and a high level of knowledge and understanding of modeling and numerical simulations, keeping a high threshold for model accessibility. On the other hand, the simple models are relatively easily implemented with a fast throughput to resulting simulations, sometimes even with a simple spreadsheet. Nonetheless, the simplifying assumptions decrease details in the model output and limit the applicability of the model.

Figure 3.2 is a schematic representation of the relationship between the different models (analytical, pseudo-analytical, 1D steady state numerical, 1D numerical dynamic and 2D/3D numerical dynamic) based on the mass balance equations for the biomass compounds. The arrow on the right hand side show an increase in amount of computations and in flexibility when going from simpler to more complex models. The left hand side arrow shows an increase in the amount of model assumptions when going from more complex to simpler models. The biofilm morphology is assumed to be flat and possibly

stratified in the models at the bottom of the figure. The 1D numerical dynamic model in the middle also assume a flat biofilm surface but allow development of biofilm thickness and a heterogeneous microbial distribution within the biofilm. Multi-dimensional models at the top of the figure include a heterogeneous biofilm surface.

Comparative studies of one- and multi-dimensional biofilm models have been performed in [67, 114, 123] with three benchmark problems (BM1-3) in [114]. In cases with heterogeneous biofilm structure the various models displayed significantly different results. A two-dimensional model was able to describe the heterogeneous structure which led to decreases in biofilm activity and an occurrence of sloughing events [123]; the one-dimensional models were unable to reproduce these local results. If global results are desired, such as reactor performance, both one- and multi-dimensional models produced largely the same results. Multi-species biofilms could also be represented by both types of models, particularly with respect to substrate concentrations and fluxes. However, microbial distributions varied considerably between the models. When the compared numerical simulations were calculated using a description of a flat biofilm the results were not significantly different. For a relatively smooth biofilm morphology there was a good agreement between the models. The difference was instead noticed in the efforts involved in producing the results [67]. Multi-dimensional models have higher requirements on input data, modifications of custom made software and ample computing resources. Numerical one-dimensional models were easily and quickly solved with available software packages. Hence, simple models like the analytical, pseudo-analytical or 1D numerical models provide a good results-to-effort-ratio and are often recommended for usage, specifically for practitioners.

From the viewpoint of the Wanner-Gujer model, additional assumptions can be made, which leads to more simplified models [93]. These models are often not dynamical and may use several approximations, but are easier to work with. On the other hand, by relaxing the assumptions more complex models are obtained [1, 28, 56, 85, 124]. Different modeling approaches are used, such as individual-based modeling, cellular automata and continuum models. Multi-dimensional, multi-species/-substrate models include many more details, but are exclusively numerical and require large computing power. Although multi-dimensional, complex models are much better at describing local biofilm development, they are unsuitable for large scale applications. In particular, these models are not aimed at reactor scale development in the context of wastewater engineering. The overall reactor system length and time scales are so much larger than the scales of detailed biofilm growth. The sophisticated, complex models are already computationally heavy and are, therefore, in practice not feasible for large scale purposes. Most often, the main interest of reactor models is the longterm behavior, in which case detailed biofilm description is not crucial and simpler biofilm models may be used instead.

Another advantage of simple models is their suitability for mathematical analysis. Biofilm models are often collections of several types of diffusion/reaction/transport equations and multi-dimensional models complicate things further. Available mathematical

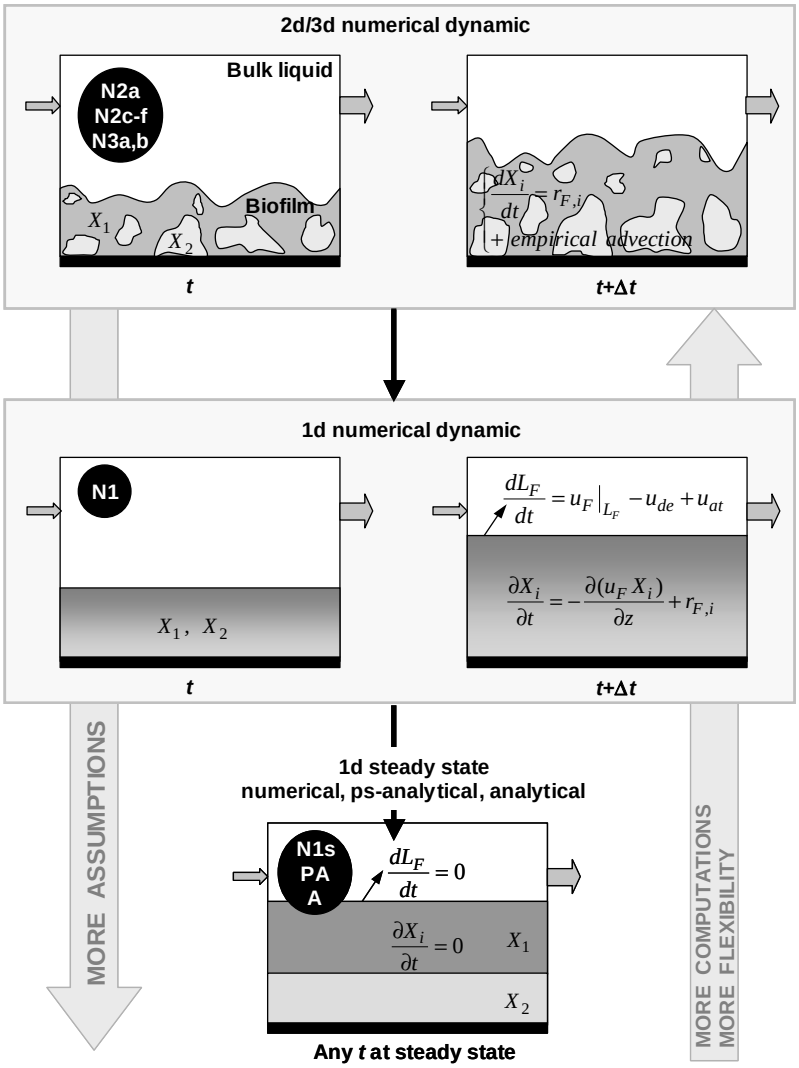

Figure 3.2: Relationship between different models with respect to mass balance equations for the biomass compounds X_i. Here, as in Table 3.3, (A) denotes the analytical, (PA) the pseudo-analytical, (N1) the 1D numerical and (N2/N3) the 2D/3D numerical model. Image used with permission from [114], courtesy of IWA Publishing.

tools can be applied to simple or even further simplified models, depending on the specific situation. Often, however, even very simple models are complex enough for reaching a limit with what is possible in mathematical analysis. There exist a few studies in which biofilms have been analyzed with mathematical tools. Steady state solutions of a single species single substrate biofilm model with a constant bulk substrate concentration were investigated in [88]. Detachment effects were not included in the model. It was shown that the existence and stability of steady state solutions depend on biomass decay rate, maximum growth rate and bulk substrate concentration. In [107] detachment was included and global existence and properties of solutions were shown. The steady state case was studied and existence and uniqueness of solutions were proven along with establishment of sufficient conditions for existence. The Freter model, describing the interaction between suspended and wall-attached bacteria, was analyzed in [49] where it was found that the trivial equilibrium (i.e. complete washout of all biomass) always exists. The stability thereof depends on the growth and decay rates of the wall-attached and suspended biomass along with the dilution rate in the continuous-flow reactor. Moreover, it was shown that a non-trivial equilibrium exists, but the model complexity prevented further analysis.

The contribution of this thesis is to develop and study a mathematical model of a biofilm reactor with suspended growth. The main application of the models used in this thesis is a (at times idealized) reactor in wastewater treatment. To this end, a simple, one-dimensional biofilm model has been used to describe the biofilm contribution to the reactor performance. Particular attention has been given to suspended biomass, which is mostly neglected in biofilm models.

Even though the term "simple" typically indicates a lack of complexity, the underlying mathematical expressions are indeed rather complicated. The model presented in Paper I, with growth of biofilm and suspended biomass in a CSTR, is a hybrid model consisting of chemostat-like mass balances for the substrate and biomass in the reactor, coupled with a free boundary value problem for the substrate in the biofilm. The model could formally be rewritten as a system of ordinary differential equations to which standard analytical techniques could be applied. It was shown that the stability conditions for the trivial equilibrium depend on the dilution rate and on the growth and decay rates of the biofilm and the suspended biomass. In comparison with the less complex Freter model it was found that the main existence and stability results carry over. In the case of an unstable washout equilibrium the system attains a non-trivial steady state at which biomass will exist in both forms. Numerical simulations showed that biofilm dominates over suspended biomass in longterm reactor behavior, but that suspended biomass is relatively more efficient at substrate consumption.

The results from the analytical and numerical analyses in Paper I raise two follow-up questions: (i) What happens if the substrate and treatment time are limited? (ii) What if the model is more biologically complex, to better represent a nitrification reactor? The first question leads to an optimal control problem in Paper IV in which a biological treat-

ment reactor is available for a limited amount of substrate stored in a buffer tank during a limited amount of time. The aim of the optimal control problem is to increase substrate removal efficiency and reduce process duration while controlling the flow between the buffer tank and the treatment reactor. A single species single substrate system is used in which biofilm and suspended biomass are present. The second question leads to an extension of the model in Paper III, where a multi-substrate multi-species nitrification model is presented. Ammonium oxidizing bacteria convert ammonium to nitrite, which is in turn converted to nitrate by nitrite oxidizing bacteria. The continuous-flow stirred tank reactor is constantly oxygenated in order to supply oxygen to the aerobic reactions. The extended model requires a larger amount of parameters, why an experimental and numerical study was performed in Paper II to validate the choice of parameters. The underlying model is a hybrid model consisting of a chemostat-like ordinary differential equation model for the substrates and the suspended biomass in the reactor, coupled with a mixed hyperbolic-parabolic free boundary value problem for the biofilm. Numerical simulations of the extended model served as a basis for the analysis.

Chapter 4

Conclusions and outlook

The main objective of the work presented in this thesis was to investigate the role of suspended biomass in biofilm reactor models. Traditional biofilm models neglect the contribution of suspended biomass to substrate conversion. On the other hand, in models of the IFAS process it needs to be included as a full activated sludge model. The model formulated in this thesis falls between these two extremes.

The model presented in Paper I is a one-dimensional biofilm reactor model of Wanner-Gujer type, based on the Freter model for wall attached bacterial growth, with a natural exchange of biomass through attachment and detachment between the biofilm and the suspended biomass. In a simple single species single substrate setting, but with a proper diffusion-reaction equation for the substrate in the biofilm, the model was already more complex than the Freter model. The analysis in Paper I showed, however, that the qualitative results for the Freter model largely carry over. Bacteria will either be washed out or coexist as biofilms and suspended biomass. Furthermore, numerical simulations showed that suspended biomass was relatively more efficient at substrate removal than biofilms, even if the main contribution to removal came from the biofilm. It was found in studies of longterm behavior that the amount of suspended biomass, relative to biofilm, depends on the dilution rate. A computational study of an extended model for the considerably more complex multi-species multi-substrate nitrification setting in Paper III revealed that the incorporation of suspended biomass is significant for detailed descriptions of the processes and products in the intermediate steps of nitrification. Nevertheless, suspended biomass did not affect the overall reactor performance results and probably need not be considered if such results are the sole objective. Preparation and validation of the nitrification biofilm model (without suspended biomass) by comparison with microelectrode measurements of oxygen profiles across the biofilm was performed in Paper II. A correspondence between the bulk flow velocity and the thickness of the biofilm and of the mass transfer boundary layer was shown in that study, along with a dependence of the erosion

parameter on the bulk flow velocity. The amount of wastewater to be treated is not always "infinite" and some situations require only a certain amount of wastewater to be treated in finite time. The optimization problem presented in Paper IV addressed this situation, where the control was the flow regime between a storage tank holding the water to be treated and a treatment reactor. It was found in that study that the potential for reactor improvement by varying the system flow rate is relatively modest. The improvement is primarily due to an initial transient phase during which the bacteria in the reactor adjust to the environmental conditions. Since the initial conditions in the reactor are usually not known, the implementation of such a control is also impractical.

Simple mathematical models are considered to be a valuable tool in biofilm process research. They provide the opportunity for quantitative and/or qualitative analysis while remaining informative on the overall reactor performance level. The mathematical analysis builds a foundation and a framework within which further modifications and developments can be made. The models presented in this thesis emphasize the significance of suspended biomass in biofilm models. Its effects are generally not visible on a large-scale reactor level, but may be important on a more detailed level such as the intermediate steps in a nitrification reactor. The non-trivial equilibrium is attained when the washout equilibrium is unstable and the two biomass forms will coexist (at some ratio). Many interesting applications may be (re-)evaluated with suspended biomass in mind.

The modeling community would benefit from further analytical progress in biofilm modeling and more attention should be given to that. Mathematical tools can be used to solidify existing or derive new models, but perhaps mostly to analyze and explain their behavior. There is much to learn from mathematical analysis, which is, however, rarely a straightforward task, even for relatively simple models.

The two core issues in biofilm models with suspended growth are the interaction between the biofilm and the suspended biomass, and the characterization of suspended biomass. Interaction is described by attachment and detachment processes, in this thesis expressed as simple functions of the suspended biomass density and biofilm thickness. These processes are poorly understood in general and in biofilm reactors in particular. Many researchers use certain expressions out of convenience, but it would be helpful to have guidelines, which expressions work best for different types of reactors. In this thesis, suspended biomass has in essence been described as detached biofilms, even by using the same parameters as for biofilms in the numerical simulations. There is a lack of experimental work that deals with suspended biomass in biofilm reactors. Such work would be crucial for mathematical modeling and for understanding the role of suspended biomass in biofilm reactors. Regardless of the possible conclusions, there would be many things to learn along the way.

In Paper II, the reactor flow rate was quantitatively correlated with the biomass erosion coefficient and the mass transfer boundary layer thickness. It would be important to investigate whether such results can be found for other reactor types, and if so, whether there is a resemblance of correlations across various reactor types.

A natural extension of the current work would be to consider a plug flow or horizontal flow biofilm reactor instead of a CSTR. For single species models some work has been done in the context of the Freter model, but not considering a biofilm model to describe wall attached bacteria. Such a setup could also allow for a mathematical investigation into the role of bacterial cell yield and biofilm dispersal as a method for downstream colonization and biofilm proliferation. Mathematically, this would require an extension to partial differential equations and therefore induce an additional level of complexity.

Although the optimization study presented in Paper IV led to the conclusion that the controlled reactor was only modestly better than the uncontrolled reactor, the approach with optimal control problems might still be interesting for biofilm models, probably in the context of other reactor types. Solving an optimal control problem can assist the progress of understanding the principal features of the model. There is more to be done in regard to the optimization problem in Paper IV, where a more general solution could be sought both analytically and numerically. The relatively simple model is still very complex, using some non-standard expressions, which makes it difficult to solve. Looking into methods from the field of automatic control could perhaps be fruitful. Moreover, it would be interesting to investigate the optimal control problem for the multi-species multi-substrate model from Paper III and compare with the results obtained in Paper IV. Would the added microbial complexity lead to qualitatively different or perhaps very similar results, in particular with respect to the off-on functions? Process optimization is not unusual in wastewater engineering and an optimal control study of biofilm reactor models would perhaps bring some new features to light. In addition, control problems for other types of biofilm reactors could be studied.

Bibliography

[1] E. Alpkvist and I. Klapper. A multidimensional multispecies continuum model for heterogeneous biofilm development. *Bull. Math. Biol.*, 69(2):765–789, 2007.

[2] R.I. Amann, W. Ludwig, and K.H. Schleifer. Phylogenetic identification and in situ detection of individual microbial cells without cultivation. *Microbiol. Mol. Biol. Rev.*, 59(1):143–169, 1995.

[3] M.M. Ballyk, D.A. Jones, and H.L. Smith. Microbial competition in reactors with wall attachment: A mathematical comparison of chemostat and plug flow models. *Microb. Ecol.*, 41(3):210–221, 2001.

[4] M.M. Ballyk, D.A. Jones, and H.L. Smith. The biofilm model of Freter: A review. In P. Magal and S. Ruan, editors, *Structured population models in biology and epidemiology*, volume 1936 of *Springer lecture notes in mathematics*, pages 265–302. Springer, Berlin, 2008.

[5] J.P. Boltz, D. Brockmann, T. Sandy, B.R. Johnson, G.T. Daigger, K. Jenkins, and K. Munirathinam. Framework for a mixed-culture biofilm model to describe oxidized nitrogen, sulfur, and selenium removal in a biofilm reactor. In *Proceedings of the Water Environment Federation, WEFTEC 2011: Session 1 through Session 10*, pages 145–156, 2011.

[6] J.P. Boltz, B.R. Johnson, G.T. Daigger, and J. Sandino. Modeling integrated fixed-film activated sludge and moving-bed biofilm reactor systems I: Mathematical treatment and model development. *Water Environ. Res.*, 81(6):555–575, 2009.

[7] J.P. Boltz, E. Morgenroth, D. Brockmann, C. Bott, W.J. Gellner, and P.A. Vanrolleghem. Critical components of biofilm models for engineering practice. In *Proceedings of the Water Environment Federation, WEFTEC 2010: Session 21 through Session 30*, pages 1072–1098, 2010.

[8] J.P. Boltz, E. Morgenroth, and D. Sen. Mathematical modelling of biofilms and biofilm reactors for engineering design. *Water Sci. Technol.*, 62(8):1821–1836, 2010.

[9] M.G. Brading, J. Jass, and H.M. Lappin-Scott. Dynamics of bacterial biofilm formation. In H.M. Lappin-Scott and J.W. Costerton, editors, *Microbial biofilms*, pages 46–63. Cambridge University Press, Cambridge, United Kingdom, 1995.

[10] D. Brockmann, K.-H. Rosenwinkel, and E. Morgenroth. Practical identifiability of biokinetic parameters of a model describing two-step nitrification in biofilms. *Biotechnol. Bioeng.*, 101(3):497–514, 2008.

[11] J.D. Bryers. Biofilms and the technological implications of microbial cell adhesion. *Colloids Surf., B*, 2(1-3):9–23, 1994.

[12] A. Cébron and J. Garnier. *Nitrobacter* and *Nitrospira* genera as representatives of nitrite-oxidizing bacteria: Detection, quantification and growth along the lower Seine River (France). *Water Res.*, 39(20):4979–4992, 2005.

[13] S. Chen, J. Ling, and J.-P. Blancheton. Nitrification kinetics of biofilm as affected by water quality factors. *Aquacult. Eng.*, 34(3):179–197, 2006.

[14] N. Cogan, B. Szomolay, and M. Dindos. Effect of periodic disinfection on persisters in a one-dimensional biofilm model. *Bull. Math. Biol.*, 75(1):94–123, 2013.

[15] D.L. Correll. The role of phosphorus in the eutrophication of receiving waters: A review. *J. Environ. Qual.*, 27(2):261–266, 1998.

[16] J.W. Costerton. Overview of microbial biofilms. *J. Ind. Microbiol.*, 15(3):137–140, 1995.

[17] J.W. Costerton and H.M. Lappin-Scott. Introduction to microbial biofilms. In H.M. Lappin-Scott and J.W. Costerton, editors, *Microbial biofilms*, pages 1–11. Cambridge University Press, Cambridge, United Kingdom, 1995.

[18] J.W. Costerton, Z. Lewandowski, D.E. Caldwell, D.R. Korber, and H.M. Lappin-Scott. Microbial biofilms. *Annu. Rev. Microbiol.*, 49:711–745, 1995.

[19] J.W. Costerton, P.S. Stewart, and E.P. Greenberg. Bacterial biofilms: a common cause of persistent infections. *Science*, 284(5418):1318–1322, 1999.

[20] M.E. Davey and G.A. O'Toole. Microbial biofilms: from ecology to molecular genetics. *Microbiol. Mol. Biol. Rev.*, 64(4):847–867, 2000.

[21] D.G. Davies. Biofilm dispersion. In H.-C. Flemming, J. Wingender, and U. Szewzyk, editors, *Biofilm highlights*, volume 5 of *Springer series on biofilms*, pages 1–28. Springer, Berlin, 2011.

[22] D. de Beer and A. Schramm. Micro-environments and mass transfer phenomena in biofilms studied with microsensors. *Water Sci. Technol.*, 39(7):173–178, 1999.

[23] D. de Beer, P. Stoodley, F. Roe, and Z. Lewandowski. Effects of biofilm structures on oxygen distribution and mass transport. *Biotechnol. Bioeng.*, 43(11):1131–1138, 1994.

[24] W.M. Deen. *Analysis of transport phenomena*. Topics in Chemical Engineering. Oxford University Press, USA, 1998.

[25] R.M. Donlan. Biofilm formation: a clinically relevant microbiological process. *Clin. Infect. Dis.*, 33(8):1387–1392, 2001.

[26] R.M. Donlan. Biofilms: microbial life on surfaces. *Emerg. Infect. Dis.*, 8(9):881–890, 2002.

[27] W.M. Dunne. Bacterial adhesion: Seen any good biofilms lately? *Clin. Microbiol. Rev.*, 15(2):155–166, 2002.

[28] H.J. Eberl, D.F. Parker, and M.C.M. van Loosdrecht. A new deterministic spatio-temporal continuum model for biofilm development. *J. Theor. Med.*, 3(3):161–175, 2001.

[29] L. Edelstein-Keshet. *Mathematical models in biology*. Classics in Applied Mathematics. Society for Industrial and Applied Mathematics, Philadelphia, USA, 2005.

[30] C.M. Falkentoft, P. Arnz, M. Henze, H. Mosbæk, E. Müller, P.A. Wilderer, and P. Harremoës. Possible complication regarding phosphorus removal with a continuous flow biofilm system: Diffusion limitation. *Biotechnol. Bioeng.*, 76(1):77–85, 2001.

[31] H. Fgaier and H.J. Eberl. A competition model between *Pseudomonas fluorescens* and pathogens via iron chelation. *J. Theor. Biol.*, 263(4):566–578, 2010.

[32] H.-C. Flemming. Biofouling in water systems - cases, causes and countermeasures. *Appl. Microbiol. Biotechnol.*, 59(6):629–640, 2002.

[33] H.-C. Flemming, T.R. Neu, and D.J. Wozniak. The EPS matrix: The "house of biofilm cells". *J. Bacteriol.*, 189(22):7945–7947, 2007.

[34] R. Freter, H. Brickner, J. Fekete, M. Vickerman, and K. Carey. Survival and implantation of *Escherichia coli* in the intestinal tract. *Infect. Immun.*, 39(2):686–703, 1983.

[35] H. Furumai and B.E. Rittmann. Evaluation of multiple-species biofilm and floc processes using a simplified aggregate model. *Water Sci. Technol.*, 29(10-11):439–446, 1994.

[36] A. Gjaltema, J.L. Vinke, M.C.M. van Loosdrecht, and J.J. Heijnen. Biofilm abrasion by particle collisions in airlift reactors. *Water Sci. Technol.*, 36(1):221–228, 1997.

[37] C. Goode. *Understanding biosolids dynamics in a moving bed biofilm reactor*. PhD thesis, University of Toronto, Canada, 2010.

[38] G. Gottschalk. *Bacterial metabolism*. Springer-Verlag, New York, second edition, 1986.

[39] C. Grunditz and G. Dalhammar. Development of nitrification inhibition assays using pure cultures of *Nitrosomonas* and *Nitrobacter*. *Water Res.*, 35(2):433–440, 2001.

[40] L. Hall-Stoodley, J.W. Costerton, and P. Stoodley. Bacterial biofilms: from the natural environment to infectious diseases. *Nat. Rev. Microbiol.*, 2(2):95–108, 2004.

[41] X. Hao, J.J. Heijnen, and M.C.M. van Loosdrecht. Model-based evaluation of temperature and inflow variations on a partial nitrification – ANAMMOX biofilm process. *Water Res.*, 36(19):4839–4849, 2002.

[42] C. Hellinga, A.A.J.C. Schellen, J.W. Mulder, M.C.M. van Loosdrecht, and J.J. Heijnen. The SHARON process: An innovative method for nitrogen removal from ammonium-rich waste water. *Water Sci. Technol.*, 37(9):135–142, 1998.

[43] M. Henze, C.P.L. Grady, W. Gujer, G.v.R. Marais, and T. Matsuo. *Activated Sludge Model No. 1*. Number 1 in IAWPRC Scientific and Technical Reports. IAWQ London, 1987.

[44] H. Horn and D.C. Hempel. Growth and decay in an auto-/heterotrophic biofilm. *Water Res.*, 31(9):2243–2252, 1997.

[45] H. Horn and D.C. Hempel. Substrate utilization and mass transfer in an autotrophic biofilm system: Experimental results and numerical simulation. *Biotechnol. Bioeng.*, 53(4):363–371, 1997.

[46] S.A. Huws, A.J. McBain, and P. Gilbert. Protozoan grazing and its impact upon population dynamics in biofilm communities. *J. Appl. Microbiol.*, 98(1):238–244, 2005.

[47] I. Ivanovic and T.O. Leiknes. Particle separation in Moving Bed Biofilm Reactor: Applications and opportunities. *Separ. Sci. Technol.*, 47(5):647–653, 2012.

[48] D. Jenkins. From total suspended solids to molecular biology tools – a personal view of biological wastewater treatment process population dynamics. *Water Environ. Res.*, 80(8):677–687, 2008.

[49] D. Jones, H.V. Kojouharov, D. Le, and H. Smith. The Freter model: A simple model of biofilm formation. *J. Math. Biol.*, 47(2):137–152, 2003.

[50] J.B. Kaplan. Biofilm dispersal: mechanisms, clinical implications, and potential therapeutic uses. *J. Dent. Res.*, 89(3):205–218, 2010.

[51] J.C. Kissel, P.L. McCarty, and R.L. Street. Numerical simulation of mixed-culture biofilm. *J. Environ. Eng.*, 110(2):393–411, 1984.

[52] I. Klapper. Productivity and equilibrium in simple biofilm models. *Bull. Math. Biol.*, 74(12):2917–2934, 2012.

[53] I. Klapper and J. Dockery. Mathematical description of microbial biofilms. *SIAM Rev.*, 52(2):221–265, 2010.

[54] T. Koshy. *Fibonacci and Lucas numbers with applications*. Pure and Applied Mathematics: A Wiley Series of Texts, Monographs and Tracts. John Wiley & Sons, New York, USA, 2011.

[55] G.A. Kowalchuk and J.R. Stephen. Ammonia-oxidizing bacteria: A model for molecular microbial ecology. *Annu. Rev. Microbiol.*, 55:485–529, 2001.

[56] J.-U. Kreft, C. Picioreanu, J.W.T. Wimpenny, and M.C.M. van Loosdrecht. Individual-based modelling of biofilms. *Microbiol.*, 147(11):2897–2912, 2001.

[57] C.G. Kumar and S.K. Anand. Significance of microbial biofilms in food industry: a review. *Int. J. Food Microbiol.*, 42(1-2):9–27, 1998.

[58] Z. Lewandowski and H. Beyenal. Mechanisms of microbially influenced corrosion. In H.-C. Flemming, P.S. Murthy, R. Venkatesan, and K. Cooksey, editors, *Marine and industrial biofouling*, Springer Series on Biofilms, pages 35–64. Springer Verlag, Berlin, 2009.

[59] Y.-M. Lin, J.-H. Tay, Y. Liu, and Y.-T. Hung. Biological nitrification and denitrification processes. In L.K. Wang, N.C. Pereira, and Y.-T. Hung, editors, *Biological treatment processes*, volume 8 of *Handbook of environmental engineering*, pages 539–588. Humana Press, Totowa, NJ, USA, 2009.

[60] Y. Liu and J.-H. Tay. Detachment forces and their influence on the structure and metabolic behaviour of biofilms. *World J. Microbiol. Biotechnol.*, 17(2):111–117, 2001.

[61] G. Mannina, D. Di Trapani, G. Viviani, and H. Ødegaard. Modelling and dynamic simulation of hybrid moving bed biofilm reactors: Model concepts and application to a pilot plant. *Biochem. Eng. J.*, 56(1–2):23–36, 2011.

[62] G. Mannina and G. Viviani. Hybrid moving bed biofilm reactors: An effective solution for upgrading a large wastewater treatment plant. *Water Sci. Technol*, 60(5):1103–1116, 2009.

[63] B. Manz, F. Volke, D. Goll, and H. Horn. Investigation of biofilm structure, flow patterns and detachment with magnetic resonance imaging. *Water Sci. Technol.*, 52(7):1–6, 2005.

[64] P.D. Marsh. Dental plaque as a biofilm and a microbial community - implications for health and disease. *BMC Oral Health*, 6(Suppl 1):S14, 2006.

[65] J. Monod. The growth of bacterial cultures. *Annu. Rev. Microbiol.*, 3:371–394, 1949.

[66] E. Morgenroth. Biofilm reactors. In M. Henze, M. van Loosdrecht, G. Ekama, and D. Brdjanovic, editors, *Biological wastewater treatment: Principles, modelling and design*, pages 493–511. IWA Publishing, London, UK, 2008.

[67] E. Morgenroth, H.J. Eberl, M.C.M. van Loosdrecht, D.R. Noguera, G.E. Pizarro, C. Picioreanu, B.E. Rittmann, A.O. Schwarz, and O. Wanner. Comparing biofilm models for a single species biofilm system. *Water Sci. Technol.*, 49(11–12):145–154, 2004.

[68] E. Morgenroth, M.C.M. van Loosdrecht, and O. Wanner. Biofilm models for the practitioner. *Water Sci. Technol.*, 41(4–5):509–512, 2000.

[69] E. Morgenroth and P.A. Wilderer. Influence of detachment mechanisms on competition in biofilms. *Water Res.*, 34(2):417–426, 2000.

[70] J.D. Murray. *Mathematical biology I: An introduction*. Interdisciplinary applied mathematics. Springer, New York, third edition, 2002.

[71] C.D. Nadell, J.B. Xavier, and K.R. Foster. The sociobiology of biofilms. *FEMS Microbiol. Rev.*, 33(1):206–224, 2009.

[72] C. Nicolella, M.C.M. van Loosdrecht, and J.J. Heijnen. Wastewater treatment with particulate biofilm reactors. *J. Biotechnol.*, 80(1):1–33, 2000.

[73] J.-C. Ochoa, C. Coufort, R. Escudié, A. Liné, and E. Paul. Influence of non-uniform distribution of shear stress on aerobic biofilms. *Chem. Eng. Sci.*, 62(14):3672–3684, 2007.

[74] H. Ødegaard. Innovations in wastewater treatment: the moving bed biofilm process. *Water Sci. Technol.*, 53(9):17–33, 2006.

[75] H. Ødegaard, M. Cimbritz, M. Christensson, and C.P. Dahl. Separation of biomass from moving bed biofilm reactors (MBBRs). In *Proceedings of the Water Environment Federation, Biofilms*, pages 212–233, 2010.

[76] H. Ødegaard, U. Mende, E. Olsen Skjerping, S. Simonsen, R. Strube, and E. Bundgaard. Compact tertiary treatment based on the combination of MBBR and contained hollow fibre UF-membranes. *Desalin. Water Treat.*, 42(1–3):80–86, 2012.

[77] S. Okabe, H. Satoh, and Y. Watanabe. In situ analysis of nitrifying biofilms as determined by in situ hybridization and the use of microelectrodes. *Appl. Environ. Microbiol.*, 65(7):3182–3191, 1999.

[78] G. Olivieri, M.E. Russo, A. Marzocchella, and P. Salatino. Modeling of an aerobic biofilm reactor with double-limiting substrate kinetics: Bifurcational and dynamical analysis. *Biotechnol. Prog.*, 27(6):1599–1613, 2011.

[79] J. Palmer, S. Flint, and J. Brooks. Bacterial cell attachment, the beginning of a biofilm. *J. Ind. Microbiol. Biotechnol.*, 34(9):577–588, 2007.

[80] J.D. Parry. Protozoan grazing of freshwater biofilms. *Adv. Appl. Microbiol.*, 54:167–196, 2004.

[81] M.R. Parsek and E.P. Greenberg. Sociomicrobiology: the connections between quorum sensing and biofilms. *Trends Microbiol.*, 13(1):27–33, 2005.

[82] D. Paul, G. Pandey, J. Pandey, and R.K. Jain. Accessing microbial diversity for bioremediation and environmental restoration. *Trends Biotechnol.*, 23(3):135–142, 2005.

[83] Y. Peng and G. Zhu. Biological nitrogen removal with nitrification and denitrification via nitrite pathway. *Appl. Microbiol. Biotechnol.*, 73(1):15–26, 2006.

[84] C. Picioreanu, J.-U. Kreft, and M.C.M. van Loosdrecht. Particle-based multidimensional multispecies biofilm model. *Appl. Environ. Microbiol.*, 70(5):3024–3040, 2004.

[85] C. Picioreanu, M.C.M. van Loosdrecht, and J.J. Heijnen. Mathematical modeling of biofilm structure with a hybrid differential-discrete cellular automaton approach. *Biotechnol. Bioeng.*, 58(1):101–116, 1998.

[86] C. Picioreanu, M.C.M. van Loosdrecht, and J.J. Heijnen. A new combined differential-discrete cellular automaton approach for biofilm modeling: Application for growth in gel beads. *Biotechnol. Bioeng.*, 57(6):718–731, 1998.

[87] C. Picioreanu, J.B. Xavier, and M.C.M. van Loosdrecht. Advances in mathematical modeling of biofilm structure. *Biofilms*, 1(4):337–349, 2004.

[88] L.A. Pritchett and J.D. Dockery. Steady state solutions of a one-dimensional biofilm model. *Math. Comput. Model.*, 33(1–3):255–263, 2001.

[89] C.W. Randall and D. Sen. Full-scale evaluation of an integrated fixed-film activated sludge (IFAS) process for enhanced nitrogen removal. *Water Sci. Technol.*, 33(12):155–162, 1996.

[90] P. Reichert. AQUASIM - A tool for simulation and data analysis of aquatic systems. *Water Sci. Technol.*, 30(2):21–30, 1994.

[91] R. Riffat. *Fundamentals of wastewater treatment and engineering*. CRC Press / IWA Publishing, 2012.

[92] B.E. Rittmann. The effect of shear stress on biofilm loss rate. *Biotechnol. Bioeng.*, 24(2):501–506, 1982.

[93] B.E. Rittmann and P.L. McCarty. Model of steady-state-biofilm kinetics. *Biotechnol. Bioeng.*, 22(11):2343–2357, 1980.

[94] M.E. Roberts and P.S. Stewart. Modeling antibiotic tolerance in biofilms by accounting for nutrient limitation. *Antimicrob. Agents Chemother.*, 48(1):48–52, 2004.

[95] M. Rodgers and X.-M. Zhan. Moving-medium biofilm reactors. *Rev. Environ. Sci. Biotechnol.*, 2(2-4):213–224, 2003.

[96] B. Rosche, X.Z. Li, B. Hauer, A. Schmid, and K. Buehler. Microbial biofilms: a concept for industrial catalysis? *Trends Biotechnol.*, 27(11):636–643, 2009.

[97] M.E. Russo, P.L. Maffettone, A. Marzocchella, and P. Salatino. Bifurcational and dynamical analysis of a continuous biofilm reactor. *J. Biotechnol.*, 135(3):295–303, 2008.

[98] K. Sauer, M.C. Cullen, A.H. Rickard, L.A.H. Zeef, D.G. Davies, and P. Gilbert. Characterization of nutrient-induced dispersion in *Pseudomonas aeruginosa* PAO1 biofilm. *J. Bacteriol.*, 186(21):7312–7326, 2004.

[99] R.P. Schneider. Conditioning film-induced modification of substratum physicochemistry – analysis by contact angles. *J. Colloid Interface Sci.*, 182:204–213, 1996.

[100] A. Schramm, L.H. Larsen, N.P. Revsbech, N.B. Ramsing, R. Amann, and K.H. Schleifer. Structure and function of a nitrifying biofilm as determined by in situ hybridization and the use of microelectrodes. *Appl. Environ. Microbiol.*, 62(12):4641–4647, 1996.

[101] B. Sharma and R.C. Ahlert. Nitrification and nitrogen removal (in waste water treatment). *Water Res.*, 11(10):897–925, 1977.

[102] H.L. Smith and P. Waltman. *The theory of the chemostat: Dynamics of microbial competition*. Cambridge University Press, Cambridge, UK, 1995.

[103] E.D. Stemmons and H.L. Smith. Competition in a chemostat with wall attachment. *SIAM J. Appl. Math.*, 61(2):567–595, 2000.

[104] P.S. Stewart. Diffusion in biofilms. *J. Bacteriol.*, 185(5):1485–1491, 2003.

[105] P.S. Stewart and M.J. Franklin. Physiological heterogeneity in biofilms. *Nat. Rev. Microbiol.*, 6(3):199–210, 2008.

[106] P. Stoodley, K. Sauer, D.G. Davies, and J.W. Costerton. Biofilms as complex differentiated communities. *Annu. Rev. Microbiol.*, 56:187–209, 2002.

[107] B. Szomolay. Analysis of a moving boundary value problem arising in biofilm modelling. *Math. Methods Appl. Sci.*, 31(15):1835–1859, 2008.

[108] B. Szomolay, I. Klapper, and M. Dindos. Analysis of adaptive response to dosing protocols for biofilm control. *SIAM J. Appl. Math.*, 70(8):3175–3202, 2010.

[109] U. Telgmann, H. Horn, and E. Morgenroth. Influence of growth history on sloughing and erosion from biofilms. *Water Res.*, 38(17):3671–3684, 2004.

[110] T. Tolker-Nielsen, U.C. Brinch, P.C. Ragas, J.B. Andersen, C.S. Jacobsen, and S. Molin. Development and dynamics of *Pseudomonas* sp. biofilms. *J. Bacteriol.*, 182(22):6482–6489, 2000.

[111] M. von Sperling. *Activated sludge and aerobic biofilm reactors*, volume 5 of *Biological wastewater treatment series*. IWA Publishing, London, UK, 2007.

[112] M. Wagner, B. Manz, F. Volke, T.R. Neu, and H. Horn. Online assessment of biofilm development, sloughing and forced detachment in tube reactor by means of magnetic resonance microscopy. *Biotechnol. Bioeng.*, 107(1):172–181, 2010.

[113] Q. Wang and T. Zhang. Review of mathematical models for biofilms. *Solid State Commun.*, 150(21–22):1009–1022, 2010.

[114] O. Wanner, H. Eberl, E. Morgenroth, D.R. Noguera, C. Picioreanu, B. Rittmann, and M. van Loosdrecht. *Mathematical modeling of biofilms*. Number 18 in Scientific and Technical Report. IWA Publishing, London, UK, 2006.

[115] O. Wanner and W. Gujer. Competition in biofilms. *Water Sci. Technol.*, 17(2–3):27–44, 1984.

[116] O. Wanner and W. Gujer. A multispecies biofilm model. *Biotechnol. Bioeng.*, 28(3):314–328, 1986.

[117] O. Wanner and P. Reichert. Mathematical modeling of mixed-culture biofilms. *Biotechnol. Bioeng.*, 49(2):172–184, 1996.

[118] Y. Watanabe, S. Masuda, and M. Ishiguro. Simultaneous nitrification and denitrification in micro-aerobic biofilms. *Water Sci. Technol.*, 26(3–4):511–522, 1992.

[119] P. Watnick and R. Kolter. Biofilm, city of microbes. *J. Bacteriol.*, 182(10):2675–2679, 2000.

[120] M. Wichern, C. Lindenblatt, M. Lübken, and H. Horn. Experimental results and mathematical modelling of an autotrophic and heterotrophic biofilm in a sand filter treating landfill leachate and municipal wastewater. *Water Res.*, 42(14):3899–3909, 2008.

[121] J. Wimpenny, W. Manz, and U. Szewzyk. Heterogeneity in biofilms. *FEMS Microbiol. Rev.*, 24(5):661–671, 2000.

[122] G.M. Wong-Chong and R.C. Loehr. The kinetics of microbial nitrification. *Water Res.*, 9(12):1099–1106, 1975.

[123] J.B. Xavier, C. Picioreanu, and M.C.M. van Loosdrecht. A modelling study of the activity and structure of biofilms in biological reactors. *Biofilms*, 1(4):377–391, 2004.

[124] J.B. Xavier, C. Picioreanu, and M.C.M. van Loosdrecht. A framework for multidimensional modelling of activity and structure of multispecies biofilms. *Environ. Microbiol.*, 7(8):1085–1103, 2005.

[125] T.C. Zhang and P.L. Bishop. Experimental determination of the dissolved oxygen boundary layer and mass transfer resistance near the fluid-biofilm interface. *Water Sci. Technol.*, 30(11):47–58, 1994.

[126] S. Zhu and S. Chen. The impact of temperature on nitrification rate in fixed film biofilters. *Aquacult. Eng.*, 26(4):221–237, 2002.

Papers

[redacted]

PAPER I

Published in *Bulletin of Mathematical Biology* 2012.

Persistence in a single species CSTR model with suspended flocs and wall attached biofilms

Alma Mašić[a,b], **Hermann J. Eberl**[c]

a) School of Technology, Malmö University, SE-20506 Malmö, Sweden.

b) Centre for Mathematical Sciences, Lund University, Box 118, SE-22100, Lund, Sweden.

E-mail: alma.masic@mah.se

c) Biophysics Interdepartmental Program and Dept. Mathematics and Statistics, University of Guelph, ON, Canada, N1G 2W1

E-mail: heberl@uoguelph.ca

Abstract

We consider a mathematical model for a bacterial population in a continuously stirred tank reactor (CSTR) with wall attachment. This is a modification of the Freter model, in which we model the sessile bacteria as a microbial biofilm. Our analysis indicates that the results of the algebraically simpler original Freter model largely carry over. In a computational simulation study, we find that the vast majority of bacteria in the reactor will eventually be sessile. However, we also find that suspended biomass is relatively more efficient in removing substrate from the reactor than biofilm bacteria.

Keywords: biofilm, mathematical model, CSTR, wall attachment.

MSC: 92D25

1 Introduction

Bacterial biofilms are microbial layers on immersed surfaces in aqueous systems. Bacteria adhere to the surface, become sessile and start producing a gel-like matrix of extracellular polymeric substances (EPS) in which they are themselves embedded [16]. Biofilms are omnipresent and can be found wherever environmental conditions sustain microbial growth. It has been suggested that the vast majority of bacteria in natural systems live in biofilm communities [9], and not in suspended communities, which have traditionally been the center of study, both in experimental microbiology and in mathematical biology.

Two primary distinctions between the biofilm and the suspended mode of growth are (i) the EPS matrix offers the cells protection against mechanical washout and (ii) in a biofilm, the bacteria experience concentration gradients of dissolved substrates, i.e. the living conditions depend on the location of the cell within the biofilm [23, 26]. The latter can lead to the establishment of micro-environments, such as anaerobic zones in aerobic biofilms [8, 26].

In environmental engineering many technologies have been developed based on biofilm processes, in particular in wastewater treatment, but also for soil remediation and ground-

water protection [23]. Some of these technologies are based on stimulating biofilm growth by providing colonizable surfaces on which biofilms can form and be sheltered. An example of this kind are Moving Bed Biofilm Reactors (MBBR) for wastewater treatment, where the vessel in which the biological treatment processes occur is augmented by biofilm carrier chips [17].

In many engineered systems, including MBBR, biofilms and suspended communities co-exist. Moreover, free swimming bacteria may adhere to an already existing biofilm, and biofilm bacteria may leave the community and go into suspension. Both processes, attachment and detachment are not very well understood. The latter process is primarily associated with shear induced erosion or sloughing of biomass [19], but it has also been documented that cells can leave the community independently of external forces [6].

Mathematical models for suspended bacterial populations have been successfully developed for many years and are frequently and routinely used in design of reactors and operating conditions, and in the analysis of microbial growth curves, e.g. for food safety and shelf-life studies. Typically these are systems of first order ordinary differential equations. In microbially relatively simple systems, these models can often be studied analytically [24]. More complex microbial systems, e.g. the ones arising in wastewater treatment studies, usually must be studied computationally [13, 14].

Also mathematical models for biofilms have been developed for many years, originally primarily in the engineering literature [29, 30]. They are more complex than models of suspended growth, because they must account for the spatial aspects of biofilms, most notably the inhomogeneous distribution of bacteria and substrates across the depth of a biofilm. Biofilm models are primarily computational models. Indeed, only very few studies are known in which biofilm models have been studied with analytical techniques [21, 27], although biofilm models have greatly contributed to our understanding of biofilm processes, in particular with respect to population and resource dynamics.

Mathematical models for systems that comprise both suspended and sessile bacteria are more scarce. Best known and well studied is the Freter model of competition between suspended and wall attached bacteria for a nutrient [4, 5, 10, 15, 25]. In this model, the amount of wall space available for colonization is limited and it is implicitly assumed that the wall attached bacteria form a relatively thin layer in which no concentration gradients develop. The cells sessile at the wall experience the same growth conditions as the suspended cells but are protected from hydrodynamical washout. Although this describes the system for which the model was originally developed (the mammalian gut) relatively well, it appears too simplistic for biofilm systems, where the wall attached bacteria can grow in thick layers in which concentration gradients can develop, and where the colonization surface is not limiting the capacity for wall attachment. A greatly simplified version of the Freter model has been used for description and analysis of gastro-intestinal *E coli* infections [7].

In this study we revisit the Freter model for a CSTR. More specifically, we replace the original wall-attachment model by a traditional Wanner-Gujer type one-dimensional

biofilm model [29, 30], in order to account for the spatial structure of the wall attached bacterial population. The resulting model is algebraically more complex than the original Freter model and naturally the question arises whether this added algebraic complexity also adds new dynamic complexity. This is investigated with analytical and computational methods. Moreover, in a numerical simulation experiment we investigate how reactor operating conditions, such as flow rate, bulk substrate concentration, and surface area available for colonization affect the reactor's performance with respect to substrate removal.

2 Model description

2.1 The Freter model of a CSTR with wall attachment

In [10] a model was proposed that describes the formation of a microbial population in an aqueous environment in the mammalian gut. Bacteria can be suspended in the aqueous phase or colonize the surface. This model was later adapted to a CSTR [15], which includes the following processes:

- continuous replenishment of the reactor with fresh medium,
- washout of substrate and suspended biomass,
- growth of bacterial biomass through consumption of substrate,
- natural cell death,
- attachment of suspended biomass to the wall,
- detachment of bacteria from the wall.

This is described by a system of three ordinary differential equations for the substrate concentration, the unattached as well as the wall-attached bacteria. The model reads

$$\dot{S} = D(S^{in} - S) - \gamma^{-1}(u\mu_u(S) + \delta w \mu_w(S)) \tag{1}$$

$$\dot{u} = u(\mu_u(S) - D - k_u) + \beta\delta w + \delta w \mu_w(S)(1 - G(W)) - \alpha u(1 - W) \tag{2}$$

$$\dot{w} = w(\mu_w(S)G(W) - \beta - k_w) + \alpha u(1 - W)\delta^{-1}. \tag{3}$$

The dependent variables are concentration of the growth limiting substrate S [gm^{-3}], the concentration of suspended bacteria u [gm^{-3}], and the amount of biomass per unit area of colonizable surface, w [gm^{-2}].

The parameter D [d^{-1}] is the dilution rate, i.e. the rate at which fresh substrate is supplied to the reactor, and at which substrate and suspended bacteria are washed out. It is obtained through $D = Q/V$ where Q [m^{3}d^{-1}] is the flow rate and V [m^3] the

reactor volume. By S^{in} [gm^{-3}] we denote the bulk concentration, i.e. the concentration at inflow. The constant δ [m^{-1}] is a reactor parameter that denotes how much surface area is available for colonization per unit volume of the reactor.

The growth rates of the unattached and wall-attached bacteria are denoted by $\mu_u(S)$ and $\mu_w(S)$, respectively. The functional relationship between growth rate and substrate concentration is described by Monod kinetics, i.e. takes the form

$$\mu_u(S) = \frac{m_u S}{a_u + S}, \quad \mu_w(S) = \frac{m_w S}{a_w + S},$$

where the constants m_u [d^{-1}] and m_w [d^{-1}] are the maximum specific growth rates, i.e. the growth rates achieved in situations of food abundance, and the parameters a_u [gm^{-3}] and a_w [gm^{-3}] are the half saturation coefficients. The constant γ [$-$] is the biomass yield per unit of substrate. The cell death rates are k_u [d^{-1}] and k_w [d^{-1}].

Daughter cells of the wall-attached bacteria compete for space; $G(W)$ cells attach to the wall at rate α [d^{-1}], $1-G(W)$ are released into the bulk liquid, where $G(W) = \frac{1-W}{1.1-W}$ and $W := w/w_{max}$ is the wall occupancy fraction. Detachment of wall attached bacteria happens at rate β [d^{-1}].

It was found in [15] that the washout steady state $(S, u, w) = (S^{in}, 0, 0)$ always exists and that it is locally asymptotically stable if both $\mu_w(S^{in}) - k_w < 0$ and $\mu_u(S^{in}) - k - D < 0$ are satisfied. It is unstable if either $\mu_w(S^{in})G(0) - k_w - \beta \geq 0$ or $\mu_u(S^{in}) - k - D - \alpha \geq 0$ is satisfied. Further, the study showed that at least one nontrivial steady state $(S, u, w) = (S^*, u^*, w^*)$ exists when the washout state is unstable. However, given the complexity of the model, a calculation of the exact coordinates of the nontrivial steady state in closed form was not possible. Instability of the washout state implies persistence of u and w, assuming nontrivial initial data.

2.2 A CSTR model with wall attachment in form of biofilms

In the model of [15] the wall attached bacteria experience the same substrate concentrations as the suspended bacteria. We will re-formulate the model for the case where the wall attached cells form bacterial biofilms. The starting point for our model is a CSTR mass balance as in the previous section, which we couple with a traditional one-dimensional biofilm model. The processes included in this model are the same as in Section 2.1. Additionally, we assume that

- the biofilm uniformly covers the surface that is available for colonization,
- substrate diffuses into the bacterial biofilm layer,
- substrate gradients in the biofilm are observed as a consequence of diffusion and reaction.

In the Freter model all sessile bacteria are assumed to be wall-attached and, therefore, compete for space. On the other hand, in a biofilm, sessile bacteria grow in thick layers that form on the substratum. In the Wanner-Gujer model it is assumed that all available substratum is homogeneously covered. The fundamental underlying assumption of the traditional one-dimensional biofilm model [29, 30] is that the biomass in a biofilm always attains maximum density. In a single-species biofilm, therefore, biomass and biofilm thickness are equivalent: production of biomass leads to a one-to-one expansion of the biofilm. Biomass that is produced in the inner layers of the biofilm pushes the cells above, i.e biomass moves with a velocity that is equivalent to the rate of biomass production. The spatial extension of the biofilm distinguishes the new model from the Freter model. The consumption of substrate by the biofilm for growth induces a substrate flux across the biofilm/water interface. In the biofilm substrate diffuses and is degraded. This results in substrate gradients and, accordingly, the bacteria in the inner layers of the biofilm, where the substrate concentration is lower, live under different conditions than the bacteria closer to the interface, where the substrate concentration is higher. In particular, the bacterial growth rates in the biofilm are not homogeneous.

For our convenience, and unlike the model in Section 2.1, we cast the model in terms of the dependent variables substrate concentration S [gm^{-3}], suspended biomass u [g] and biofilm thickness λ [m]. The modified CSTR model with homogeneous biofilm wall attachment then reads

$$\dot{S} = D(S^{in} - S) - \frac{u\mu_u(S)}{V\gamma} - \frac{J(S,\lambda)}{V} \tag{4}$$

$$\dot{u} = u(\mu_u(S) - D - k_u) + A\rho d(\lambda)\lambda - \alpha u \tag{5}$$

$$\dot{\lambda} = v(\lambda, t) + \frac{\alpha u}{A\rho} - d(\lambda)\lambda \tag{6}$$

Here, as above, D is again the dilution rate, S^{in} the inflow concentration, γ the yield coefficient, k_u the cell death rate for suspended bacteria, and α is the rate at which suspended bacteria attach to the biofilm. In contrast to the model of the previous section, it does not depend on available wall space but models the attachment of suspended biomass to the biofilm.

In (4)-(6), V [m^3] is the reactor volume and A [m^2] the colonizable surface area. The biomass density in the biofilm is ρ [gm^{-3}].

In (6), the function $v = v(z,t)$ [md^{-1}] denotes the growth induced velocity of the biomass at a location z in the biofilm. Due to the incompressibility assumption that the biomass density is constant across the biofilm, biofilm expansion is essentially equivalent to biomass growth. Velocity v is obtained as the integral of the biomass production rate

$$v(z,t) = \int_0^z (\mu_\lambda(C(\zeta)) - k_\lambda)d\zeta, \tag{7}$$

where k_λ [d^{-1}] is the cell death rate for biofilm bacteria.

Similarly as μ_u, μ_w in Section 2.1, we define the substrate dependent growth rates via Monod kinetics, i.e.

$$\mu_u(S) = \frac{\mu_u^{max} S}{K_u + S}, \quad \mu_\lambda(C(z)) = \frac{\mu_\lambda^{max} C(z)}{K_\lambda + C(z)}, \tag{8}$$

where $\mu_u^{max}, \mu_\lambda^{max}$ are the maximum specific growth rates, K_u, K_λ the half-saturation coefficients and $C(z)$ [gm^{-3}] denotes the substrate concentration in the biofilm at thickness z [m] from the substratum. It is obtained as the solution of the two-point boundary value problem

$$D_c C''(z) = \frac{\rho}{\gamma}\mu_\lambda(C(z)), \quad C'(0) = 0,\ C(\lambda) = S. \tag{9}$$

Here D_c [$m^2 d^{-1}$] is the diffusion coefficient. The boundary condition at the substratum, $z = 0$, describes that substrate does not leave the reactor through the walls, while the boundary condition at $z = \lambda$ implies that external mass transfer resistance at the biofilm/water interface is neglected. In (9) we used that substrate diffusion is a much faster process than biofilm growth, i.e. that (9) can be considered in a quasi-steady state.

In (4), the sink J [gd^{-1}] denotes the substrate flux from the aqueous phase into the biofilm, i.e.

$$J(S, \lambda) = AD_c \frac{dC}{dz}(\lambda). \tag{10}$$

Detachment of biomass from the biofilm is described by the volumetric detachment rate $d(\lambda)$ [d^{-1}]. The frequently used detachment rate expression in biofilm modeling is to assume that d is proportional to λ,

$$d(\lambda) = E\lambda, \tag{11}$$

leading to a quadratic sink term in (6); E [$d^{-1}m^{-1}$] is the erosion or detachment parameter.

We assume all model parameters to be positive.

3 Analysis of the model

In this section we present some analytical results about the equilibrium of the mathematical CSTR biofilms model. The following result shows that the model is well-posed and that the total mass in the system is bounded.

Proposition 3.1. *Model (4)-(10) with nonnegative initial data*

$$S(t_0) = S^0, \quad u(t_0) = u^0, \quad \lambda(t_0) = \lambda^0, \tag{12}$$

possesses a unique, non-negative solution that exists for all $t > 0$ and satisfies

$$V\gamma S(t) + u(t) + A\rho\lambda(t) \leq a + bt \tag{13}$$

where a, b depend on model parameters and initial data.

Proof. First we formally re-write our model as an ordinary initial value problem. Note that integrating (9) once and using the boundary conditions gives

$$\frac{dC}{dz}(\lambda) = \frac{\rho}{\gamma D_c}\int_0^\lambda \mu_\lambda(C(z))dz. \tag{14}$$

We define

$$j(\lambda, S) := \begin{cases} \frac{\rho}{\gamma D_c}\int_0^\lambda \mu_\lambda(C(z))dz, & \lambda > 0 \\ 0 & \lambda = 0. \end{cases} \tag{15}$$

Note that $C(z)$ is indirectly a function of S due to the boundary condition in (9), therefore also j is a function of S. Then (4)-(10) becomes

$$\dot{S} = D(S^{in} - S) - \frac{1}{V}\Big(\frac{u\mu_u(S)}{\gamma} + AD_c j(\lambda, S)\Big) \tag{16}$$

$$\dot{u} = u(\mu_u(S) - D - k_u) + A\rho d(\lambda)\lambda - \alpha u \tag{17}$$

$$\dot{\lambda} = \frac{\gamma D_c}{\rho} j(\lambda, S) - \lambda k_\lambda + \frac{\alpha u}{A\rho} - d(\lambda)\lambda. \tag{18}$$

Some properties of the function $j(\lambda, S)$ are summarized in Lemma 3.3 below. In particular we note that $j(0, \cdot) = 0$ and $j(\cdot, 0) = 0$. Thus using the tangent criterion, see [28], it follows that the non-negative cone is positively invariant. Moreover, in the non-negative cone, the right hand sides of (16)-(18) are continuously differentiable, so the system satisfies a Lipschitz condition. This implies the local existence and uniqueness of a non-negative solution of the initial value problem with non-negative initial data.

Furthermore, adding the equations (16)-(18) gives the estimate

$$V\gamma\dot{S} + \dot{u} + A\rho\dot{\lambda} = Q\gamma(S^{in} - S) - uD - uk_u - A\rho\lambda k_\lambda \leq Q\gamma S^{in}.$$

Thus

$$V\gamma S(t) + u(t) + A\rho\lambda(t) \leq V\gamma S^0 + u^0 + A\rho\lambda^0 + Q\gamma S^{in}t.$$

Therefore, since S, u, λ are non-negative, they exist and are bounded by a positive linear function for every $t > 0$. □

Remark 3.2. It is easily verified through eqs. (5) and (6) that all solutions S, u, λ to the initial value problem (4)-(6) are such that either $u = \lambda = 0$ or $u > 0$, $\lambda > 0$ for all t.

Thus, if biomass is not absent from the system, it exists simultaneously in suspended and wall attached form.

In the following lemma we derive a result that will be used later on in the stability analysis.

Lemma 3.3. *The function $j(\lambda, S)$ for $\lambda \geq 0$, $S \geq 0$ is well-defined, nonnegative and differentiable. It has the following properties:*

(a) $j(\cdot, 0) = 0$, $j(0, \cdot) = 0$,

(b) $\frac{\partial j}{\partial S}(0, S) = 0$,

(c)

$$\frac{S\vartheta}{K_\lambda + S} \leq \frac{\partial j}{\partial \lambda}(0, S) \leq \frac{S\vartheta}{K_\lambda}, \tag{19}$$

where $\vartheta = \frac{\rho \mu_\lambda^{max}}{\gamma D_c}$ and K_λ is the half-saturation coefficient from (8).

Proof. The function $j(\lambda, S)$ is well-defined since the boundary value problem (9) has a unique solution. If λ and S are positive, this solution is positive; since $C(z)$ is differentiable with respect to the parameters λ and S, also $j(\lambda, S)$ is.

(a) For $S = 0$ we have $C(\lambda) = 0$ from the boundary conditions in (9). Since $C(z)$ is a continuous nonnegative function we have $C(z) \equiv 0 \Rightarrow \mu_\lambda(C(z)) \equiv 0 \Rightarrow j(\cdot, 0) = 0$.

(b) The derivative of j with respect to S for $\lambda = 0$ is by definition

$$\frac{\partial j}{\partial S}(0, S) = \lim_{h \to 0} \frac{j(0, S + h) - j(0, S)}{h} \overset{(a)}{=} 0.$$

(c) We non-dimensionalize (9) with $x = z/\lambda$ and $c(z) = C(z)/S$. The equation now becomes

$$\begin{aligned} c''(x) &= \lambda^2 \frac{\rho \mu_\lambda^{max}}{\gamma D_c} \frac{c(x)}{K_\lambda + Sc(x)}, \\ 0 < x < 1, &\quad c'(0) = 0,\ c(1) = 1. \end{aligned} \tag{20}$$

Further, we consider the two linear auxiliary problems

$$c''(x) = \vartheta \lambda^2 \frac{c(x)}{K_\lambda + S} \tag{21}$$

and

$$c''(x) = \vartheta\lambda^2 \frac{c(x)}{K_\lambda}, \tag{22}$$

with the same boundary conditions as in (20), where $\vartheta = \frac{\rho\mu_\lambda^{max}}{\gamma D_c}$. The solution $c(x)$ of (20) is continuous and bounded by $0 < c(x) < 1$. Therefore $K_\lambda < K_\lambda + cS < K_\lambda + S$. We denote the solutions to (21) and (22) by c_1 and c_2 respectively. With comparison theorems for Sturm-Liouville type boundary value problems, e.g. [28], we get

$$c_1(x) \geq c(x) \geq c_2(x) \tag{23}$$

for all $0 < x < 1$. Since $c_1(1) = c(1) = c_2(1) = 1$ we conclude that

$$c_1'(1) \leq c'(1) \leq c_2'(1). \tag{24}$$

By reversing the non-dimensionalization, we obtain $c'(1) = \frac{\lambda}{S} C'(\lambda)$ and with (14) and (15) from (24)

$$j_1(\lambda, S) \leq j(\lambda, S) \leq j_2(\lambda, S), \tag{25}$$

where j_1 and j_2 are defined in analogy with (15) for the estimates c_1 and c_2. For a fixed S, $j_1(0, S) = j(0, S) = j_2(0, S) = 0$ together with (25) gives us

$$\frac{\partial j_1}{\partial \lambda}(0, S) \leq \frac{\partial j}{\partial \lambda}(0, S) \leq \frac{\partial j_2}{\partial \lambda}(0, S). \tag{26}$$

The solution to (21) is

$$c_1(x) = B_1(\lambda, S)\left(e^{x\sqrt{\vartheta_1(\lambda,S)}} + e^{-x\sqrt{\vartheta_1(\lambda,S)}}\right) \tag{27}$$

with $\vartheta_1(\lambda, S) = \frac{\vartheta\lambda^2}{K_\lambda + S}$ and $B_1(\lambda, S) = \left(e^{\sqrt{\vartheta_1(\lambda,S)}} + e^{-\sqrt{\vartheta_1(\lambda,S)}}\right)^{-1}$. Similarly, the solution to (22) is

$$c_2(x) = B_2(\lambda)\left(e^{x\sqrt{\vartheta_2(\lambda)}} + e^{-x\sqrt{\vartheta_2(\lambda)}}\right) \tag{28}$$

with $\vartheta_2(\lambda) = \frac{\vartheta\lambda^2}{K_\lambda}$ and $B_2(\lambda) = \left(e^{\sqrt{\vartheta_2(\lambda)}} + e^{-\sqrt{\vartheta_2(\lambda)}}\right)^{-1}$. The fluxes are now

$$j_1(\lambda, S) = SB_1(\lambda, S)\sqrt{\frac{\vartheta}{K_\lambda + S}}\left(e^{\lambda\sqrt{\frac{\vartheta}{K_\lambda+S}}} - e^{-\lambda\sqrt{\frac{\vartheta}{K_\lambda+S}}}\right), \tag{29}$$

$$j_2(\lambda, S) = SB_2(\lambda)\sqrt{\frac{\vartheta}{K_\lambda}}\left(e^{\lambda\sqrt{\frac{\vartheta}{K_\lambda}}} - e^{-\lambda\sqrt{\frac{\vartheta}{K_\lambda}}}\right) \tag{30}$$

with

$$\frac{\partial j_1}{\partial \lambda}(\lambda, S) = \frac{S\vartheta B_1(\lambda, S)}{K_\lambda + S}\left(e^{\lambda\sqrt{\frac{\vartheta}{K_\lambda+S}}} - e^{-\lambda\sqrt{\frac{\vartheta}{K_\lambda+S}}}\right), \tag{31}$$

$$\frac{\partial j_2}{\partial \lambda}(\lambda, S) = \frac{S\vartheta B_2(\lambda)}{K_\lambda}\left(e^{\lambda\sqrt{\frac{\vartheta}{K_\lambda}}} - e^{-\lambda\sqrt{\frac{\vartheta}{K_\lambda}}}\right) \tag{32}$$

which gives us

$$\frac{\partial j_1}{\partial \lambda}(0, S) = \frac{2S\vartheta B_1(0, S)}{K_\lambda + S} = \frac{S\vartheta}{K_\lambda + S}, \tag{33}$$

$$\frac{\partial j_2}{\partial \lambda}(0, S) = \frac{2S\vartheta B_2(0)}{K_\lambda} = \frac{S\vartheta}{K_\lambda}. \tag{34}$$

The assertion follows from (26).

□

Remark 3.4. We observe that the estimates of $j(\lambda, S)$ are in fact

$$j_1(\lambda, S) = S\sqrt{\frac{\vartheta}{K_\lambda + S}}\tanh\sqrt{\frac{\lambda^2\vartheta}{K_\lambda + S}}, \tag{35}$$

$$j_2(\lambda, S) = S\sqrt{\frac{\vartheta}{K_\lambda}}\tanh\sqrt{\frac{\lambda^2\vartheta}{K_\lambda}}, \tag{36}$$

with $\vartheta = \frac{\rho\mu_\lambda^{max}}{\gamma D_c}$ and $j_1(\lambda, S) \le j(\lambda, S) \le j_2(\lambda, S)$, where j_1, j_2 are the substrate fluxes of limiting first-order kinetic models. An illustration for $S = 10$ g/m^3 is given in Figure 1. An improved upper estimate for j for small enough λ could be obtained from the zero-order kinetics problem

$$c''(x) = \frac{\vartheta S}{K_\lambda + S},$$

which leads to a linear function in λ, see also [1].

Proposition 3.5. *Let $\alpha > 0$ and $d(\lambda) > 0$. Then for the system of equations (4)-(6) the washout equilibrium $E_0 = (S^{in}, 0, 0)$ exists for all parameters. It is asymptotically stable if*

$$\mu_u(S^{in}) < D + k_u + \alpha \quad \textbf{\textit{and}} \quad \frac{\partial j}{\partial \lambda}(0, S^{in}) < \frac{k_\lambda \rho}{\gamma D_c}$$

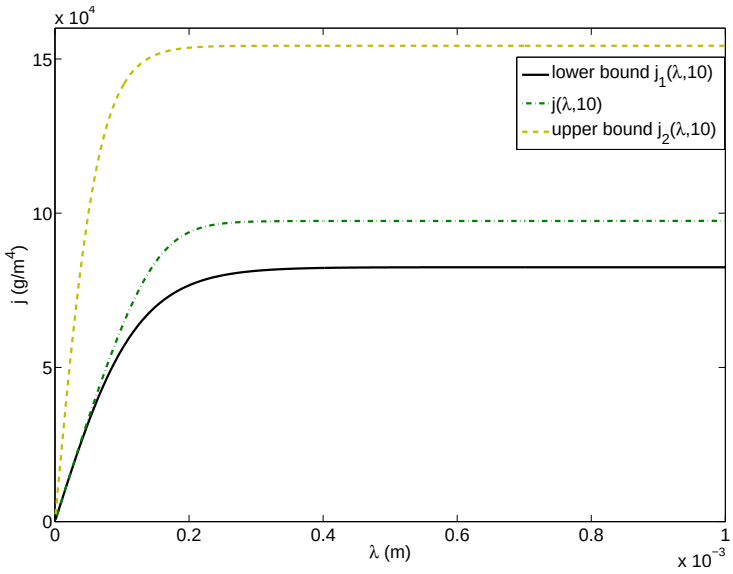

Figure 1: Numerical approximation of $j(\lambda, 10)$ with its upper (yellow dashed) and lower (black solid) bound using parameters from Tables 1 and 2.

and unstable if either

$$\mu_u(S^{in}) > D + k_u + \alpha \quad \textbf{\textit{or}} \quad \frac{\partial j}{\partial \lambda}(0, S^{in}) > \frac{k_\lambda \rho}{\gamma D_c}.$$

Proof. It is easily verified that the trivial equilibrium $E_0 = (S^{in}, 0, 0)$ always exists. To determine the stability of the equilibrium we calculate the Jacobian $J(S, u, \lambda)$ of the right hand side of (16)-(18)

$$\begin{pmatrix} -D - \frac{u\mu_u'(S)}{V\gamma} - \frac{AD_c}{V}\frac{\partial j}{\partial S}(\lambda, S) & -\frac{\mu_u(S)}{V\gamma} & -\frac{AD_c}{V}\frac{\partial j}{\partial \lambda}(\lambda, S) \\ u\mu_u'(S) & \mu_u(S) - D - k_u - \alpha & A\rho(d(\lambda) + \lambda d'(\lambda)) \\ \frac{\gamma D_c}{\rho}\frac{\partial j}{\partial S}(\lambda, S) & \frac{\alpha}{A\rho} & \frac{\gamma D_c}{\rho}\frac{\partial j}{\partial \lambda}(\lambda, S) - (d(\lambda) + \lambda d'(\lambda)) - k_\lambda \end{pmatrix}$$

which for E_0 simplifies to

$$J(S^{in}, 0, 0) = \begin{pmatrix} -D & -\frac{\mu_u(S^{in})}{V\gamma} & -\frac{AD_c}{V}\frac{\partial j}{\partial \lambda}(0, S^{in}) \\ 0 & \mu_u(S^{in}) - D - k_u - \alpha & 0 \\ 0 & \frac{\alpha}{A\rho} & \frac{\gamma D_c}{\rho}\frac{\partial j}{\partial \lambda}(0, S^{in}) - k_\lambda \end{pmatrix}.$$

The eigenvalues of $J(S^{in},0,0)$ are

$$\begin{aligned}\sigma_1 &= -D,\\ \sigma_2 &= \mu_u(S^{in}) - D - k_u - \alpha,\\ \sigma_3 &= \frac{\gamma D_c}{\rho}\frac{\partial j}{\partial \lambda}(0,S^{in}) - k_\lambda.\end{aligned}$$

For asymptotic stability we need all eigenvalues to be negative. From this follows the assertion. □

The function $j(\lambda,S)$ and its derivatives are not easy to evaluate. Instead, using the estimates from Lemma 3.3, we can derive the following weaker criterion

Corollary 3.6. *A sufficient condition for asymptotic stability of the trivial equilibrium* $E_0 = (S^{in},0,0)$ *is*

$$\mu_u(S^{in}) < D + k_u + \alpha \quad \textbf{\textit{and}} \quad \frac{S^{in}}{K_\lambda} < \frac{k_\lambda}{\mu_\lambda^{max}}.$$

On the other hand,

$$\mu_u(S^{in}) > D + k_u + \alpha \quad \textbf{\textit{or}} \quad \frac{S^{in}}{K_\lambda + S^{in}} > \frac{k_\lambda}{\mu_\lambda^{max}}$$

is sufficient for instability.

Observe that the stability criterion in Corollary 3.6 consists of two parts. One refers to the suspended biomass only and presents the classical persistence criterion where a population will not establish if the growth rate is smaller than the sum of dilution and death rate. The second criterion only refers to the biofilm: this stability and instability result is independent of the reactor flow rate and of the detachment rate coefficient E, in agreement with the analysis of [3].

Figure 2 illustrates the numerical approximation of $\frac{\partial j}{\partial \lambda}(0,S^{in})$ with its upper and lower estimate. We observe that the approximation of $\frac{\partial j}{\partial \lambda}(0,S^{in})$ corresponds to the lower estimate $\frac{\rho \mu_\lambda^{max} S^{in}}{\gamma D_c (K_\lambda + S^{in})}$. This is in good agreement with the results of [1], where an analytical approximation of the form $j(\lambda,S) \approx const \cdot \frac{\lambda S}{K_\lambda + S}$ was derived with a Homotopy Perturbation Method argument, which could be numerically verified for an extended range of biofilm parameters. Stability of the trivial equilibrium E_0 is attained for S^{in} such that $\frac{\partial j}{\partial \lambda}(0,S^{in})$ lies beneath $\frac{k_\lambda \rho}{\gamma D_c}$, which is represented by the dotted line in Figure 2.

In summary, with Proposition 3.1 we determine the existence of a unique, non-negative solution to our model (4)-(10), introducing the function $j(\lambda,S)$ in (15) and

Lemma 3.3. Stability of the trivial equilibrium $E_0 = (S^{in}, 0, 0)$ is determined in Proposition 3.5, where E_0 is asymptotically stable if $\mu_u(S^{in}) < D + k_u + \alpha$ and $\frac{\partial j}{\partial \lambda}(0, S^{in}) < \frac{k_\lambda \rho}{\gamma D_c}$ are satisfied and it is unstable if either $\mu_u(S^{in}) > D + k_u + \alpha$ or $\frac{\partial j}{\partial \lambda}(0, S^{in}) > \frac{k_\lambda \rho}{\gamma D_c}$ is satisfied.

The stability conditions for E_0 obtained here are essentially the same as found in [15] for the Freter model with wall attachment. Since it was not possible to compute and analyze the non-trivial equilibria in the algebraically simpler Freter model, we did not attempt this here. Instead, we have investigated the model numerically in Section 4.

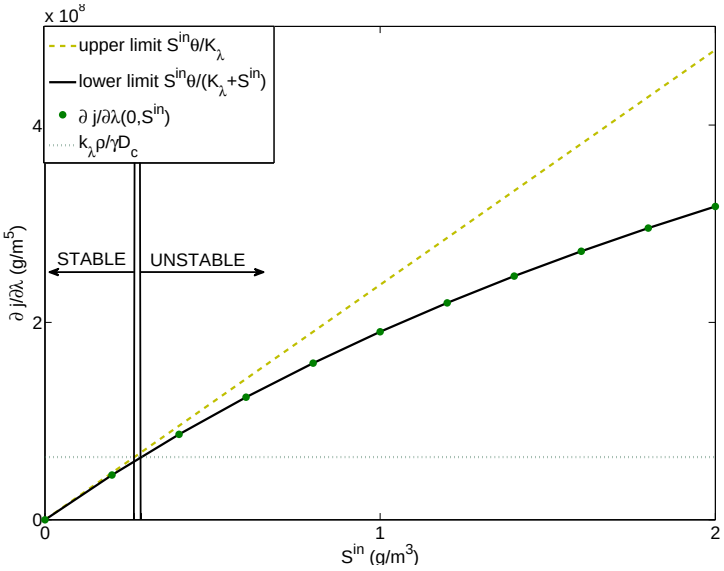

Figure 2: Numerical approximation of $\frac{\partial j}{\partial \lambda}(0, S^{in})$ (green dots) with its upper (yellow dashed) and lower (black solid) bound using parameters from Tables 1 and 2. The dotted line represents the constant $\frac{k_\lambda \rho}{\gamma D_c}$ from Proposition 3.5.

4 Results

4.1 Computational details

Numerical simulations of (4)-(6) were performed in Matlab with the built-in initial value problem solver ode15s. The embedded two-point boundary value problem (9) was solved with the routine bvp5c. The initial value problem was solved until a steady state was

reached upon which the simulations were terminated. The initial conditions were

$$S(0) = S^{in}\ \mathrm{g/m^3}, \quad u(0) = 10^{-6}\ \mathrm{g}, \quad \lambda(0) = 0\ \mathrm{m},$$

where the reactor parameter S^{in} was varied together with colonizable surface area A and dilution rate D. This specific choice for $S(0)$ implies that the medium that is added to the reactor is the same as the medium with which the reactor is initially filled, which seems a reasonable assumption. Assuming a cylindrical reactor with dimensions specified in Table 1 we have a volume $V \approx 0.00118\ \mathrm{m^3}$ and an inner surface area $A_{\mathrm{reactor}} \approx 0.055\ \mathrm{m^2}$. The surface area A can be increased by adding suspended carriers on which biofilms can form [17], i.e. we always have $A \geq A_{\mathrm{reactor}}$.

Table 1: Reactor dimensions.

Parameter	Value	Reference
radius	0.05 m	assumed
height	0.15 m	assumed
suspended carrier area	0.0068 $\mathrm{m^2}$/carrier	[17]

The model parameters are summarized in Table 2. To allow better comparison, we used the same growth parameter values for both biofilm and suspended biomass, i.e. we interpret the latter as microbial flocs, i.e. bacterial communities without substratum. The specific choices of model parameters are taken from Benchmark Problem 1 of the International Water Association's Taskgroup on Biofilm Modelling, i.e. our reactor models a sufficiently aerated system in which carbon is the only growth limiting substrate.

The values for the attachment rate α and erosion parameter E were assumed. The erosion parameter E was chosen large enough so that the results from our 1D model could be comparable to the results from a 2D model, as shown by [31]. In their study the authors investigate values ranging from $E = 22.8/d$ to $E = 2280/d$ and show that the biofilm thickness $\lambda(t)$ originating from a 1D model is very different from $\lambda(t)$ from a 2D model for small values of E and very similar for large values of E. We picked a value in the middle of the range tested by these authors, which however can be viewed at the higher end of the range used by other authors. Of all the processes considered in our model, biofilm attachment is probably the least understood one. Also here we choose a relatively high value, assuming that one bacterium attaches to the wall for every six bacteria that grow in the bulk liquid.

4.2 Typical simulations

We solved (4)-(10) numerically, stopping the simulations once the solutions had attained steady state. In accordance with our analysis, two steady state forms were observed, de-

Table 2: Model parameters.

Symbol	Parameter	Value	Reference
α	attachment rate	1/day	assumed
D_c	diffusion coefficient	10^{-4} m^2/day	[30]
E	erosion parameter	1000/(m·day)	assumed
γ	yield of biomass from substrate	0.63 -	[30]
K_λ, K_u	half-saturation coefficients	4 g/m^3	[30]
k_λ, k_u	death rates	0.4 /day	[30]
μ_λ^{max}, μ_u^{max}	maximum specific growth rates	6 /day	[30]
ρ	biofilm biomass density	10000 g/m^3	[30]

pending on initial substrate concentration and dilution rate: complete washout of all biomass and co-existence of both biomass types, suspended and biofilm. Variation of the initial suspended biomass u^0 did not have an impact on the steady state values.

For a small initial substrate concentration $S^0 = 0.1$ g/m^3 and a small dilution rate $D = 0.42$/day we observed washout, see Figure 3. Here D was much lower than the maximal growth rate $\mu_\lambda^{max} = \mu_u^{max} = 6$/day, wherefore we expected little biomass to be flushed out of the reactor, compared to the amount of suspended biomass being produced. However, the initial substrate concentration was also very low and the slow dilution rate did not supply much substrate with the influent. Even though biofilm initially started growing it was limited by the low substrate concentration, eventually being completely washed out of the reactor. The suspended biomass started at $u^0 = 10^{-6}$ g and decreased toward zero. The low initial substrate concentration in combination with the dilution rate sufficed to wash out all biomass from the reactor.

By increasing the bulk substrate concentration S^{in}, we expected the biomass to have access to enough nutrients to persist. Keeping the same dilution rate and increasing S^0 to 10 g/m^3, we observed biomass growth and co-existence. Both biomass types increased until they reached a steady state while the substrate was consumed, see Figure 4. The steady state values indicate prevalence of biofilm biomass.

4.3 Trivial equilibrium

Using the estimates from Corollary 3.6 and the parameters from Table 2 we know that asymptotic stability of the trivial equilibrium $\mathrm{E}_0 = (S^{in}, 0, 0)$ is achieved if $S^{in} < 0.2667$ g/m^3 and instability if $S^{in} > 0.2857$ g/m^3. The nature of the interval between these two extremal values is unknown and cannot be determined with the estimates. Therefore, we performed numerical simulations for $S^{in} \in [0.26, 0.29]$ g/m^3 at the relatively high dilution rate $D = 85/d \gg 6/d = \mu$ to investigate the interval in more detail. A close-up of the interval is presented in Figure 5 with steady state values of the solutions. Both

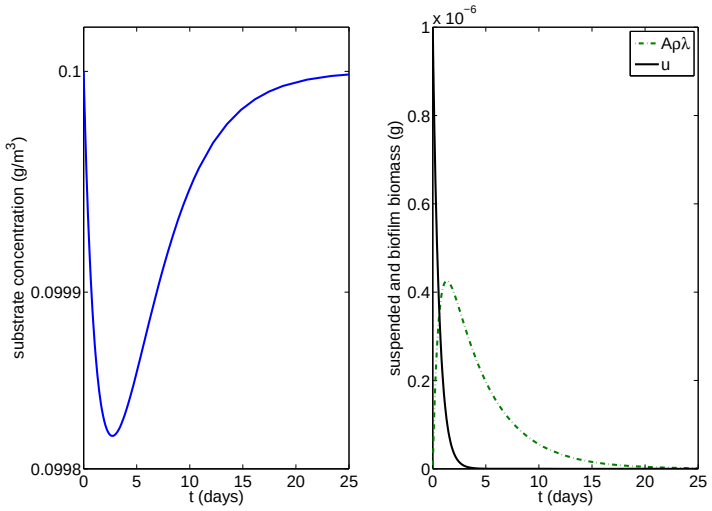

Figure 3: Typical time-dependent simulation at $D = 0.42/\text{day}$ and $S^0 = 0.1$ g/m^3 with substrate concentration S (left) and suspended biomass u and biofilm biomass $A\rho\lambda$ (right).

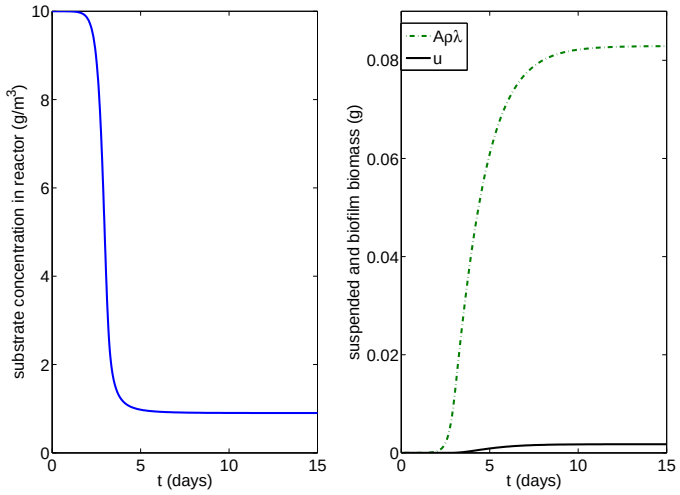

Figure 4: Typical time-dependent simulation at $D = 0.42/\text{day}$ and $S^0 = 10$ g/m^3 with substrate concentration S (left) and suspended biomass u and biofilm biomass $A\rho\lambda$ (right).

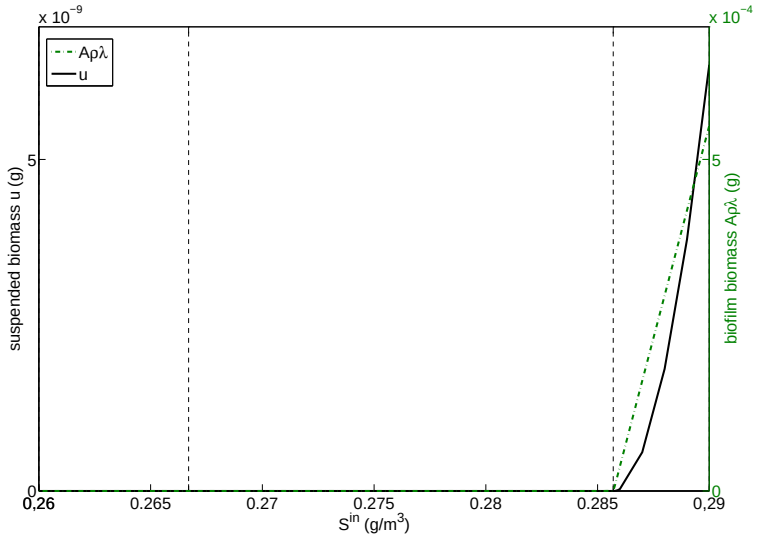

Figure 5: Steady state values of suspended and biofilm biomass, on two different axes, for $S^{in} \in [0.26, 0.29]$ g/m^3 at $D = 85$/day, showing a close-up of E_0 becoming unstable. Two vertical dashed lines indicate the critical values given by Corollary 3.6.

biomass types were washed out for the lower values of S^{in}. The critical value of S^{in}, when both suspended and biofilm biomass are positive, was in fact closer to 0.2857 g/m^3, given by the upper bound in Corollary 3.6.

Led by the conclusions of Proposition 3.5 we were interested in the behavior of our model for variations in parameters D and S^{in}. We rendered a coarse two dimensional grid and performed numerical simulations for $0 < S^{in} \leq 1$ g/m^3 and $0 < D < 85$ /day, presented in Figures 6 and 7. We expected impact on the stability of the trivial equilibrium from both D and S^{in}, depending on the signs of the eigenvalues in Proposition 3.5. Our results, however, show that the stability was governed solely by S^{in}. Washout of all biomass occurred for $S^{in} < 0.3$ g/m^3, independent of the values of D. This is a value much smaller than the half saturation concentration, i.e. indicates a regime of nutrient scarcity. The critical value of S^{in} for which the third eigenvalue σ_3 becomes positive is rather small. In this range of S^{in}, the second eigenvalue σ_2 remains negative, implying that σ_3 is always the first eigenvalue to become positive as S^{in} varies. Since D is not a part of the expression for σ_3, the stability of E_0 is governed by the reaction processes only, but does not depend on the bulk hydrodynamics. An increase in S^{in} beyond the critical value caused instability of E_0 expressed by an increase in biomass.

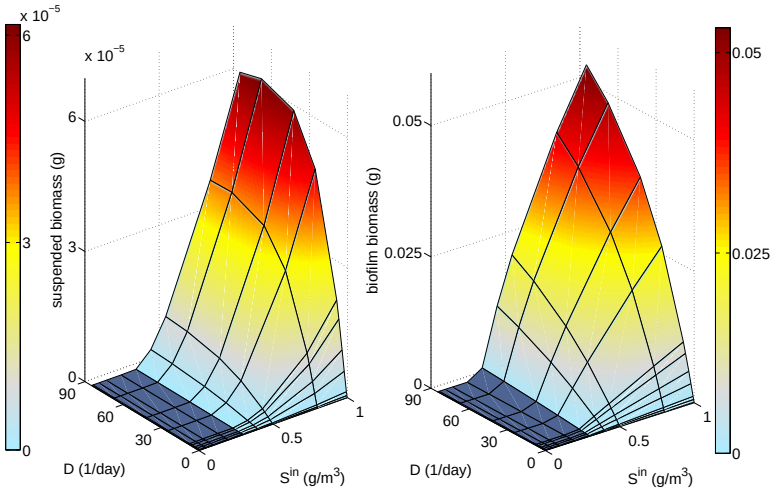

Figure 6: Suspended biomass u (left) and biofilm biomass $A\rho\lambda$ (right) at steady state as functions of the dilution rate D and the initial substrate concentration S^{in}. Trivial equilibrium $E_0 = (S^{in}, 0, 0)$ marked in dark blue.

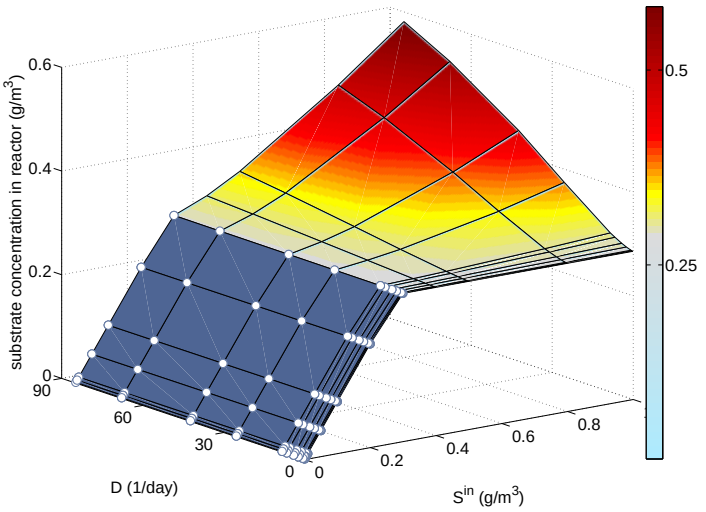

Figure 7: Substrate concentration S in the reactor at steady state as function of the dilution rate D and the initial substrate concentration S^{in}. Trivial equilibrium $E_0 = (S^{in}, 0, 0)$ marked in dark blue with white circles.

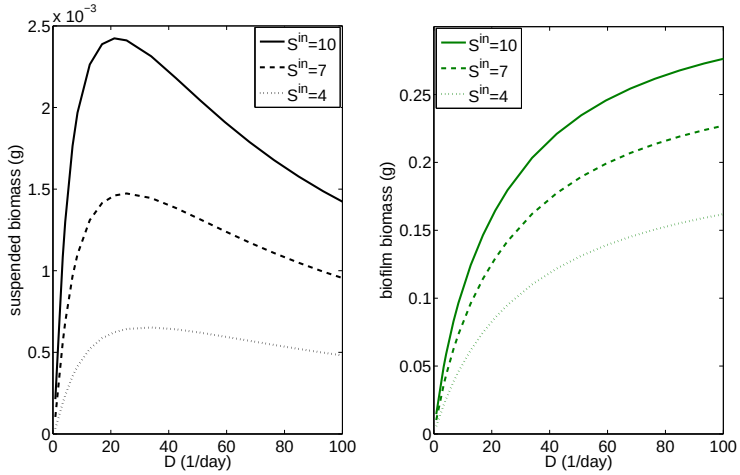

Figure 8: Suspended biomass u (left) and biofilm biomass $A\rho\lambda$ (right) at steady state as functions of the dilution rate D at $S^{in} = 10$, 7 and 4 g/m^3.

4.4 Persistence equilibrium

We know from Proposition 3.5 that the trivial equilibrium is unstable, i.e. $S, u, \lambda > 0$, when S^{in} is large enough. Therefore, the longterm behavior of the model was investigated numerically through variation of S^{in} and D. Washout occurred for $S^{in} < 0.3$ g/m^3, as previously discussed. Persistence of both biomass types was achieved in every simulation for $S^{in} \geq 0.3$ g/m^3. The two biomass types behaved differently as S^{in} and D varied. Suspended biomass increased in the lower range of D while the dilution rate was still comparable to the growth rate. But as D rose to multiples of $\mu_u^{max} = 6$/day it acted as the stronger force, wherefore more suspended biomass was washed out before it could notably contribute to suspended growth. Eventually, for very large D, there was very little suspended biomass in the reactor, however never vanishing completely. An increase in S^{in} increased the peak of suspended biomass before it declined due to washout. Figure 8 is a snapshot of steady states of u and $A\rho\lambda$ at $S^{in} = 4$, 7 and 10 g/m^3 as they vary along D. Biofilm biomass increased for both S^{in} and D, eventually reaching a plateau for large D.

Figure 8 indicates that the suspended biomass will decrease eventually as D increases, whereas the biofilm will persist and, in fact, keep growing. Larger D brings more nutrients to the reactor wherefore the biofilm thickness increases. Since the detachment rate (11) has no connection to the dilution rate, it is not affected by variation in D. Eventually, suspended biomass will decrease to a minimum due to washout from the reactor for a large enough dilution rate.

In our model (4)-(6), the bulk flow rate contributes to substrate supply and to washout

of suspended biomass. Experimental results indicate that also the rate of detachment is coupled to the bulk hydrodynamics, more specifically, that detachment forces increase as the bulk flow rate increases [19]. This is not reflected in the simple standard detachment model (11), which assumes that the detachment rate is proportional to the biofilm thickness only.

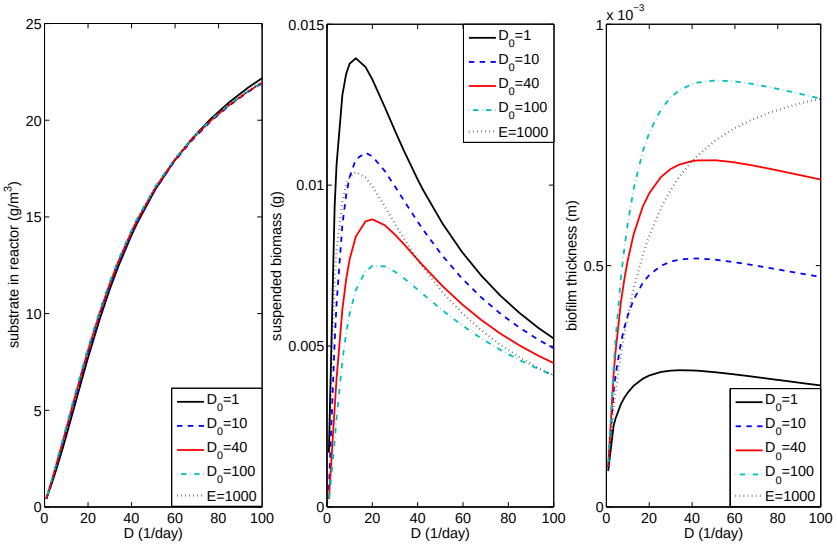

Figure 9: Substrate concentration S (left), suspended biomass u (center) and biofilm thickness λ (right) at steady state for dilution rate dependent detachment coefficients as in (37) at $S^{in} = 30$ g/m^3.

In order to investigate the possible contribution of the reactor flow rate to detachment and the effect that this has on the reactor behavior, we coupled the detachment rate E to the dilution rate D. Motivated by [22] we chose the relationship as

$$\tilde{E} = E\left(\frac{D}{D_0}\right)^{0.58}, \tag{37}$$

where by D_0 we denote a reference dilution rate. For $D > D_0$ we have $\tilde{E} > E$, while for $D < D_0$ we have $\tilde{E} < E$. In Figure 9 we plot the substrate concentration S, the suspended biomass u and the wall attached biomass λ for four different choices of D_0, along with the data for the corresponding model with $E = const$ as previously. The surface area was kept at $A = A_{reactor} \approx 0.055$ m^2 in all simulations. We note that the choice of the detachment rate did not affect the substrate concentration, i.e. it did not

affect the prediction of reactor performance. It did, however, affect the biofilm thickness. This is in agreement with [2], a study of biofilm on a porous medium where it was concluded that changes in the mesoscopic detachment rate do not affect the macroscopic reactor performance. On the other hand, larger D_0, i.e. smaller detachment rates led to thicker biofilms and lower suspended biomass. For larger dilution rates, the detachment rates increased. In contrast to the constant detachment rate, we observed that the biofilm thickness eventually decreased as the dilution rate increased. This did not imply an increase of the suspended biomass for increasing flow rates, which indicates that most of the detached biomass was washed out of the reactor. The observation that a thinner biofilm did not affect the reactor's substrate removal performance indicates that much of the biofilm did not contribute to substrate removal, i.e. that substrate was limited in the inner layers. This is also supported by Figure 10, where we plot the substrate concentration in the biofilms at steady state attained for the various values of D_0 at dilution rate $D = 20$/day. In all four cases the bulk substrate concentration is approximately the same and the substrate concentrations are approximately translations by the difference in biofilm thickness. Thicker biofilms have a thicker inactive inner layer with low substrate concentration.

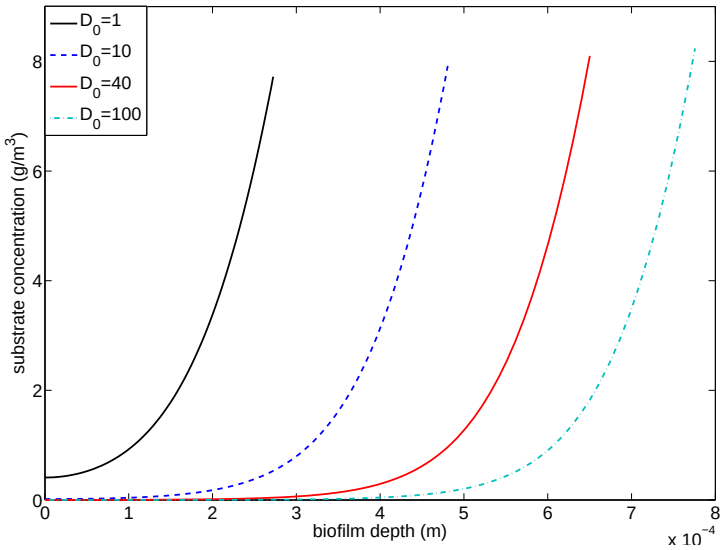

Figure 10: Substrate concentration $C(z)$ within the biofilm at steady state for dilution rate dependent detachment coefficients as in (37) at $S^{in} = 30$ g/m^3 and $D = 20$/day. The substratum is located to the left and the biofilm-bulk liquid interface to the right in the plot.

4.5 Dependence on reactor parameters

A possible application of our model is wastewater treatment, where high amounts of biomass are desired. Existing treatment methods use biofilms and suspended biomass (activated sludge) to treat the wastewater. In methods where biofilm is allowed to grow on suspended carriers it is often not known how much the suspended biomass contributes to the removal of unwanted compounds. Often, reactor parameters are designed in such a way that one can assume that most of the suspended biomass is washed out. To investigate this further, we performed numerical simulations of our model varying the reactor parameters D and A. The total available colonization area A consists of the reactor's inner walls and bottom and the area provided by a certain amount of suspended carriers. In our simulations we considered an empty reactor with $A \approx 0.055$ m^2 up to 200 extra carriers with $A \approx 1.4150$ m^2. Each suspended carrier was assumed to have an area of 0.0068 m^2 [17]. The dilution rate D was varied between 1 and 93/day, while S^{in} was kept at 30 g/m^3.

Higher D resulted in a larger concentration of S in the reactor, due to a higher inflow that transports more substrate into the reactor (see Figure 11). A larger colonization area A contributed to a decrease in substrate concentration due to higher consumption by the increasing biofilm biomass. In fact, even though the biofilm thickness decreased as A increased, the total amount of biofilm biomass increased with A. The graph for biofilm biomass in Figure 11 basically reflects the graph for substrate concentration in the reactor.

The behavior of suspended biomass was governed by several forces. For small dilution rates the amount of suspended biomass decreased as the surface area for colonization increased. The increase of A resulted in a larger biofilm biomass (see Figure 11), which in turn limited the substrate, thereby causing a decrease in suspended biomass due to substrate limitation. Initially this decrease was rapid but leveled off as A increased. For larger dilution rates, the suspended biomass increased for small surface areas but then declined and plateaued (see Figure 12). The increasing dilution rate D brought more substrate to the reactor, but it also increased washout of biomass. The peak value for suspended biomass decreased and was attained at larger values of A as D increased. In all cases, the plateaued value for suspended biomass increased with the dilution rate. Since the biofilm biomass increased with A and D, there was a larger contribution of biomass to the bulk liquid through erosion as both A and D increased. The washout effect was smaller for larger A due to the larger contribution of biomass from the biofilm, balancing out the washout. In summary, suspended biomass increased with D and decreased with A, except for low ranges of A where the washout effect of higher D was noticeable.

Generally we observe that increasing dilution rate increased the substrate removal efficiency which is easily calculated through $Q(S^{in} - S^*)$ [g/day], where S^* is the steady state substrate concentration. For small dilution rates, $D < \mu_u^{max}$, the surface colonization rate had no effect on the substrate removal rate. However, as D became larger than the growth rate, i.e. as the washout of suspended bacteria began to dominate growth, the substrate removal rate increased initially as A increased and then leveled off for larger A.

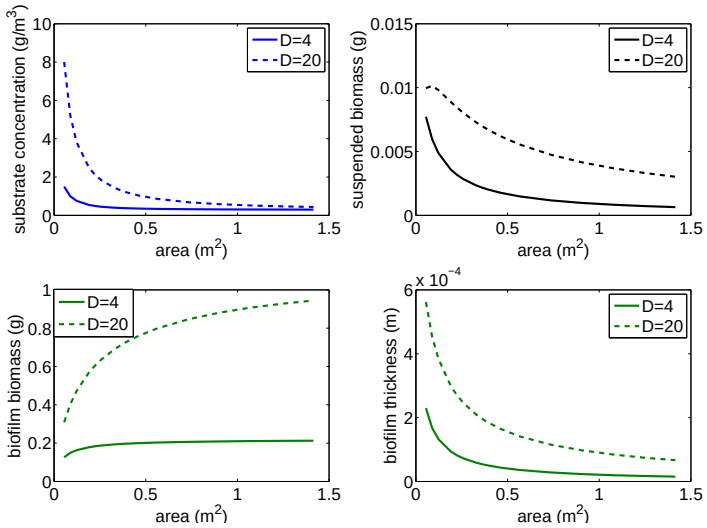

Figure 11: Substrate concentration S (top left), suspended biomass u (top right), biofilm biomass $A\rho\lambda$ (bottom left) and biofilm thickness λ (bottom right) at steady state as functions of colonizable area A for dilution rates $D = 4$ and $D = 20$/day at $S^{in} = 30$ g/m^3.

The bigger the dilution rate the more pronounced was this effect and the later the leveling off occurred (see Figure 13). Interestingly, by increasing A we could increase the overall removal but were not able to decrease the final concentration of S in the effluent beyond a lower limit, regardless of the dilution rate. Hence, addition of suspended carriers would improve removal (significantly for higher D) to a certain extent.

We denote the contribution of suspended biomass to the overall substrate removal by φ and calculate it through

$$\varphi = \frac{\frac{u^* \mu_u(S^*)}{\gamma}}{Q(S^{in} - S^*)} = \frac{u^* \mu_u^{max} S^*}{\gamma Q(S^{in} - S^*)(K_u + S^*)} \tag{38}$$

where u^* denotes the steady state suspended biomass. φ decreased at all dilution rates as the colonization area increased, indicating that the biofilm dominated as the main actor in substrate removal (see Figure 14). However, the suspendeds contributed to the removal significantly in medium ranges of D and low colonization areas, although never reaching beyond 16%. This indicates that the suspended biomass can make a considerable contribution to reactor performance, even if the amount of suspendeds is small compared to the amount of biofilm. In fact, suspended biomass was relatively more efficient in substrate removal than the biofilm. This is due to the fact that in biofilms the bacteria in

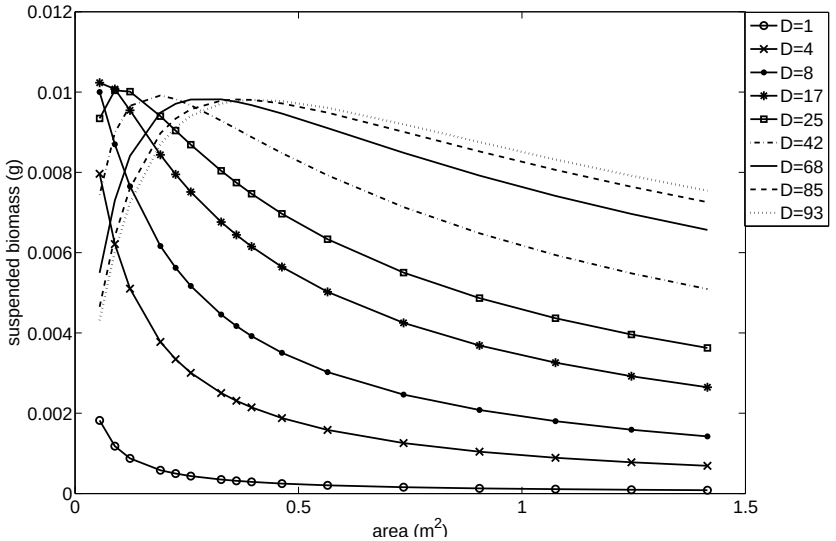

Figure 12: Suspended biomass u at steady state as a function of colonizable area A for different dilution rates D at $S^{in} = 30$ g/m^3.

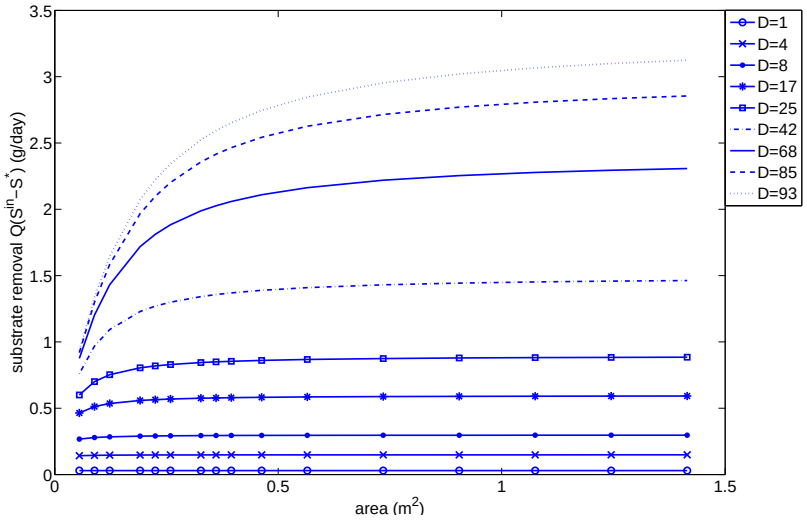

Figure 13: Substrate removal at steady state as a function of colonizable area A for different dilution rates D at $S^{in} = 30$ g/m^3.

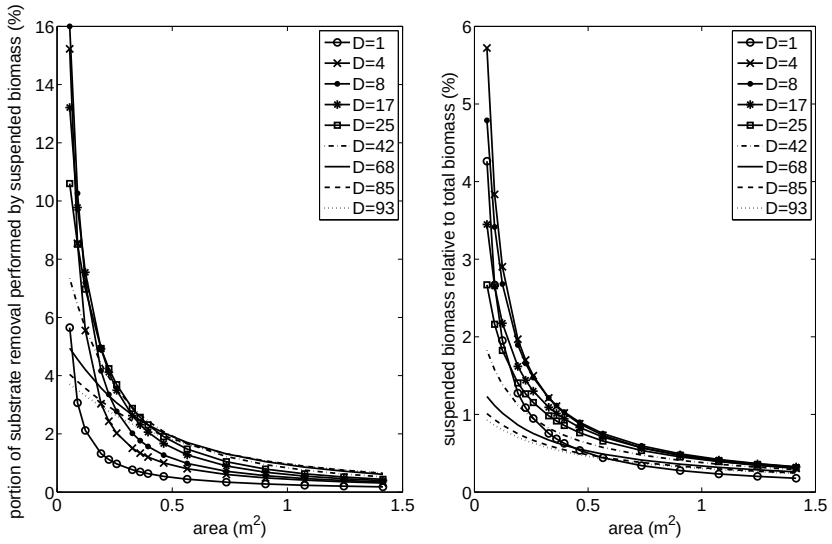

Figure 14: Percentage of substrate removal performed by suspended biomass (left) and amount of suspended biomass relative to total biomass (right), at steady state as a function of colonizable area A for different dilution rates D at $S^{in} = 30$ g/m^3.

the inner layers often, particularly in thick biofilms, live under nutrient limitations and do not contribute greatly to substrate degradation. φ corresponded to the behavior of the suspended biomass for the different dilution rates, i.e. it increased initially in the lower ranges of D until it reached a peak and subsequently decreased due to higher washout.

5 Conclusion

In this paper we studied a mathematical model of bacterial population and resource dynamics in a CSTR with wall attachment. This is a modification of Freter's model, in which we treat the wall attached bacteria as biofilms. The resulting mathematical model is more complex than the original Freter model, because the reactor mass balance is coupled with a diffusion-reaction equation for the substrate in the biofilm. The added algebraic and physical complexity did not add increased dynamic complexity. The stability conditions for the trivial equilibrium of the modified model are essentially the same as for the original Freter model. If the trivial equilibrium is unstable, the system attains a non-trivial equilibrium, in which both suspended and biofilm biomass co-exist. Overall, the model shows a preference of the biomass for the biofilm mode of growth, as also observed in natural systems. In particular for large reactor flow rates suspended biomass is washed

out faster than it can reproduce.

Numerical simulations of the model highlight that changes in the detachment rate affect the biofilm thickness, but do not affect the overall reactor performance.

Although the amount of suspended biomass is small compared to the biomass accumulated in the biofilm, its contribution to the reactor's substrate removal performance is significant in medium ranges of the dilution rate and small colonization areas. In fact, it appears that suspended biomass is relatively more efficient than the biofilm. This can be explained by the fact that in the deeper layers of the biofilm substrate can become limited, wherefore the bacteria there do not contribute to the removal process greatly.

In engineering applications, the performance of a reactor is often increased by increasing the colonizable surface area on which biofilms can grow. Our model reflects that this indeed increases reactor performance, but only to a certain extent, after which the performance levels off, as we observed a lower threshold for the steady-state bulk substrate concentration. In general, the higher the reactor flow rate and thus the substrate supply, the more is gained by providing additional surface area for biofilm formation.

While our study was motivated by wastewater engineering applications, we should point out that the mathematical model used here is too simplified to be quantitative. On the other hand, complicated engineering models, such as the International Water Association's Activated Sludge Models [13] or the Anaerobic Digestion Model [14] are much too involved and depend on too many parameters to be accessible for qualitative studies. Under this light, focusing on simplified and idealized scenarios can be a useful first step toward a mathematical and qualitative understanding of more involved systems [11, 12, 18, 20]. Moreover, they can be the starting point for targeted computational studies of more involved models. This is the next step in our research program.

Nomenclature

A	area	(m^2)
a_u	half-saturation Monod const. of suspended bacteria (Freter)	(g/m^3)
a_w	half-saturation Monod const. of wall-attached bacteria (Freter)	(g/m^3)
D	dilution rate	(1/day)
D_c	diffusion coefficient	(m^2/day)
E	erosion parameter	(1/m·day)
F	flow (velocity) through the reactor (Freter)	(m^3/day)
K_λ	half-saturation Monod constant of biofilm	(g/m^3)
K_u	half-saturation Monod constant of suspended bacteria	(g/m^3)
k_λ	death rate of biofilm	(1/day)
k_u	death rate of suspended bacteria	(1/day)
k_w	death rate of wall-attached bacteria in Freter model	(1/day)
m_u	maximum growth rate of suspended bacteria (Freter)	(1/day)
m_w	maximum growth rate of wall-attached bacteria (Freter)	(1/day)
Q	flow (velocity) through the reactor	(m^3/day)
S	substrate concentration	(g/m^3)
S^{in}	substrate concentration at inlet	(g/m^3)
u	suspended bacteria	(g)
u	concentration of suspended bacteria (Freter)	(g/m^3)
V	volume of the reactor	(m^3)
w	areal biomass density of wall-attached bacteria	(g/m^2)
w_{max}	maximum areal biomass density of wall-attached bacteria	(g/m^2)
$W = w/w_{max}$	wall occupancy fraction	(-)

Greeks

α	attachment rate	(1/day)
β	detachment rate (Freter)	(1/day)
λ	biofilm thickness	(m)
μ_λ^{max}	maximum growth rate of biofilm	(1/day)
μ_u^{max}	maximum growth rate of suspended bacteria	(1/day)
γ	yield	(-)
ρ	biofilm biomass density	(g/m^3)

Bibliography

[1] F. Abbas and H.J. Eberl, (2011). Analytical flux approximation for the Monod boundary value problem. *Appl. Math. Comp. 218(4)*:1484-1494.

[2] F. Abbas and H.J. Eberl, (accepted). Investigation of the role of mesoscale detachment rate expressions in a macroscale model of a porous medium biofilm reactor. *Int. J. Biomath. Biostats. [scheduled for 2(1), 2011]*

[3] F. Abbas, R. Sudarsan and H.J. Eberl, (accepted). Longtime behavior of one-dimensional biofilm models with shear dependent detachment rates. *Math. Biosc. Eng.*

[4] M.M. Ballyk, D.A. Jones, and H.L. Smith, (2001). Microbial competition in reactors with wall attachment. *Microbial Ecology 41(3)*:210-221.

[5] M.M. Ballyk, D.A. Jones, and H.L. Smith, (2008). The biofilm model of Freter: a review. In P. Magal, S. Ruan (eds), *Structured population models in biology and epidemiology*, Springer Lecture Notes in Mathematics Vol.1936.

[6] E. Bester, E.A. Edwards and G.M. Wolfaardt, (2009). Planktonic cell yield is linked to biofilm development. *Can. J. Microbiology, 55(10)*:1195-1206.

[7] B. Boldin, (2008). Persistence and spread of gastro-intestinal infections: the case of enterotoxigenic *Escherichia coli* in piglets. *B. Math. Biol., 70(7)*:2077-2101.

[8] J.W. Costerton, Z. Lewandowski, D.E. Caldwell, D.R. Korber and H.M. Lappin-Scott, (1995). Microbial Biofilms. *Ann. Rev. Microbiology 49*:711-745.

[9] H.C. Flemming, (2000). Biofilme – das Leben am Rande der Wasserphase *Nachr. Chemie 48*:442-447.

[10] R. Freter, H. Brickner, J. Fekete, M. Vickerman and K. Carey, (1983). Survival and implantation of Escherichia coli in the intestinal tract. *Infect. Immun. 39*:686-703.

[11] E.V. Grigorieva and E.N. Khailov, (2010). Minimization of pollution concentration on a given time interval for the waste water cleaning plant. *J. Control Sci. Eng. vol. 2010*, Article ID 712794, 10 pages.

[12] M. El Hajji, F. Mazenc, and J. Harmand, (2010). A mathematical study of a syntrophic relationship of a model of anaerobic digestion process. *Math. Biosci. Eng. 7(3)*:641-656.

[13] M. Henze, W. Gujer, M. Takashi, and M. van Loosdrecht, (2002). Activated Sludge Models ASM1, ASM2, ASM2d and ASM3. IWA Publishing.

[14] IWA Task Group, (2002). Anaerobic Digestion Model No. 1 (ADM1). IWA Publishing.

[15] D. Jones, H. V. Kojouharov, and D. Le, H. Smith, (2003). The Freter model: A simple model of biofilm formation. *Math. Bio. 47*:137-152.

[16] Z. Lewandowski and H. Beyenal, (2007). Fundamentals of biofilm research. CRC Press, Boca Raton.

[17] A. Masic, J. Bengtsson, and M. Christensson, (2010). Measuring and modeling the oxygen profile in a nitrifying Moving Bed Biofilm Reactor. *Math. Biosci. 227*:1-11.

[18] J. Moreno, (1999). Optimal time control of bioreactors for the wastewater treatment. *Optim. Control Appl. Meth. 20*:145-164.

[19] E. Morgenroth, (2003). Detachment: an often-overlooked phenomenon in biofilm research and modeling. In: S. Wuertz et al (eds), *Biofilms in Wastewater Treatment*, pp 246-290, IWA Publishing, London.

[20] T.G. Müller, N. Noykova, M. Gyllenberg, and J. Timmer, (2002). Parameter identification in dynamical models of anaerobic waste water treatment. *Math. Biosci. 177-178*:147-160.

[21] L.A. Pritchett and J.D. Dockery, (2001). Steady state solutions of a one-dimensional biofilm model. *Math. Comput. Model. 33*:255-263.

[22] B.E. Rittmann, (1982). The effect of shear stress on biofilm loss rate. *Biotech. Bioeng. 24*:501-506.

[23] B.E. Rittmann and P.L. McCarty, (2001). Environmental Biotechnology. McGraw-Hill.

[24] H.L. Smith and P. Waltman, (1995). The theory of the chemostat. Cambridge University Press, Cambridge, UK.

[25] E.D. Stemmons and H.L. Smith, (2000). Competition in a chemostat with wall attachment. *SIAM J. Appl. Math. 61(2)*:567-595.

[26] P.S. Stewart, (2003). Diffusion in biofilms. *J. Bacteriol. 185(5)*:1485-1491.

[27] B. Szomolay, (2008). Analysis of a moving boundary value problem arising in biofilm modeling. *Math. Meth. Appl. Sci. 31*:1835-1859.

[28] W. Walter, (2000). Gewöhnliche Differentialgleichungen. 7th ed, Springer-Verlag, Berlin.

[29] O. Wanner and W. Gujer, (1986). A multispecies biofilm model. *Biotech. Bioeng. 28*:314-328.

[30] O. Wanner, H. Eberl, E. Morgenroth, D.R. Noguera, C. Picioreanu, B. Rittmann, and M. van Loosdrecht, (2006). Mathematical modeling of biofilms, Scientific and Technical Report No.18. IWA Publishing.

[31] J.B. Xavier, C. Picioreanu, and M.C.M. van Loosdrecht, (2004). A modeling study of the activity and structure of biofilms in biological reactors. *Biofilms 1(4)*:377-391.

PAPER II

Published in *Mathematical Biosciences* 2010.

Mathematical Biosciences 227 (2010) 1–11

Contents lists available at ScienceDirect

Mathematical Biosciences

journal homepage: www.elsevier.com/locate/mbs

Measuring and modeling the oxygen profile in a nitrifying Moving Bed Biofilm Reactor

Alma Mašić [a,b,*], Jessica Bengtsson [c], Magnus Christensson [d]

[a] Centre for Technological Studies, Malmö University, SE-20506 Malmö, Sweden
[b] Centre for Mathematical Sciences, Lund University, Box 118, SE-22100, Lund, Sweden
[c] Alfa Laval Copenhagen A/S, Maskinvej 5, DK-2860 Søborg, Denmark
[d] AnoxKaldnes AB, Klosterängsvägen 11A, SE-22647 Lund, Sweden

ARTICLE INFO

Article history:
Received 27 August 2009
Received in revised form 7 May 2010
Accepted 16 May 2010
Available online 24 May 2010

Keywords:
Biofilm model
Microelectrode
MBBR
Moving Bed Biofilm Reactor
Nitrifying biofilms
Oxygen profile

ABSTRACT

In this paper we determine the oxygen profile in a biofilm on suspended carriers in two ways: firstly by microelectrode measurements and secondly by a simple mathematical model.

The Moving Bed Biofilm Reactor is well-established for wastewater treatment where bacteria grow as a biofilm on the protective surfaces of suspended carriers. The flat shaped BiofilmChip P was developed to allow good conditions for transport of substrates into the biofilm. The oxygen profile was measured *in situ* the nitrifying biofilm with a microelectrode and it was simulated with a one-dimensional mathematical model. We extended the model by adding a CSTR equation, to connect the reactor to the biofilm through the boundary conditions.

We showed the dependence of the thickness of the mass transfer boundary layer on the bulk flow rate. Finally, we estimated the erosion parameter λ to increase the concordance between the measured and simulated profiles. This lead to a simple empirical relationship between λ and the flow rate. The data gathered by *in situ* microelectrode measurements can, together with the mathematical model, be used in predictive modeling and give more insight in the design of new carriers, with the ambition of making process operation more energy efficient.

1. Introduction

The Moving Bed Biofilm Reactor (MBBR) is well-established for wastewater treatment where bacteria grow as a biofilm on the protective surfaces of suspended carriers [19]. The reactor is aerated and mixed through rising air bubbles from the bottom blowers. In nitrification, oxygen acts as an electron acceptor in the two-step conversion of ammonium to nitrate:

$$\begin{aligned} &\text{Step 1}: \quad 2NH_4^+ + 3O_2 \rightleftharpoons 2NO_2^- + 4H^+ + 2H_2O, \\ &\text{Step 2}: \quad 2NO_2^- + O_2 \rightleftharpoons 2NO_3^-. \end{aligned} \tag{1}$$

The overall conversion rate is usually limited by the first step of the reaction, i.e. conversion of ammonium to nitrite [10, Section 3.4.4]. In wastewater conditions, the availability of ammonium is generally maintained on a high level due to influent water. In the presence of a biofilm oxygen limitation occurs when [8]:

$$D_{O_2} \cdot S_{O_2} < \nu_{NH_4^+,O_2} \cdot D_{NH_4^+} \cdot S_{NH_4^+}, \tag{2}$$

where $D_{O_2}, D_{NH_4^+}$ are diffusion coefficients, $\nu_{NH_4^+,O_2}$ is the stoichiometric coefficient of the overall ratio of oxygen consumption to ammonium removal and $S_{O_2}, S_{NH_4^+}$ are the bulk concentrations of oxygen and ammonium, respectively.

In a biofilm process, transport of oxygen through diffusion limits the nitrification rate to a larger degree compared to what is found in a suspended biomass where convection is more significant. Previous studies on the AnoxKaldnes™ carrier media type K1 have shown that the nitrification rate was close to first order kinetics with respect to dissolved oxygen (DO) when oxygen limiting conditions were established [9]. To maintain a higher DO concentration in the bulk liquid an increase in oxygen transfer from the air bubbles is required, obtained by supplying more air from the blowers, thereby increasing the energy demand per aerated volume. However, the total energy demand for a MBBR biological process operated at elevated DO concentration may not be higher than for a biological process operated at a lower DO concentration, since less aerated volume is needed in the first case due to the higher efficiency. A key factor in the development of new suspended carriers is then not only to increase the available protective surface area, thereby directly contributing to a larger biofilm, but also to allow good conditions for transport of substrates into the biofilm. The flat shaped AnoxKaldnes™ carrier media type

* Corresponding author at: Centre for Technological Studies, Malmö University, SE-20506 Malmö, Sweden. Tel.: +46 40 6657738; fax: +46 40 6657646.
E-mail addresses: alma.masic@mah.se (A. Mašić), jessica.bengtsson@alfalaval.com (J. Bengtsson), Magnus.Christensson@anoxkaldnes.com (M. Christensson).

0025-5564/$ - see front matter © 2010 Elsevier Inc. All rights reserved.
doi:10.1016/j.mbs.2010.05.004

Nomenclature

A	total biofilm area (m^2)
D_k	diffusion constant of substrate k (m^2/day)
DO	dissolved oxygen
$f_i(t,z)$	volume fraction in the biofilm of species i
K_k	half-saturation Monod constant of substrate k (g/m^3)
$L(t)$	thickness of biofilm (m)
MBBR	Moving Bed Biofilm Reactor
Q	flow (velocity) through the reactor (m^3/day)
r_k	net production rate of substrate k (g/m^3 day)
s_p	sum of squared distances for oxygen profile p
S_k	concentration profile of substrate k across the biofilm (g/m^3)
S_k^*	concentration of substrate k in the bulk liquid (g/m^3)
S_k^{in}	concentration of substrate k in the influent (g/m^3)
$u(t,z)$	flow of biomass (m/day)
V	volume of the reactor (m^3)
Y_i	yield coefficient of species i (g COD/g N)

Greeks

$\varphi_k(S^*(t))$	outward flux of substrate k from the biofilm, at the biofilm–liquid interface (g/m^2 day)
λ	erosion parameter (1/m day)
λ_{BL}	erosion parameter when boundary layer removed (1/m day)
$\mu_i(t,z)$	specific growth rate of species i (1/day)
μ_i^{max}	maximum growth rate of species i (1/day)
ρ	density of biofilm (g COD/m^3 biofilm)

Subscripts

A	ammonium oxidizers
BL	boundary layer
I	inert matter
N	nitrite oxidizers
NH_4^+	ammonium
NO_2^-	nitrite
NO_3^-	nitrate
O_2	oxygen

BiofilmChip P (Fig. 1) was developed to meet both these criteria (see Table 1).

We are interested in determination of the oxygen profile in a biofilm on suspended carriers, on BiofilmChip P in particular. One way to determine the oxygen profile in biofilms experimentally is to use microelectrodes [6]. However, for a suspended carrier with a small mesh, a microelectrode measurement can be very challenging to set up and is perhaps not always possible. Therefore, we investigate the possibility of using a simple one-dimensional mathematical model [22] instead, to obtain an estimation of the oxygen profile.

The use of microelectrodes to measure concentrations in biofilms has previously been addressed by Horn and Hempel [12], where the authors measured the oxygen concentration in a biofilm tube reactor and by Hille et al. [11], where they focused on oxygen in biofilm pellets. However, measurements on MBBR are novel to our knowledge. With today's available technology, it is very difficult, even impossible, to carry out measurements on moving suspended carriers. Even when fixated, it can be ambitious to reach deep into all compartments of the plastic carrier. Our work aims to investigate the oxygen profiles on Biofilm Chip P, having in mind what has already been measured in biofilms on other substrata.

In previous studies, simulation and determination of oxygen profiles have been dealt with by Horn and Hempel [13], Rauch et al. [18]. Concentration profiles are greatly influenced by boundary layers and flow of bulk liquid, making the models more complex. Alpkvist et al. [1] developed a 2D model for a similar system of suspended carriers. Our interest is to see whether a simple 1D model can be used to obtain oxygen profiles for biofilms on MBBR. More complex models tend to have more parameters and a higher data requirement, making them difficult to work with. A simpler model with almost the same accuracy in results would be preferable for everyday use.

In this paper, the oxygen profile of the biofilm within the BiofilmChip P carriers is presented, based on two different methodologies. Firstly, the oxygen profile was measured on actual carriers that have been used in a MBBR and secondly, the oxygen profile was estimated, based on a mathematical model of the biofilm growth and development for this reactor.

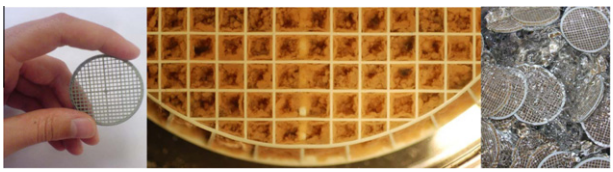

Fig. 1. Images of BiofilmChip P.

Table 1
Characteristics of BiofilmChip P.

Length	3 mm
Diameter	45 mm
Protected surface per carrier	6.818×10^{-3} m^2
Protected surface per m^3 carriers	900 m^2

2. Experimental set-up

A bench-scale Moving Bed Biofilm Reactor (7 l) with flat shaped BiofilmChip P carriers was operated for nitrification using a synthetic medium containing ammonia chloride without any organic substrates (Appendix A). Air was injected through small holes (2 mm) in the bottom of the reactor to guarantee a completely mixed environment and a constant dissolved oxygen concentration. Temperature was regulated by a cooling bath connected to the mantled reactor. Dissolved oxygen and temperature were maintained at 5 mg/l and 10–12 °C, respectively, to replicate design conditions for nitrification in colder climates. The medium flow was adjusted manually to achieve an effluent concentration of 5–8 mg NH_4–N/l to ensure ammonia not being a limiting factor in the first step of nitrification. The nitrification rate was determined through measurements of ammonia, nitrate and nitrite in influent and effluent of the system. After more than a year of continuous operation, establishing a mature biofilm, carriers were taken out for microelectrode measurements in a tube flow cell.

Four carriers from the reactor were placed inside a long plastic tube cell, completely enclosed by the surrounding wall, to ensure that all flow would pass through the holes of the carriers, see Figs. 2 and 3. Each carrier had a quarter cut off to facilitate the insertion of the microelectrode into the biofilm. Altogether, the four carriers, with one quarter removed from each, had an efficient surface area equal to the area of three whole carriers. The same medium compo-

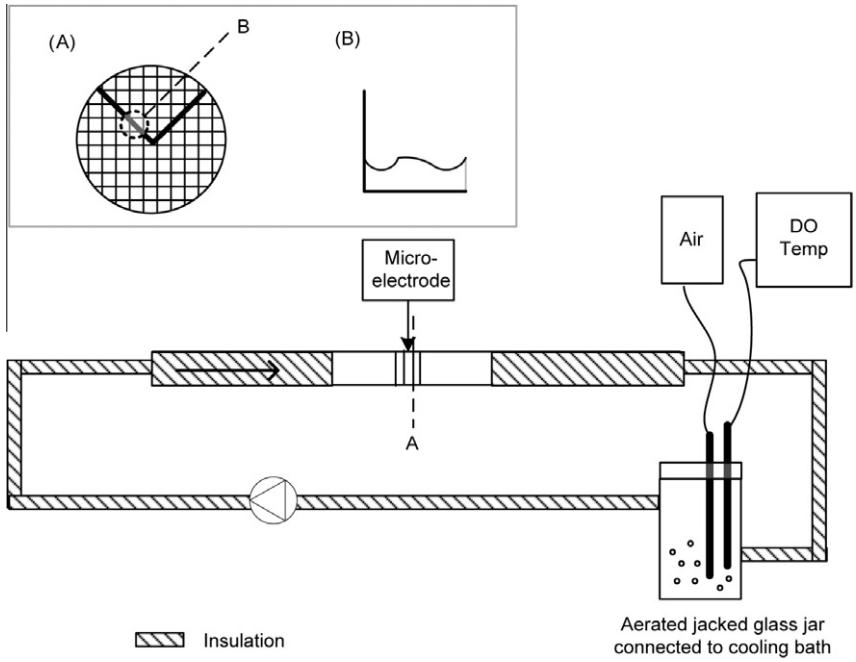

Fig. 2. Sketch of the experimental set-up.

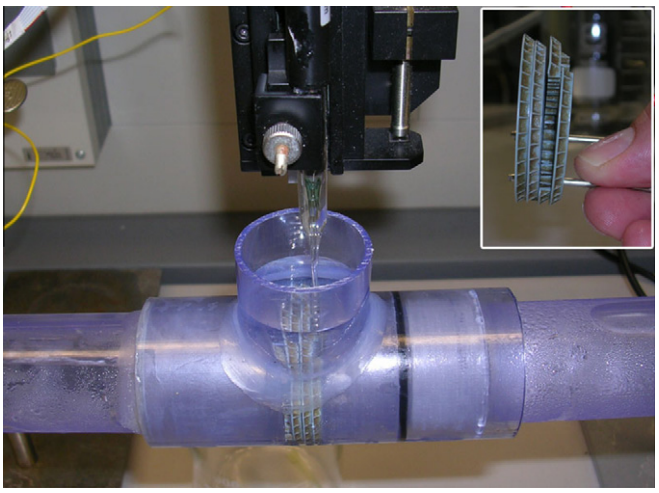

Fig. 3. Photograph of the microelectrode and the four carriers.

sition, as for the continuously operated MBBR, was circulated through the test tube. DO and temperature of the medium were controlled in a small jacked glass in connection with the test tube. The initial concentrations were: 12 mg NH_4–N/l, 1 mg NO_3–N/l and 0 mg NO_2–N/l.

A Clark type oxygen microelectrode [15] was used to measure the oxygen profile *in situ* the nitrifying biofilm. The sensor was inserted into the biofilm, positioned with a micromanipulator, that enables positioning with a precision of 10 μm in z-direction. Since, the holes are very narrow, the biofilm of the nearby perpendicular walls was scraped off in order not to influence the profile of the measured boundary layer. The DO concentration was measured *in situ* along the depth of the biofilm at different positions in x–y-direction. Each profile measurement lasted approx. 10 min. Due to the short duration and a small amount of biomass, the change in concentrations of ammonia, nitrite and nitrate was not significant.

The oxygen profiles were measured on the same carrier to visualize the instantaneous effect of variations in flow rate. The flow through the tube varied from 0.65 l/h to 2.18 l/h.

A longer test was performed to verify the activity of the biofilm on the carriers. Six samples were taken out during 4 h of continuous recirculation through the test tube for measurements of ammonia, nitrite and nitrate concentrations. The nitrification rate was calculated with known water volume and effective biomass surface area, to 2 g N/m^2 d.

3. Mathematical model

3.1. Original model

We used the one-dimensional mathematical model proposed by Wanner and Gujer [22] to estimate the oxygen profile. The model has been adapted to the specific wastewater treatment process mentioned above (MBBR), which contains two types of autotrophic bacteria (ammonium oxidizers and nitrite oxidizers), inert matter and two substrates (ammonium and nitrite) as well as nitrate and oxygen. Using our parameters, based on Eq. (2) oxygen is limiting when $S_{O_2} < 3.14 \cdot S_{NH_4^+}$, assuming ammonium oxidation only to nitrite (1). This condition is fulfilled for the concentrations used in our experiment. For stoichiometry and kinetics, see Table 3.

Our model assumptions are: that the biofilm is one-dimensional, continuous, homogeneous and grows in a direction perpendicular to the substratum; the processes are biomass growth, endogenous respiration and inactivation; Monod kinetics are used to describe the substrate reactions in relation to the bacterial growth rate (with oxygen and ammonium being limiting for the ammonium oxidizers, oxygen and nitrite for the nitrite oxidizers).

Mathematically this results in a system of partial differential equations with a free boundary. The different types of bacteria are described by volume fractions $f_i(t,z)$ in the biofilm and tracked over time with the transport equation

$$\frac{\partial f_i}{\partial t} + \frac{\partial}{\partial z}(u f_i) = \mu_i f_i, \quad i = 1,2,3 \quad (\text{or } i = A,N,I) \tag{3}$$

with the constraint

Table 3
Stoichiometric matrix.

Process j	Dissolved components k				Solid components i			Process rate P_j
	$\mathbf{S}_{O_2}$	$\mathbf{S}_{NH_4^+}$	$\mathbf{S}_{NO_2^-}$	$\mathbf{S}_{NO_3^-}$	$\mathbf{f_A}$	$\mathbf{f_N}$	$\mathbf{f_I}$	
Ammonium oxidizers (A)								
1. Growth	$-\frac{(3.43-Y_A)}{Y_A}$	$-\frac{1}{Y_A}-i_A$	$\frac{1}{Y_A}$	–	*1*	–	–	$\mu_A^{max}\cdot\frac{S_{O_2}}{K_{A,O_2}+S_{O_2}}\cdot\frac{S_{NH_4^+}}{K_{NH_4^+}+S_{NH_4^+}}\cdot f_A\cdot\rho$
2. Endogenous respiration	$-(1-f_{XI})$	$i_A-i_f f_{XI}$	–	–	-1	–	f_{XI}	$b_A\cdot\frac{S_{O_2}}{K_{A,O_2}+S_{O_2}}\cdot f_A\cdot\rho$
3. Inactivation	–	–	–	–	-1	–	*1*	$b_A\cdot\eta\cdot\frac{S_{O_2}}{K_{A,O_2}+S_{O_2}}\cdot f_A\cdot\rho$
Nitrite oxidizers (N)								
4. Growth	$-\frac{(1.14-Y_N)}{Y_N}$	$-i_A$	$-\frac{1}{Y_N}$	$\frac{1}{Y_N}$	–	*1*	–	$\mu_N^{max}\cdot\frac{S_{O_2}}{K_{N,O_2}+S_{O_2}}\cdot\frac{S_{NO_2^-}}{K_{NO_2^-}+S_{NO_2^-}}\cdot f_N\cdot\rho$
5. Decay/endogenous respiration	$-(1-f_{XI})$	$i_A-i_f f_{XI}$	–	–	–	-1	f_{XI}	$b_N\cdot\frac{S_{O_2}}{K_{N,O_2}+S_{O_2}}\cdot f_N\cdot\rho$
6. Inactivation	–	–	–	–	–	-1	1	$b_N\cdot\eta\cdot\frac{S_{O_2}}{K_{N,O_2}+S_{O_2}}\cdot f_N\cdot\rho$

We have $r_k(t,z)=\sum_{j=1}^{6}\nu_{kj}P_j\ \left[\frac{g}{m^3\cdot d}\right]$ and $\mu_i(t,z)=\sum_{j=1}^{6}\frac{\nu_{ij}P_j}{f_i\rho}\ [1/d]$.

$$\sum_{i=1}^{3} f_i(t,z)=1,$$

where $\mu_i(t,z)$ denote the specific growth rates for each biomass component (1/day) and $u(t,z)$ denotes the velocity with which the biomass moves in the biofilm (m/day). The growth rates can be calculated from Tables 3 and 4, for example

$$\begin{aligned}\mu_A&=\sum_{j=1}^{6}\frac{\nu_{Aj}\cdot P_j}{f_A\cdot\rho}=\frac{1}{f_A\cdot\rho}\left(1\cdot\mu_A^{max}\cdot\frac{S_{O_2}}{K_{A,O_2}+S_{O_2}}\cdot\frac{S_{NH_4^+}}{K_{NH_4^+}+S_{NH_4^+}}\right.\\&\left.\cdot f_A\cdot\rho-1\cdot b_A\cdot\frac{S_{O_2}}{K_{A,O_2}+S_{O_2}}\cdot f_A\cdot\rho-1\cdot b_A\cdot\eta\cdot\frac{S_{O_2}}{K_{A,O_2}+S_{O_2}}\cdot f_A\cdot\rho\right)\\&=\mu_A^{max}\cdot\frac{S_{O_2}}{K_{A,O_2}+S_{O_2}}\cdot\frac{S_{NH_4^+}}{K_{NH_4^+}+S_{NH_4^+}}-(1+\eta)\cdot b_A\cdot\frac{S_{O_2}}{K_{A,O_2}+S_{O_2}}\end{aligned}$$

and u from

$$\begin{aligned}&u(t,z)=\int_0^z\left(\sum_{i=1}^{3}f_i(t,z')\cdot\mu_i(t,z')\right)dz',\\&u(t,0)=0\quad\forall t\geqslant 0.\end{aligned}\tag{4}$$

The thickness of the biofilm L is described by an ordinary differential equation

$$\frac{dL(t)}{dt}=u(t,L(t))-\lambda L(t)^2,\tag{5}$$

where λ (1/m d) is the erosion parameter from [22].

The substrate fields are found as the solution to a boundary value problem for four coupled diffusion–reaction equations

$$\begin{aligned}&\frac{\partial S_k(t,z)}{\partial t}=D_k\frac{\partial^2 S_k(t,z)}{\partial z^2}+r_k(t,z),\\&k=1,\ldots,4\\&\left(\text{or } k=O_2,NH_4^+,NO_2^-,NO_3^-\right)\end{aligned}\tag{6}$$

Table 4
Model parameters. (*) Adapted for 10 °C from [26].

Parameter	Label	Value	Unit	Reference
Maximum growth rates				
Ammonium oxidizers	μ_A^{max}	0.3082*	/day	Wyffels et al. [26]
Nitrite oxidizers	μ_N^{max}	0.4015*	/day	Wyffels et al. [26]
Monod constants				
Ammonium	$K_{NH_4^+}$	0.169	g NH_4–N/m^3	Own study
Nitrite	$K_{NO_2^-}$	0.302	g NO_2–N/m^3	Wiesmann [24]
Oxygen, A	K_{A,O_2}	0.5	g O_2/m^3	Pai [16]
Oxygen, N	K_{N,O_2}	0.5	g O_2/m^3	Pai [16]
Yield coefficients				
Ammonium oxidizers	Y_A	0.15	g COD/g NH_4–N	Wyffels et al. [26]
Nitrite oxidizers	Y_N	0.041	g COD/g NO_2-N	Wyffels et al. [26]
Reaction rate constants				
Decay of ammonium oxidizers	b_A	0.04	/day	Salem et al. [20]
Decay of nitrite oxidizers	b_N	0.08	/day	Salem et al. [20]
Anoxic reduction factor for b_A or b_N	η	0.5	–	Elenter et al. [5]
N content of active biomass	i_A	0.07	g N/g COD	Picioreanu et al. [17]
N content of inert biomass	i_I	0.02	g N/g COD	Picioreanu et al. [17]
Fraction of inert biomass produced by endogenous respiration	f_{XI}	0.1	g COD/g COD	Picioreanu et al. [17]
Density	ρ	10 000	g COD/m^3 biofilm	Picioreanu et al. [17]
Diffusion coefficients at temperature T °C				
Oxygen	D_{O_2}	$(682+29.8T-0.0343\ T^2+0.016T^3)\times10^{-7}$	m^2/day	Wik [25]
Ammonium	$D_{NH_4^+}$	$(730+12.8T+0.606\ T^2-0.00533T^3)\times10^{-7}$	m^2/day	Wik [25]
Nitrite	$D_{NO_2^-}$	$(610+12.8T+0.606\ T^2-0.00533T^3)\times10^{-7}$	m^2/day	Wik [25]
Nitrate	$D_{NO_3^-}$	$(610+12.8T+0.606\ T^2-0.00533T^3)\times10^{-7}$	m^2/day	Wik [25]

with the boundary conditions

$$S_k(t,L) = S_k^*, \quad \frac{\partial S_k(t,0)}{\partial z} = 0. \tag{7}$$

Here, S_k denotes the substrate profile (concentration (g/m^3)) across the biofilm and S_k^* the concentration in the bulk liquid. D_k is the diffusivity (m^2/day) and r_k the net production rate $\left[\frac{g}{m^3 \cdot d}\right]$. The boundary conditions state that the concentration at the surface of the biofilm, i.e. the biofilm-bulk interface, should be the same as in the bulk liquid and that there is no flux of concentration through the substratum. The net production rates can be calculated from Table 3, for example

$$r_{NO_2^-} = \sum_{j=1}^{6} \nu_{NO_2^- j} \cdot P_j = \frac{1}{Y_A} \cdot \mu_A^{max} \cdot \frac{S_{O_2}}{K_{A,O_2} + S_{O_2}} \cdot \frac{S_{NH_4^+}}{K_{NH_4^+} + S_{NH_4^+}} \cdot f_A \cdot \rho - \frac{1}{Y_N} \cdot \mu_N^{max} \cdot \frac{S_{O_2}}{K_{N,O_2} + S_{O_2}} \cdot \frac{S_{NO_2^-}}{K_{NO_2^-} + S_{NO_2^-}} \cdot f_N \cdot \rho.$$

The biomass equations and the substrate equations are coupled to each other through the growth rates μ_i and production rates r_k, as seen in Table 3.

When solving the system of Eq. (6), one usually assumes pseudo steady-state [14, Section 2.6.3] setting the time derivative equal to zero, i.e.

$$-D_k \frac{\partial^2 S_k(t,z)}{\partial z^2} = r_k(t,z). \tag{8}$$

Thus we assume that the substrate field equilibrates rapidly and follows changes in the biomass tightly. This reduces the equations in (6) to a two-point boundary value problem.

Note that this model does not include the boundary layer (BL), i.e. the 'layer' of bulk liquid found at the fluid–biofilm interface where mass transfer resistance occurs. The thickness of this boundary layer varies depending on flow velocities and biofilm structure [4], greatly affecting the substrate profiles.

3.2. CSTR model

We incorporated another equation into our model, originally to improve the numerics. This equation, basically a mass balance for substrate concentrations, is well known for continuously stirred tank reactors (CSTR) [7, Sections 4.2 and 4.3.1]. Since, our reason for including the CSTR equation was not to describe the impact of fluid flow, but to determine the bulk concentration levels of all dissolved substrates, a mass transfer coefficient was not suitable. With the CSTR equation we have a two-way interaction between the bulk and the biofilm concentrations. It is also a straightforward way of describing the MBBR system, considering the suspended carriers floating around in a completely mixed reactor.

We connected the equation to the original model through the boundary condition (7) in the diffusion–reaction equation. Due to the method of aeration, oxygen concentration is assumed to be constant in the bulk liquid and, therefore, not included in the CSTR equation. We now have a time-dependent boundary condition for ammonium, nitrite and nitrate:

$$S_k(t,L) = S_k^*(t), \quad k = 2,\ldots,4 \tag{9}$$

and, hence, a differential equation for the concentrations S_k^* in the reactor

$$V \frac{dS_k^*(t)}{dt} = A \cdot \varphi_k(S^*(t)) + Q(S_k^{in} - S_k^*(t)), \quad k = 2,\ldots,4 \tag{10}$$

with initial condition

$$S_k^*(0) = S_k^{in}, \quad k = 2,\ldots,4. \tag{11}$$

Here, $\varphi_k(S^*(t))\left[\frac{g}{m^2 \cdot d}\right]$ denotes the outward flux from the biofilm at the biofilm–liquid interface, V is the volume of the reactor (m^3), A the total biofilm area (m^2) and Q the flow through the reactor (m^3/d). This system of equations describes the time evolution of the substrate concentrations in the reactor. The initial condition (11) states that the concentrations in the reactor at time = 0 should be equal to the concentrations in the influent S_k^{in}. The boundary condition for oxygen remains a constant $S_1(t,L) = S_1^*$.

Note that

$$\varphi_k(S^*(t)) = -D_k \cdot S_k'(t,L), \quad k = 2,\ldots,4,$$

where $S_k'(t,L)$ is the first spatial derivative from the diffusion–reaction system (6), evaluated at $z = L$, using $S^*(t) = S_1^*(t),\ldots,S_4^*(t)$ as boundary conditions (9) for each substrate respectively.

We observe that $S_k'(t,L)$ is indirectly a function of the growth rates μ_i, the production rates r_k and the volume fractions f_i. A schematic illustration of the connection between the two parts in the model can be seen in Fig. 4. The CSTR equation describes the reactor, taking into account the influent and the outward fluxes from the biofilm, calculating the effluent from the reactor. The biofilm part uses the concentrations given by the reactor and incorporates them into the boundary conditions (7). In contrast to the steady state solutions of [1], the concentrations are updated in every time step, making the influence from the bulk on the biofilm and vice versa almost instantaneous.

3.3. Statistics

Even though erosion is not the main focus of our paper, we need to determine the erosion parameter λ in (5). This parameter controls the thickness of the biofilm and indirectly the position and form of the oxygen profile. Although erosion is a very complicated mechanism in a MBBR, considering that water flows through the carriers in several directions, we have chosen to use this simple model of biofilm detachment from [22]. There exist other model components that more accurately describe erosion and sloughing [2], however greatly increasing the model complexity.

To our knowledge, there is no general way of determining λ for use in simulations of oxygen profiles at different flow rates. We know from experimental studies [21] that a higher flow rate causes greater erosion, i.e. a thinner biofilm, while a lower flow rate leads to thicker biofilms. Therefore, we use our measured oxygen profiles to estimate the erosion parameter λ. This will then be used in our model to achieve a better fit in simulations. For every oxygen profile p, the parameter λ_p is determined by minimizing the Euclidean distance between the model solution and the measured data, i.e. by minimizing

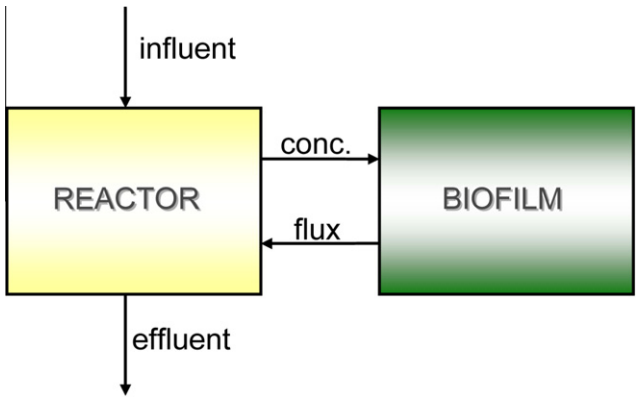

Fig. 4. Schematic view of the model.

$$E_p(\lambda_p) = \sum_{i=1}^{M_p} d_{p,i}^2(\lambda_p), \tag{12}$$

where M_p is the number of data points of the oxygen profile. For the pth oxygen profile the distance $d_{p,i}$ is computed as

$$d_{p,i}^2(\lambda_p) = \min_j \left((\hat{z}_{p,i}(\lambda_p) - z_{p,j})^2 + (\hat{y}_{p,i}(\lambda_p) - y_{p,j})^2 \right), \tag{13}$$

where $(z_{p,j}, y_{p,j})$ are measured and $(\hat{z}_{p,i}(\lambda_p), \hat{y}_{p,i}(\lambda_p))$ are modeled points on the curves. Since the scales in z- and y-direction are different (ca 4 orders of magnitude), we will standardize the axes by dividing with the length of the interval in z and y, respectively.

Due to our choice of the minimization function as the Euclidean distance, we cannot use the coefficient of determination R^2 to assess the goodness of fit. Instead, we will use the sums of squared distances to evaluate our model, i.e.

$$s_p = \sum_i d_{p,i}^2,$$

where a smaller s_p indicates a better fit.

3.4. Numerics

For our analysis we require the steady state of the dynamic biofilm model equations (3), (5) and (10). We computed this iteratively by time-stepping to equilibrium. In every time-step conducted, the dissolved substrate concentrations were computed by solving the two-point boundary value problem (8), see Fig. 5.

We used Matlab to solve all our equations, following the scheme in Fig. 5. The diffusion–reaction system of equations (8) was converted to a first-order system of ordinary differential equations (assuming steady-state in (6)) and was solved using a built-in solver `bvp4c`. By vectorizing the input to the solver (and the system of equations) one can significantly reduce computing time. The transport Eq. (3), as well as the biofilm thickness Eq. (5) and the CSTR Eq. (10), were solved with our own finite difference implementation. We used `lsqnonlin` from the Optimization Toolbox, a built-in solver of nonlinear least squares problems, to find the optimal λ that minimizes the functional (12).

We started with an initial biofilm thickness of 50 μm with an equidistant grid and an equal distribution of ammonium and nitrite oxidizers. The initial value for the fraction of inert biomass was set to zero. As can be seen in the experimental set-up in Fig. 3, the overall biofilm area equaled the area of three carriers.

The system of equations was then iterated with time steps of $\Delta t = 0.1$ days, until $t_{end} = 60$ days. We chose 60 days to make sure that the biofilm thickness had reached steady-state.

4. Results

For the comparison between the mathematical model and the experiments, we have 13 oxygen concentration profiles, measured at five different flow rates, ranging from 0.65 l/h to 2.18 l/h. Four representatives are plotted in Fig. 6. With increasing flow rate, a shift of the slope of the oxygen profile to the left occurred, as previously observed in [11]. This indicates that, despite increased oxygen supply as a consequence of increased bulk flow, the biofilm becomes thinner, the faster the bulk flow is. Hence, the increasing flow rate must have a stronger effect on biofilm erosion, than on biofilm growth. Unfortunately, the model parameter describing biofilm erosion is not a priori known. Therefore, the comparison of the mathematical model with the experimental data was conducted in two steps. (i) In the first step, we determined the biofilm erosion parameter λ, for which no reliable estimates can be found in the literature, from the experimentally measured oxygen profiles. (ii) In the second step we compared the oxygen profiles computed with the mathematical model against the experimental data.

The oxygen concentration profiles measured by the microelectrodes cover three distinct phases: (a) the bulk liquid, in which the oxygen concentration can be assumed in good approximation to be constant, (b) the mass transfer boundary layer, in which all the resistance to oxygen transfer outside the biofilm occurs [14], and (c) the actual biofilm, in which oxygen is reduced by the bacteria, see also Fig. 9 from [23]. Our simple mathematical model (8) for the dissolved substrate concentrations only captures phase (c), but is not able to describe the mass transfer boundary layer well. Hence, it must be expected, that using the experimental measurements without further postprocessing of data introduces errors when comparing model predictions and measurements.

Therefore, and in order to estimate the effect that this may have on the modeling results, both steps (i) and (ii) were carried out twice: First we used the raw data as determined in the experiments. Then, we repeated steps one and two above after removing the concentration measurements in the boundary layer and the bulk. This postprocessing of the experimental data had to be performed manually. Neither the biofilm/liquid interface nor the transition from the boundary layer to the bulk can be clearly inferred from the oxygen profiles in a straightforward manner. According to [23] and based on theoretical considerations, the oxygen profile should have a point of inflection at the biofilm/liquid interface, i.e. where the biofilm ends and the boundary layer begins. This point of inflection is a consequence of the increased diffusive resistance in the biofilm, compared to the liquid phase. However, since for small molecules like oxygen the difference between the diffusion coefficient in the biofilm and in the liquid phase is not very large [3], this point of inflection cannot be expected to be very pronounced and is easily overshadowed by measurement uncertainties. Therefore, the manual detection of the concentration boundary layer from the experimental data was to some degree subjective. In Fig. 7 we plot the concentration boundary layer thicknesses that have been estimated manually from the oxygen concentration profiles. While no quantitative co-relation between bulk flow velocity and boundary layer thickness appears to be known in the literature, to which these data could be compared, our results confirm the expectation that higher bulk flow rates imply a smaller mass transfer boundary layer, i.e. a faster transport of oxygen from the bulk into the biofilm.

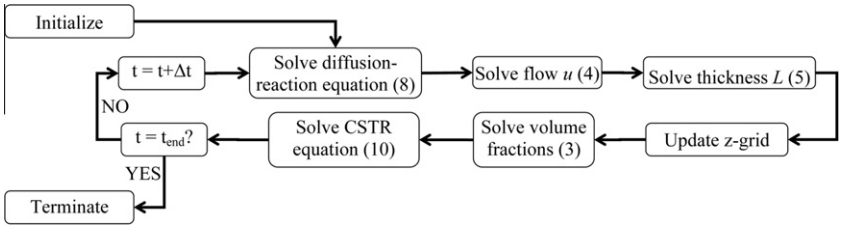

Fig. 5. Numerical scheme.

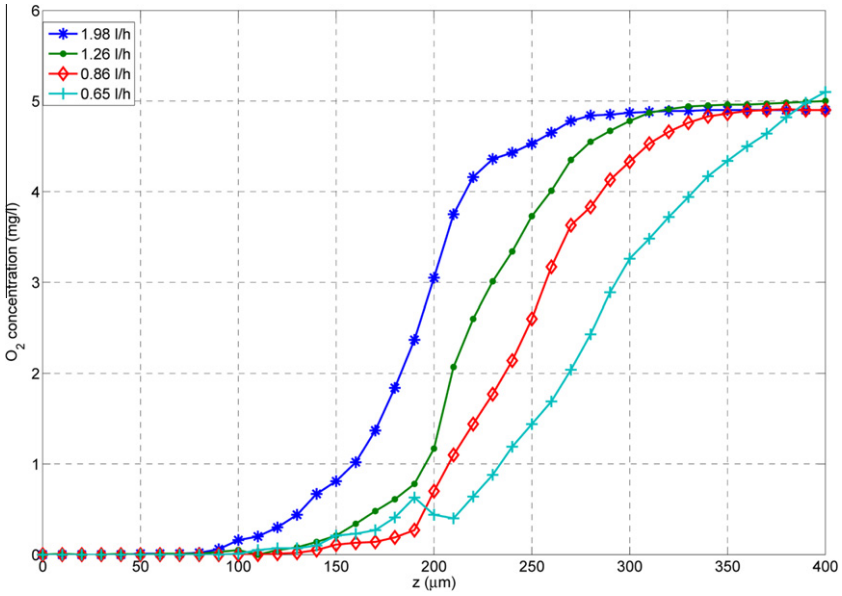

Fig. 6. Oxygen profiles measured at different flow rates.

4.1. Estimation of erosion parameter λ

The erosion parameter λ was estimated from the experimental oxygen profiles using the optimization procedure outlined above. For each data set this was conducted twice, once with the concentration boundary layer in the data, denoted by λ, and once after it was removed, denoted by λ_{BL}. The results are plotted in Fig. 8. The erosion parameters obtained in both cases were rather similar, but slightly higher for the data after removing the boundary layer than for the data sets with the boundary layer values. In both cases, the erosion parameter λ increased as Q increased, which confirms the impact of the reactor flow rate on detachment. At the lowest flow rates of 0.65 l/h the measured erosion parameters lied between 200 and 250 $(\mathrm{md})^{-1}$. These values doubled as the flow rate was increased to 2.18 l/h. In good approximation, the relationship between λ and Q can be described as linear. The lines of best fit were obtained as

$$\lambda(Q) = 179 + 124Q$$

for the oxygen profiles including the data in the boundary layer, and

$$\lambda_{BL}(Q) = 162 + 146Q$$

for the data without. The corresponding goodness of fit was determined as $R^2 = 0.88$ and $R^2_{BL} = 0.89$. This allows us to express the a priori unknown erosion parameter in terms of the known model parameter Q.

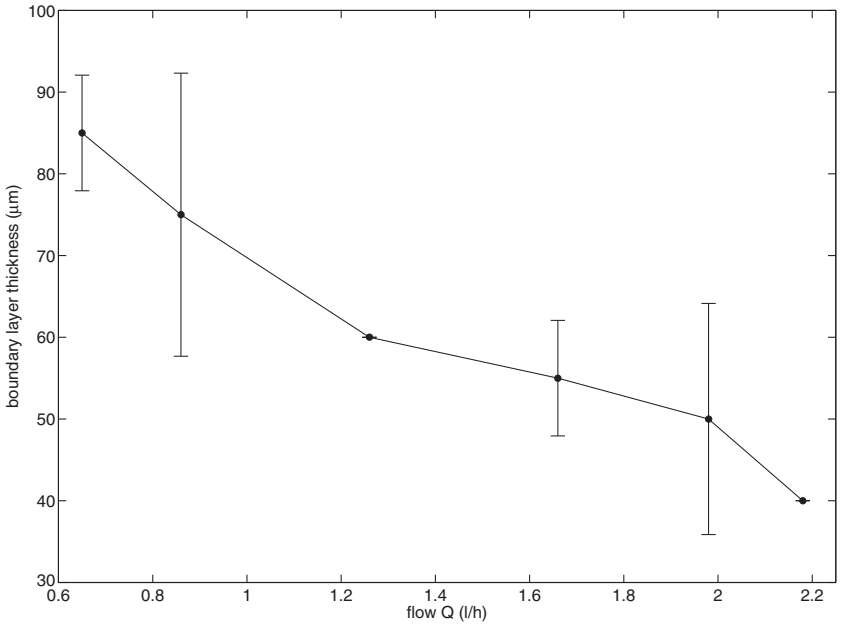

Fig. 7. Boundary layer thickness as function of the flow Q.

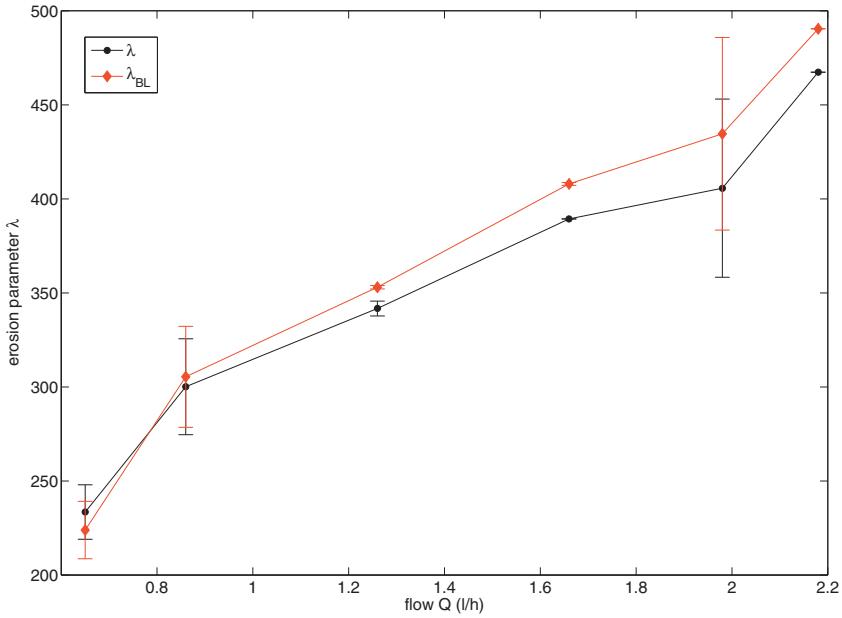

Fig. 8. Erosion parameters λ and λ_{BL} as functions of the flow Q.

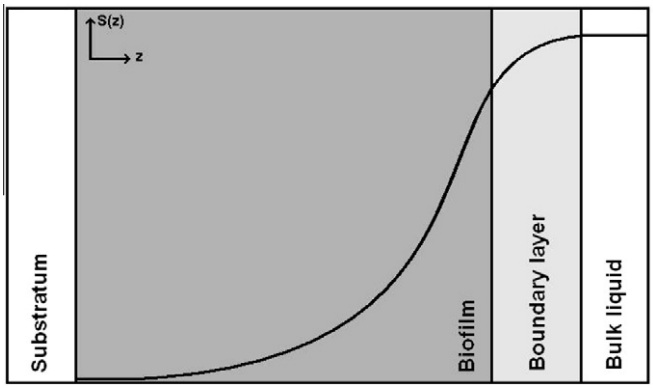

Fig. 9. The oxygen profile through different phases, as shown in [23].

4.2. Oxygen profiles

In the first set of simulations, the oxygen profiles were used including the measurements in the boundary layer. For illustration, the oxygen profiles computed by the model and the experimental data are shown in Fig. 10a for a high flow rate $Q = 1.98$ l/h and in Fig. 11a for the low flow rate $Q = 0.65$ l/h. Overall, the computed and measured profiles agreed well, although the deviation increased for values z closer to the biofilm/liquid interface. This is the effect of the boundary layer measurements which cannot be captured by our model. In a second set of simulations, the boundary layer data were removed from the experimental profiles. This resulted in a better fit of the model with the data, as shown in Figs. 10b and 11b for the data discussed above. In particular in Fig. 11b, the match between simulation and experiment was very close. The deviations around $z = 200$ μm can be attributed to experimental uncertainties; the slight oscillations in the oxygen profile are unphysical and not supported by diffusion–reaction theory (e.g. they violate the maximum principle). For values z larger or smaller the simulated and the measured curve lied nearly on top of each other.

We calculated the sums of squared distances s_p, $p = 1, \ldots, 13$ for the oxygen profiles. Table 2 presents the mean, standard deviation, minimum and maximum values of s_p for profiles estimated with and without the boundary layer. We observe that s_p has larger mean and standard deviation for the oxygen profiles with boundary layer than for the profiles estimated without the boundary layer. The minimum and maximum values are also considerably larger for the profiles with the boundary layer. This confirms that removing the data in the boundary layer stabilizes and improves the fit of model and experimental data.

Table 2
Evaluation of model with sums of squared distances s_p for the oxygen profiles.

Profile estimated	Mean	Standard deviation	Min	Max
With boundary layer	0.1746	0.1623	0.0459	0.5969
Without boundary layer	0.0874	0.0334	0.0273	0.1368

5. Discussion

5.1. Model

The simulation corresponded with the measured oxygen profile to a significant extent, comparing the slope and the spatial position of the profile. Since the model neglects the boundary layer, we assumed that the concentration at the biofilm surface was the same as in the bulk phase. This resulted in differences between the measured and simulated curve, as can be seen in Figs. 10a and 11a. The model overestimated the part where oxygen is depleted and underestimated the steep slope. Oxygen was not completely depleted in the simulation, probably due to our chosen values of the half-saturation constants for oxygen, i.e. the bacteria's affinity for oxygen was too low. The underestimation was then likely a consequence of not enough oxygen being depleted, but also of the way we estimated our parameter λ. The estimation was based on finding the shortest distance between the modeled curve and the measured points. The constant values from the bulk liquid and the boundary layer were pulling the simulated curve to the right to achieve the shortest distance between all points. Therefore, the simulated curve was slightly shifted to the right.

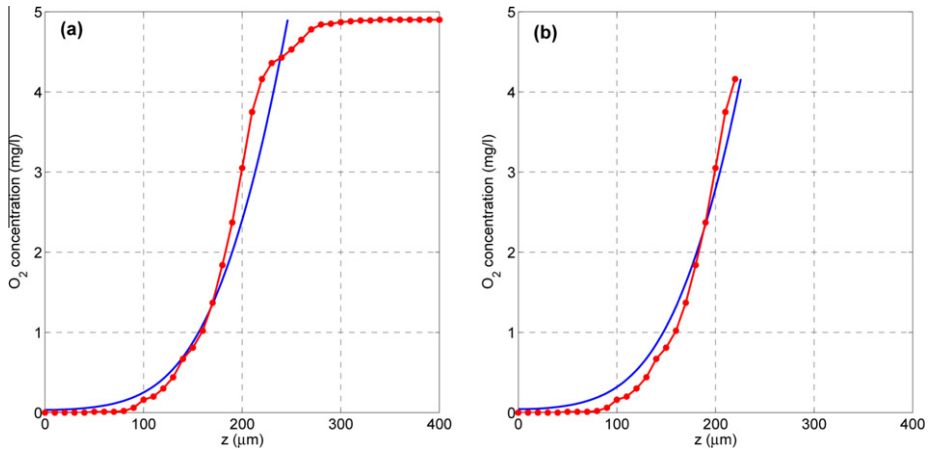

Fig. 10. Measured (•) and simulated (–) oxygen concentration at high flow rate; optimized (**a**) with, and (**b**) without boundary layer.

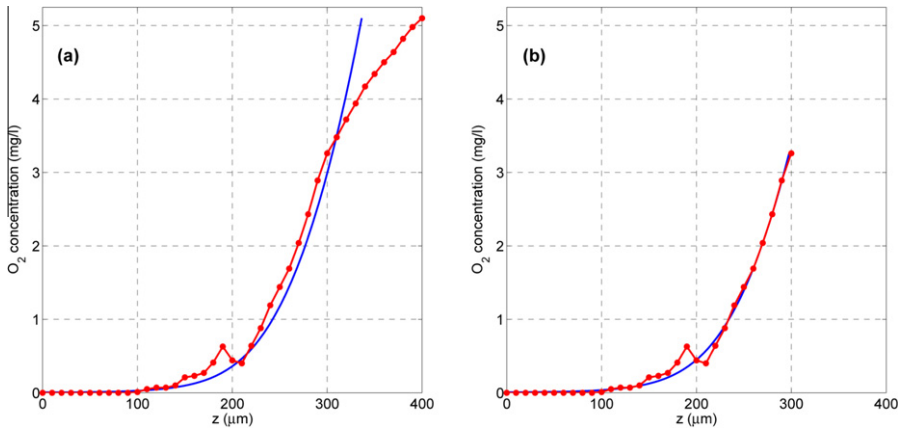

Fig. 11. Measured (•) and simulated (–) oxygen concentration at low flow rate; optimized (**a**) with, and (**b**) without boundary layer.

We obtained a better correspondence between the simulated curve and the measured points (Figs. 10b and 11b) when we removed the bulk phase and the boundary layer. Our evaluation, summarized in Table 2, showed that the sums of squared distances s_p were considerably smaller for the profiles estimated without the boundary layer, and also the standard deviation decreased indicating a stabilizing effect. By removing the boundary layer, we set the correct boundary value in Eq. (11) for our diffusion–reaction equation. This means that the oxygen concentration at the biofilm–liquid interface was no longer assumed to be equal to the concentration that was measured in the bulk liquid, but to the much lower and more reasonable concentration at the biofilm-boundary layer interface. Even though the location of this interface was chosen manually and to some degree subjective, it improved the correspondence of model and experiment.

We see in Fig. 10b that the correspondence was better than in 10a, but the over- and underestimation was still present. One avenue of investigation would be the model constants and parameters, obtained from literature, which may not accurately reflect the MBBR in question. A more exact estimation of the model constants and parameters may improve accordance. The general appearance of the oxygen profile was however well represented. In Fig. 11b we see that the simulated curve overlapped almost all of the measured values (apart from the ones that seemed to be outliers). Our results suggest that this was an appropriate approximation of the measured profile, showing that our model is an adequate representation of an oxygen profile in biofilms attached to a suspended carrier.

The estimation of the erosion parameter λ was necessary to perform, to achieve good correspondence between the modeled and the measured profiles. The amount of erosion is affected by the flow velocity in the bulk liquid surrounding the biofilm. When the velocity is high, more bacteria are eroded off the biofilm surface than when the velocity is low. It should be reflected in the values of λ, i.e. large values for high velocity and smaller values for low velocity. This effect can be observed in Fig. 8 where the values of λ rise with increasing flow velocity. A basic linear fitting has a positive slope for both λ and λ_{BL} and gives an a priori empirical correlation between the erosion parameter and the reactor flow rate that can be used in modeling studies of similar systems in the absence of measurements. It is, however, not necessary to know the exact profile in advance to be able to estimate λ, it would suffice to know the approximate thickness of the biofilm. We can see that the biofilm in Fig. 10 was thinner than the biofilm in Fig. 11. Instead of finding the shortest distance between the points when estimating the parameter, one could have compared the simulated thickness of the biofilm with the measured one. The estimation of λ can in fact be interpreted as training of an unknown parameter from the mathematical model. This is an often used technique to improve models, when experimental data is available. One could then use the trained model to predict oxygen profiles for MBBR in similar environmental conditions. A downside to the estimation is that it can be very time consuming.

5.2. Measurements

Using microelectrodes, we could measure the depth of oxygen penetration and thickness of the active layer. We could also estimate a minimal biofilm thickness by measuring the distance from

the origin to the assumed biofilm-boundary layer interface; in Fig. 10 it was approx. 220 μm and in Fig. 11 approx. 300 μm. It was however not possible to measure the actual thickness, since we did not reach substratum with the microelectrode.

It can easily be seen in the Figures that a higher flow rate gave a thinner boundary layer, while a lower flow rate gave a thicker layer. This impacted the actual oxygen concentration at the biofilm surface. In Fig. 10a, the oxygen concentration dropped ca 0.8 mg/l over the boundary layer, but in Fig. 11a it dropped ca 1.7 mg/l. This means that the true oxygen concentration at the biofilm surface in Fig. 11 was lower than in Fig. 10, even if the bulk oxygen concentrations suggested the opposite. The amount of oxygen available to the biofilm is certainly important for the nitrification rate.

Our expectation on the effect of a higher flow was a deeper penetration of oxygen due to higher convection, resulting in a thicker active layer. A short term change in flow velocity was not expected to influence the structure of the biofilm.

However, measurements at varying flow showed that the active layer was thinner at instantaneous higher flow. If the measurements were made long term on two separate systems with high versus low flow, the explanation would be more related to morphology. A biofilm created at higher flow rate, with thinner boundary layer and, therefore, higher oxygen concentration at the biofilm surface, would have a limited biofilm thickness due to a higher erosion factor. It would, therefore, benefit by having a more compact morphology, due to the presence of more active bacteria per volume unit, which contradictory would have a negative effect on diffusion within the biofilm. At lower flow rate, with thicker boundary layer and lower oxygen concentration at the biofilm surface, the biofilm would then preferably have a thicker, but open and diffuse structure that maximized the surface area towards the bulk phase. An open biofilm structure would allow further oxygen diffusion until a point where extended growth had a negative effect, i.e. it would clog the holes in the carriers, inhibiting both convection and diffusion of oxygen.

These long term effects could however not explain the outcome from our experiment. A potential effect on the biofilm at a higher flow rate was an immediate increase of pressure, making the biofilm more compact. Similar observations have been made by Hille et al. [11] for low density biomass, implying our biofilm being voluminous.

Note that the microelectrode measurements have been performed *in situ* on carriers. Since measurements on moving suspended carriers are extremely difficult to carry out, even impossible with today's techniques, we had to fixate our carriers. Even when fixated, it was challenging to reach into the depths of a biofilm on a carrier, given the complexity of their design. Our measurements on BiofilmChip P are an important step towards acquiring a better understanding of biofilms on suspended carriers. They illustrated the morphology and function of the biofilm and explained the importance of decreasing the boundary layer to achieve efficient utilization of oxygen.

The data gathered could be used in design of new carriers. It is also possible to build a model specifically for MBBR, perhaps using more *in situ* measurements. It is apparent that the flow velocity has large impact, even when working with suspended carriers. The under- and overestimation by the mathematical model of the oxygen profile at high flow rate in Fig. 10 indicated that the model does not take into account the compression caused by increased flow rate. This should be incorporated into mathematical models, in particular when studying short term effects.

To improve the oxygen utilization in process design by decreasing the boundary layer, it would be necessary to increase the mixing in the reactor either mechanically or by enhanced aeration. Thus, the potential gain is counteracted by increased energy consumption. The mathematical model will help us to go beyond the process design and instead evaluate the effect of different carrier shapes, with the ambition of making process operation more energy efficient.

6. Conclusions

Simulations and measurements of oxygen profiles in a nitrifying biofilm on suspended BiofilmChip P carriers were performed for different flow velocities. The following conclusions were drawn from these experiments:

- Instead of using the inflow concentration of the MBBR reactor as the bulk concentration value for the biofilm model, we added a balance equation in form of a CSTR equation. This allowed to account for the decreased concentration of ammonium, nitrite and nitrate in the suspended phase due to microbial activity in the biofilm and improved the computation of the oxygen concentration profile. It increased the accuracy of the boundary condition and gave a more detailed model description. Even though we used a simple one-dimensional mathematical model, we were able to mimic the development of a biofilm in general and to calculate the concentration profiles in particular. Advantages of a simpler model are easier set up and faster calculations.
- For various bulk flow rates, we carried out microelectrode measurements *in situ* on suspended carriers, on BiofilmChip P in particular. The measured oxygen concentration profiles were used for comparison with and validation of the mathematical model. It is however important to note that our measurements were performed on fixated carriers, since no currently available technique makes it possible to measure on moving carriers.
- Using microelectrodes, it was possible to estimate the biofilm thickness as well as the thickness of the mass transfer boundary layer. In particular, we were able to show the dependence of the latter two on the bulk flow rate. Our results confirm the importance of decreasing the boundary layer thickness to achieve efficient utilization of oxygen.
- Measurements of oxygen profiles with microelectrodes gave suitable information for training of the erosion parameters λ for different flow rates. This lead to a simple empirical relationship between erosion parameters and bulk flow rate, which can be used in predictive mathematical modeling of the oxygen concentration profiles under similar conditions.

Acknowledgments

The authors thank Sami Brandt (CTS, Malmö University 2008), Mattias Hansson (CTS, Malmö University) and Roland Möhle (ibvt, TU Braunschweig 2007) for their help and many engaging discussions.

We would also like to thank *Biofilms – Research Center for Biointerfaces* at Malmö University, Sweden for supporting our work.

Appendix A. Medium composition

All amounts quoted as mg/l: NH_4Cl 595, KH_2PO_4 6.0, Peptone water 3.0, $NaHCO_3$ 2×10^3, NaOH 50, $MgSO_4 \cdot 7H_2O$ 0.48, $CaCl_2 \cdot 2H_2O$ 0.58, $MnCl_2 \cdot 4H_2O$ 0.192, $CoCl_2 \cdot 6H_2O$ 0.048, $NiCl_2 \cdot 6H_2O$ 0.024, $ZnCl_2$ 0.026, $CuSO_4 \cdot 5H_2O$ 0.01, $FeSO_4 \cdot 7H_2O$ 0.2, BH_3O_3 0.52×10^{-4}, $NaMoO_4 \cdot 2H_2O$ 2.2×10^{-4}, $Na_2SeO_3 \cdot 5H_2O$ 1.125×10^{-4}, $NaWO_3 \cdot 2H_2O$ 1.4×10^{-4}.

References

[1] E. Alpkvist, J. Bengtsson, N.C. Overgaard, M. Christensson, A. Heyden, Simulation of nitrification of municipal wastewater in a moving bed biofilm

process: a bottom-up approach based on a 2d-continuum model for growth and detachment, Water Science and Technology 55 (2007) 247.
[2] E. Alpkvist, I. Klapper, Description of mechanical response including detachment using a novel particle model of biofilm/flow interaction, Water Science and Technology 55 (2007) 265.
[3] J. Bryers, F. Drummond, Local macromolecule diffusion coefficients in structurally non-uniform bacterial biofilms using fluorescence recovery after photobleaching (frap), Biotechnology and Bioengineering 60 (1998) 462.
[4] D. De Beer, P. Stoodley, Z. Lewandowski, Liquid flow and mass transport in heterogeneous biofilms, Water Research 30 (1996) 2761.
[5] D. Elenter, K. Milferstedt, W. Zhang, M. Hausner, E. Morgenroth, Influence of detachment on substrate removal and microbial ecology in a heterotrophic/autotrophic biofilm, Water Research 41 (2007) 4657.
[6] Y. Fu, T. Zhang, P. Bishop, Determination of effective oxygen diffusivity in biofilms grown in a completely mixed biodrum reactor, Water Science and Technology 29 (1994) 455.
[7] C.P.L. Grady, G.T. Daigger, H.C. Lim, Biological Wastewater Treatment: Principles and Practice, second ed., CRC Press, 1999.
[8] P. Harremoës, Criteria for nitrification in fixed film reactors, Water Science and Technology 14 (1982) 167.
[9] L. Hem, B. Rusten, H. Ødegaard, Nitrification in a moving bed biofilm reactor, Water Research 28 (1994) 1425.
[10] M. Henze, P. Harremoës, J. La Cour Jansen, E. Arvin, Wastewater Treatment: Biological and Chemical Processes, third ed., Springer-Verlag, Berlin, 2002.
[11] A. Hille, T. Neu, D.C. Hempel, H. Horn, Oxygen profiles and biomass distribution in biopellets of *Aspergillus niger*, Biotechnology and Bioengineering 92 (2005) 614.
[12] H. Horn, D.C. Hempel, Growth and decay in an auto-/heterotrophic biofilm, Water Research 31 (1997) 2243.
[13] H. Horn, D.C. Hempel, Substrate utilization and mass transfer in an autotrophic biofilm system: experimental results and numerical simulation, Biotechnology and Bioengineering 53 (1997) 363.
[14] IWA Task Group on Biofilm Modeling, Mathematical Modeling of Biofilms. IWA Scientific and Technical Report No.18, IWA Publishing, 2006.
[15] R. Lu, T. Yu, Fabrication and evaluation of an oxygen microelectrode applicable to environmental engineering and science, Journal of Environmental Engineering and Science 1 (2002) 225.
[16] T.-Y. Pai, Modeling nitrite and nitrate variations in A^2O process under different return oxic mixed liquid using an extended model, Process Biochemistry 42 (2007) 978.
[17] C. Picioreanu, J.-U. Kreft, M.C. van Loosdrecht, Particle-based multidimensional multispecies biofilm model, Applied and Environmental Microbiology 70 (2004) 3024.
[18] W. Rauch, H. Vanhooren, P.A. Vanrolleghem, A simplified mixed-culture biofilm model, Water Research 33 (1999) 2148.
[19] B. Rusten, H. Ødegaard, Design and operation of nutrient removal plants for very low effluent concentrations, in: Proceedings of the Water Environment Federation conference on Nutrient Removal 2007, Baltimore, Maryland, USA, March 2007, pp. 1307–1331.
[20] S. Salem, M. Moussa, M.C. van Loosdrecht, Determination of the decay rate of nitrifying bacteria, Biotechnology and Bioengineering 94 (2006) 252.
[21] R. Santos, M. Callow, T. Bott, The structure of Pseudomonas fluorescens biofilms in contact with flowing systems, Biofouling 4 (1991) 319.
[22] O. Wanner, W. Gujer, A multispecies biofilm model, Biotechnology and Bioengineering 28 (1986) 314.
[23] S. Wäsche, H. Horn, D. Hempel, Influence of growth conditions on biofilm development and mass transfer at the bulk/biofilm interface, Water Research 36 (2002) 4775.
[24] U. Wiesmann, Biological nitrogen removal from wastewater, Advances in Biochemical Engineering and Biotechnology 51 (1994) 113.
[25] T. Wik, On modeling the dynamics of fixed biofilm reactors, Ph.D. Thesis, Chalmers University of Technology, Göteborg, Sweden, 1999.
[26] S. Wyffels, S.W. van Hulle, P. Boeckx, E.I. Volcke, O. van Cleemput, P.A. Vanrolleghem, W. Verstraete, Modeling and simulation of oxygen-limited partial nitritation in a membrane-assisted bioreactor (MBR), Biotechnology and Bioengineering 86 (2004) 531.